Monthly Scientific-Technical and Production Journal

The Paton WELDING JOURNAL

May 2001 # 5

English translation of the monthly «Avtomaticheskaya Svarka» journal published in Russian since 1948

The National Academy of Sciences of Ukraine
The E.O. Paton Electric Welding Institute of the NAS of Ukraine
International Association «Welding»

«The Paton Welding Journal»
is published monthly by the
International Association «Welding»

Promotion group:
V.N.Lipodaev, V.I.Lokteva
A.T.Zelnichenko (Exec. director)
Translators:
S.A.Fomina, I.N.Kutianova,
T.K.Vasilenko

Editorial and advertising offices
are located at PWI,
International Association «Welding»,
11, Bozhenko str., 03680,
Kyiv, Ukraine
Tel.: (38044) 227 67 57
Fax: (38044) 268 04 86
E-mail: tomik@mac.relc.com
E-mail: office@paton.kiev.ua

State Registration Certificate
KV 4790 of 09.01.2001

Subscriptions:
$460, 12 issues, postage included

«The Paton Welding Journal» Website:
http://www.nas.gov.ua/pwj

CONTENTS

MODELLING OF COMPOSITION OF NON-METALLIC INCLUSIONS IN WELD METAL OF HIGH-STRENGTH LOW-ALLOYED STEELS

V.V. GOLOVKO
The E.O. Paton Electric Welding Institute, NASU, Kyiv, Ukraine

ABSTRACT

Experiments on validation of adequacy of the developed computer software for prediction of the amount and composition of non-metallic inclusions (NMI) in the low-alloyed steel weld metal are described. In addition to modelling of the final amount and composition of NMI, this software allows also the calculation of characteristics of the inclusions which are contained in the weld pool metal in a pre-solidification period of its existence.

Key words: *welding, low-alloyed steel, weld metal, non-metallic inclusions, computer modelling, prediction of composition, adequacy validation*

The quality of welded joints from carbon and low-alloyed steels is determined mostly by the level of physical and physical-chemical characteristics of the weld metal which are affected significantly by the morphology, composition and distribution of the NMI. Earlier, the main attention was paid to the problem of formation of inclusions in the process of weld solidification, and the formation of oxides during metal solidification was not much studied. The steel cooling both in molten and solid state is accompanied by decrease in solubility of oxygen and its evolution either into a gas phase or in the composition of NMI. The formation of different types of inclusions in the metal structure is caused, first of all, by a selective chemical affinity of oxygen to the elements-deoxidizers. At different stages of formation of metal of welded joints this affinity is different. It is shown in [1], that during the steel solidification the volumetric share of secondary (forming in the process of cooling of deoxidized metal to the liquidus temperature), tertiary (forming in the process of cooling between the liquidus and solidus lines) and quaternary (forming at temperatures below the solidus temperature) NMI can reach 70 – 80 %. These investigations were not performed for weld metal. However, it is known that the NMI themselves in weld metal represent the multilayer formations with most refractory compounds in the center and the compound with the lowest melting temperature, which is lower than that of steel solidification in the periphery [2 – 4]. Coming from this it can be assumed naturally that the formation of NMI is not completed at the solidus temperature of steel, but it is continuing for some time in a two-phase zone, which is formed around the inclusion nuclei and maintained by liquation processes. It is shown in [2] that the time of existence of this zone in weld metal during its solidification exceeds the time of existence of molten metal in a pre-solidification period.

It was stated from the numerous investigations that the NMI influence the conditions of formation of structural constituents of weld metal, and this, in turn, influences the service properties of the welded joints. This influence can be determined both by the total amount of inclusions in metal [5, 6] and also by the peculiarities of their chemical composition [7 – 9].

At the condition of a multilayer morphology of the inclusions a surface layer, i.e. the layer formed at the final stage of the inclusion formation, plays the most important role in these processes. The conditions of contact of the surface layer with a metallic matrix define the feasibility of formation of discontinuities around the inclusion which are traps during hydrogen diffusion in weld metal [10, 11], or the feasibility of occurrence of a stressed state in surrounding volumes of metal [12, 13].

It is clear, that the direct experimental investigations in the dynamics of the process of formation of NMI in weld metal are almost impossible. Coming from this, the problems of investigation of composition, sizes and content of NMI in welds made from high-strength low-alloyed steels using the methods of a mathematical modelling and numerical experiment are actual.

Methodology of work. To describe the processes of formation and growth of NMI a deterministic dynamic model with distributed parameters was selected. These models are versatile and do not become almost outdated (at the present level of process knowledge) and easily adapted to the definite technologies [14]. The adaptation of these models to the conditions which meet the definite processes of welding, is made by specifying the model parameters on the basis of experimental data, characteristic of the certain technological conditions of welding. Experimental part of the work was accomplished using the SAW.

In experiments, the agglomerated fluxes in combination with 4 mm diameter Sv-08GA (C – ≤ 0.1; Mn – 0.8 – 1.0 wt.%; Fe – balance) wire were used. The welding was performed at DCRP using the following condition parameters: I_w = 640 – 650 A, U_a =

= 30 – 31 V; v_w = 27 – 28 m/h. During experiments the 25 mm thick low-alloyed steel of 10KhSND (C — ≤ 0.12; Mn — 0.5 – 0.8; Si — 0.8 – 1.1; Cu — 0.4 – 0.65; Cr — 0.6 – 0.9; Ni — 0.5 – 0.8 wt.%; Fe — balance) grade welded joints were made with 60° angle of grooves and 20 mm gap in the weld root. The templets for manufacture of samples for metallographic examination were cut from the metal of a last pass located in the middle of the upper layer.

The metallographic examinations were made on transverse sections cut from welded joints. The quantitative analysis on NMI was performed in instruments «Omnimet» and «Quantimet-720». The total contamination of weld with inclusions was determined in «Quantimet-720», equipped with a scanning TV camera, which can reveal and process the objects of sizes of up to 0.5 μm. The distribution of inclusions by sizes and plotting of corresponding graphs were made by «Omnimet» directly from the sections. According to the preset program the instrument can count the number of inclusions in each sample by dimensional groups, from minimum to maximum sizes. The analysis of the phase composition of NMI was made in electron microscope JSM-35 with the help of an energy-dispersed spectrometer «Link-860» in «point-by-point» way to avoid the background radiation.

Physical-chemical modelling. In general, the process of formation of inclusions consists actually of two processes being different in their physical-chemical principle: process of formation of inclusion in molten steel and also the subsequent precipitation of a condensed phase at the interface in two-phase zone during the post-solidification period. In this connection, the modelling was made separately for each of the mentioned processes.

When creating the physical-chemical model of the process of formation of inclusions in the molten steel, the assumption was used that the high intensity of metal and slag stirring in the weld pool, heating of molten electrode metal at the stage of a drop to the 2000 °C temperature and higher provide the system approaching to the equilibrium conditions at the fixed moment of time which is sufficient for making true predictions. The thermodynamic calculations of equilibrium for metal–slag–gas reactions allow establishment of the most favourable conditions for the formation of inclusions of a definite composition. Calculations made by Vagner's formula [15] showed that even 2 s after the formation of the weld pool the medium size of inclusions in the molten metal is 0.5 μm and continues to grow in time. Consequently, when analyzing the amount, composition and distribution of NMI it is sufficient to be limited by examination of inclusions of sizes of not less than 0.5 μm.

In modelling the processes of condensation of inclusions in the range of temperatures below the crystallization temperature the statements of the quasi-equilibrium theory of a two-phase zone were used [16]. In this case the intensity of growth of the oxide phase at the interface is determined by a share of the liquid constituent in the two-phase region S.

During the arc processes of welding the slag, as a rule, is an oxidizing medium with respect to the molten metal. Therefore, the reaction of interaction between the elements-deoxidizers dissolved in the weld pool, and a slag can be written in a general form as

$$n_i[R_i] + m_i[O] = Rn_iOm_i, \qquad (1)$$

resulting in formation of M_i, which is the number of products of i-th reaction. However, in this case the concentration of oxygen C_O will change as a result of proceeding of these reactions and also liquation processes, and the oxygen balance in moles can be written as follows [17]:

$$d(SC_O)/dt = k_0 C_O dS/dt - \sum_{i=1}^{N} m_i dM_i/dt. \qquad (2)$$

The feasibility of these reactions and yield of their products depend on the concentration of the i-th element-deoxidizer C_i. The equation of balance (in moles) for each i-th element-deoxidizer has a form

$$d(SC_i)/dt = k_i C_i dS/dt - n_i dM_i/dt. \qquad (3)$$

At a local thermodynamic equilibrium for concentration of oxygen C_O and i-th element-deoxidizer, reacting with it, C_i, we shall have

$$C_i^n \, C_0^m = \frac{1}{K_i f_i^n f_0^m}, \qquad (4)$$

where K_i is the constant of equilibrium of reaction of oxidation of the i-th element-deoxidizer.

The system of equations (2) – (4) is composed of $2N + 1$ closed equations and makes it possible to determine the concentration of oxygen and N elements-deoxidizers, reacting with it, and also the content of oxides M_i, forming at all the stages of the solidification.

The amount of pre-solidification inclusions can be determined from the system N of the equations of the type

$$\left(C_i^0 - \frac{M_i}{1 + 16m_i/n_i A_i}\right)^n \times \left(C_O^0 - \sum_{i=1} \frac{M_i}{1 + n_i A_i/16m_i}\right)^m = \frac{1}{K_i f_i^n f_i^m}, \qquad (5)$$

where C_O^0, C_i^0 are the initial concentrations of oxygen and element-deoxidizer in melt before the solidification, respectively; A_i is the atomic weight of the i-th element-deoxidizer.

Then, the initial content of the element-deoxidizer in the melt will have the form

$$C_i^* = \frac{C_i^0 - M_i^*}{(1 + 16m_i/n_i A_i)}, \qquad (6)$$

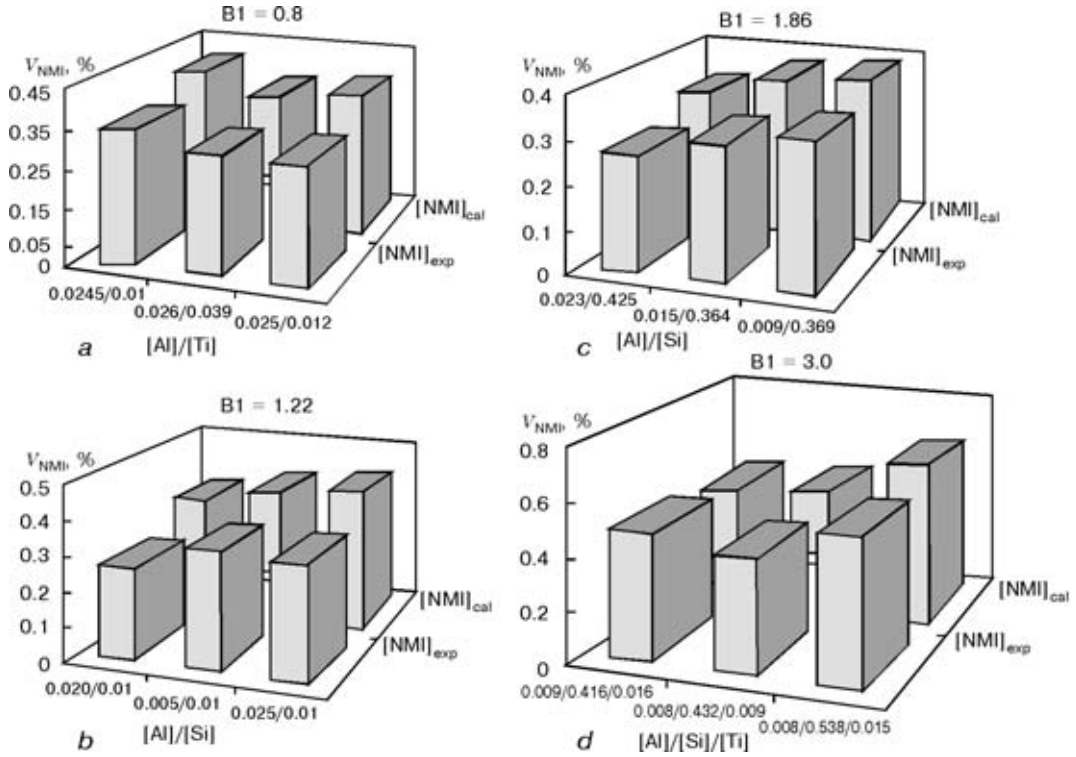

Figure 1. Comparison of calculated $[NMI]_{cal}$ and experimental $[NMI]_{exp}$ volumes depending on the ratio of aluminium, silicon, titanium in weld metal, made under fluxes of different basicity

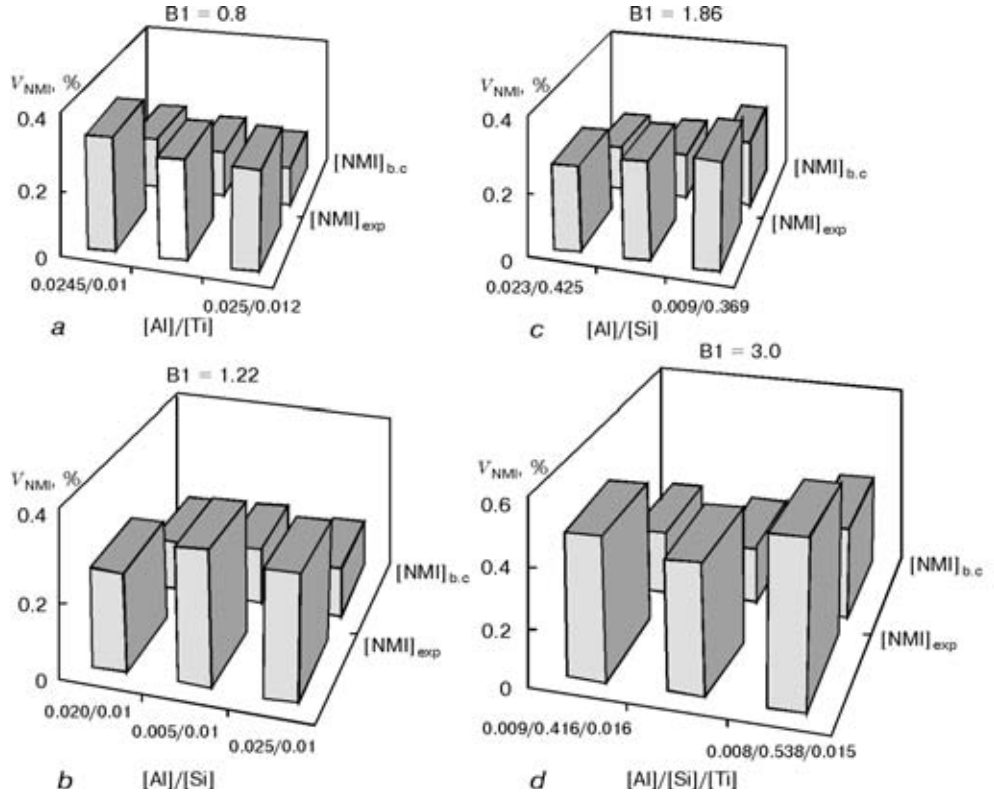

Figure 2. Comparison of calculated (pre-solidification) and experimental volumes depending on ratios of aluminium, silicon, titanium in weld metal, made under fluxes of basicity B1 = 0.8 – 3.0

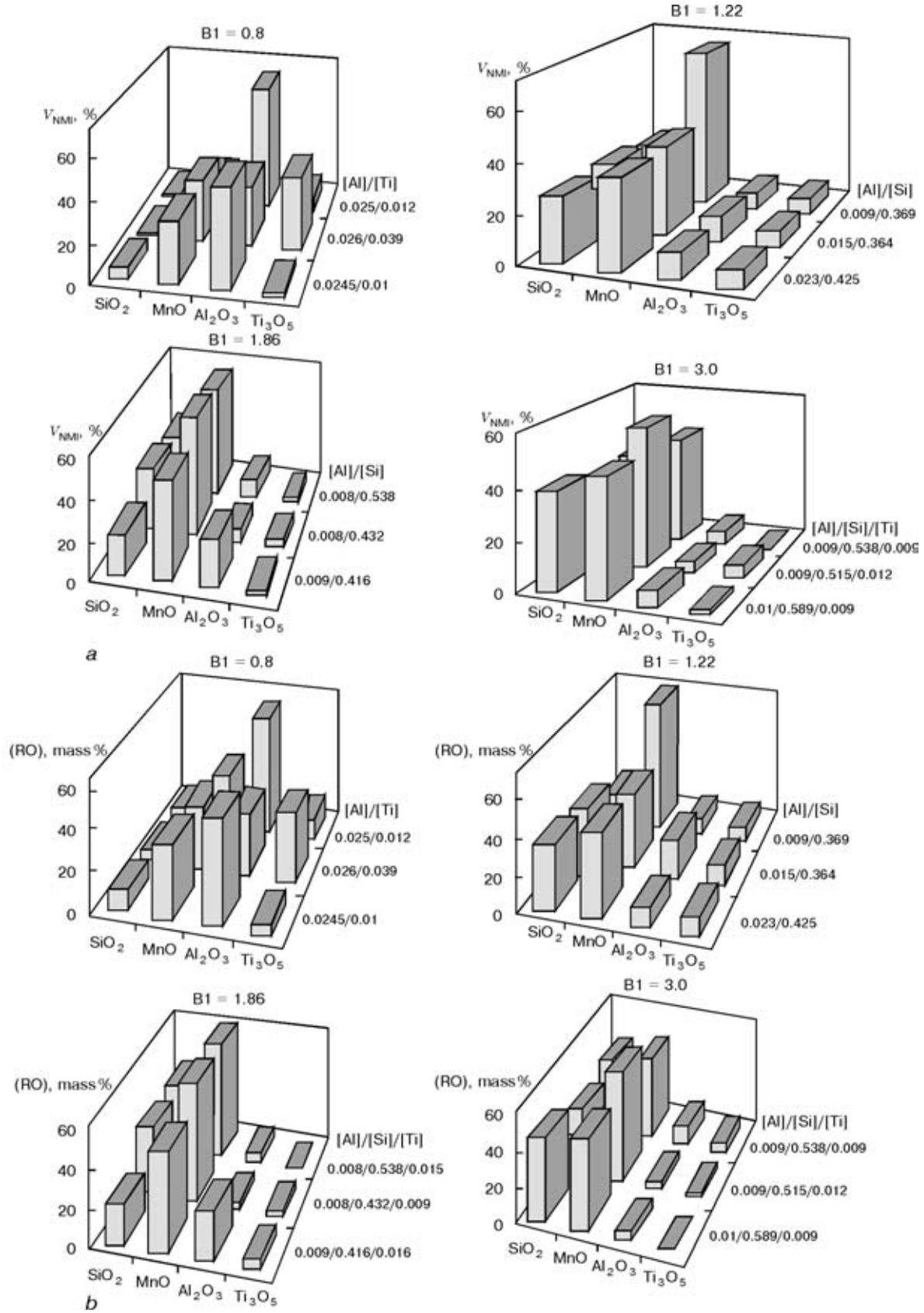

Figure 3. Experimental (*a*) and calculated (*b*) data about composition of NMI depending on ratio of aluminium, silicon and titanium in weld metal, made under flux of basicity B1 = 0.8 – 3.0 (*a*) and with allowance for action of elements-deoxidizers (*b*)

and that of oxygen

$$C_O^* = \frac{C_O^0 - \sum_{i=1}^{N} M_i^*}{(1 + n_k A_i / 16 m_i)}. \quad (7)$$

The obtained complex system of algebraic and ordinary equations (2) – (4) and (5), as well as algorithms of their solution should be specified in each definite case.

Using the algorithm, described in FORTRAN, the program was compiled and tested (in collaboration with Dr. L.A. Taraborkin) for the calculation of processes of formation of NMI in accordance with the developed mathematical model.

To check the adequacy of the developed model, five agglomerated fluxes of different types and basicity were selected. Fluxes of a fluoride-basic type had an index of basicity B1 = 3.0 and B1 = 1.86. Flux of aluminate-basic type had B1 = 1.22, and the manganese–silicate flux had the basicity index B1 = 0.8.

To intensify the processes of formation of NMI, such elements-deoxidizers as silicon, titanium and aluminium in the amount of 1 % were introduced to the experimental fluxes. Samples for metallographic examination were manufactured from the metal of the last pass of butt joints, made by welding using the experimental fluxes and the above-described procedure.

Figures 1 and 2 compare the results of calculation of amount and composition of NMI, which was made using the program with data of experiments, which were obtained during the metallographic analysis of weld metal samples. Data in Figure 1 show a good correlation of calculated and experimental results. It can be considered from this, that the results of calculation of amount of pre-solidification inclusions (Figure 2) also correspond to the real situation in the weld pool. Thus, the given program can analyze the content of inclusions in the weld pool before the beginning of the processes of its solidification that is difficult to make now experimentally.

As is seen from the data given in Figure 3, the developed model can describe the conditions of formation of NMI in the wide range of compositions of fluxes at their different basicity and with allowance for action of the elements-deoxidizers, introduced into the flux composition, that is confirmed by the adequacy of the calculated and experimental data.

Thus, the developed computer model makes it possible to describe the processes of formation of the NMI in the weld metal at the different stages of their formation. Investigations, made with the use of this program, confirmed not only a good correlation of calculated data with the results of experiments, but they also showed the feasibility of prediction of content and composition of NMI in the molten metal of the weld pool that is difficult to obtain experimentally.

The application of the developed program for the analysis of the conditions of formation of structure of the high-strength low-alloyed steel weld metal will provide opportunity to use the methods of a computer modelling for the solution of the problem of improving the serviceability of welded joints, development of welding consumables of the new generation with predicted properties.

REFERENCES

1. Yavoisky, V.I., Tyong, V.M., Gorokhov, L.S. (1961) Deoxidation of carbon and low-alloyed open-hearth steels. In: *Non-metallic inclusions in steel*.
2. Kluken, A.O., Grong, O. (1989) Mechanisms of inclusion formation in Al–Ti–Si–Mn deoxidized steel weld metals. *Metallurgical Transact. A*, **8**, 1335 – 1349.
3. Devillers, L., Kaplan, D., Ribes, A. *et al*. (1986) Metalurgie et proprietes mecaniques du metal fondu en soudage multipasse sous flux d'acier au C–Mn micro-allie. *Memories et Etudes Scientifiques Revue de Metallurgie*, **1**, 43 – 62.
4. Dowling, J.M., Corbett, J.M., Kerr, H.W. (1986) Inclusion phases and the nucleation of acicular ferrite in submerged-arc welds in high-strength low-alloy steels. *Metallurgical Transact. A*, **10**, 1611 – 1623.
5. Boniszewski, T. (1972) Fine oxide particles in mild steel CO_2 weld metal. *Welding J*., **1**, 19 – 22.
6. Irvine, K.J., Pickering, F.B. (1960) Relationship between microstructure and mechanical properties of mild steel weld deposits. *British Welding J*., **5**, 353 – 364.
7. Quintana, M., McLane, J.E., Babu, S.S. *et al*. (1999) Inclusion formation in self-shielded flux-cored arc welds. In: *Abstracts of papers AWS Meeting*.
8. Terashima, H., Hart, P.H.M. (1984) Effect of flux TiO_2 and Ti content on tolerance to high Al content of submerged-arc welds made with basic fluxes. In: *Proc. of Int. Conf. on Effects of Residual, Impurity and Microalloying Elements on Weldability and Weld Properties*, London, Nov. 15 – 17. Abington, Cambridge.
9. Horii, Y., Ichikawa, K., Ohkita, S. *et al*. (1995) Chemical composition and crystal structure of oxide inclusions promoting acicular ferrite transformation in low-alloy submerged-arc weld metal. *Q. J. of JWS*, **4**, 500 – 507.
10. Olson, D.L., Liu, S., Wang, W. *et al*. (1995) Martensite start temperature as a weldability index. In: *Proc. of the 4th Int. Conf. on Trends in Welding Research*, June 5 – 8, Gatiinburg, USA
11. Knyazev, A.A., Volkov, V.A., Chernukha, L.G. (1984) About the mechanism of effect of NMI on the hydrogen diffusion in steel. *Metally*, **4**, 43 – 49.
12. Shulga, A.V., Nikishanov, V.V. (1990) Analysis of stresses state in precipitation of particles of interstitial phases. *Ibid*., **5**, 128 – 134.
13. Tsivirko, E.I., Gontarenko, V.I., Byalik, G.A. (1992) Behaviour of NMI in the conditions of thermodeformational processing of steel. *Izv. Vuzov., Chyornaya Metallurgia*, **2**, 20 – 23.
14. Kabanova, O.V., Maksimov, Yu.A., Ruzinov, L.P. (1989) *Statistic methods of construction of physical-chemical models of metallurgical processes*. Moscow: Metallurgia.
15. Babu, S.S., David, S.A., Vitek, J.M. *et al*. (1995) Development of macro- and microstructures of carbon–manganese low-alloy steel welds: inclusion formation. *Materials Science and Technology*, **2**, 186 – 199.
16. Grigorian, V.A., Stomakhin, A.Ya., Ponomarenko, A.G. *et al*. (1989) *Physical-chemical calculations of electric steel melting processes*. Moscow: Metallurgia.
17. Borisov, V.T. (1961) Theory of formation of NMI in two-phase zone of solidifying ingot. In: *Non-metallic inclusions in steel*.

ALLOWING FOR RESIDUAL STRESSES IN THE CROSS-SECTIONS OF COMPRESSED I-SHAPED COLUMNS DURING THEIR DESIGN

A.I. GOLODNOV
The E.O. Paton Electric Welding Institute, NASU, Kyiv, Ukraine

ABSTRACT

A procedure has been developed for evaluation of the stress-strain state of I-shaped steel columns at all the stages of loading, including the hypercritical region. Design has been performed allowing for the fields of residual stresses, arising in the cross-sections of these columns.

Key words: *load-carrying capacity, I-shaped column, residual stresses, design*

Fabrication of metal structures and items, irrespective of the technological processes, invariably leads to development of residual stresses that later on affect the element performance under load. For this reason, the problem of residual stresses distribution in the cross-sections of I-shaped columns and their influence on the structure performance under load, is the subject of numerous investigations, both in FSU and abroad.

Study [1] gives the results of experimental investigations of the influence of the residual stress fields on the load-carrying capacity of columns loaded by compression, that have an I-shape in the cross-section. Longitudinal deformations (stresses) are determined in the median section of two kinds of samples, namely welded I-shaped elements and similar samples, subjected to high-temperature annealing. Deformations were measured with strain gauges located opposite each other (mean arithmetic value was used). The derived data were the basis for plotting the characteristic graphs of stress variation and led to the conclusion on the influence of inherent stresses on the load-carrying capacity of welded elements with medium values of slenderness ratio. The results of compressive testing of the columns showed that the load-carrying capacity of welded columns is lower than a similar value for the columns subjected to high-temperature annealing after fabrication. This is caused by a high level of residual compressive stresses in the welded column flanges.

The authors of [2] have conducted a series of tests of welded column samples of low-alloyed steel. Three types of samples were taken, namely those subjected to post-weld annealing (A), regular welded columns (W), samples with initial tensile stresses at the edges (R). During testing, it was found that their load-carrying capacity depends on the value and nature of distribution of residual stresses, as well as the shape of the samples cross-section. As was anticipated, W type samples had lower load-carrying capacity, because of the presence of residual compressive stresses in the flanges, compared to samples of type A and R, which had no residual compressive stresses in the flanges.

Study [3] describes the results of investigations, conducted to determine the extent of residual stresses influence on the value of critical load. Tested were the rolled and welded profiles, where the chords developed residual compressive stresses, as well as columns with deposits on the edges. Surfacing of the edges induced additional tensile residual stresses that acted simultaneously with the initial compressive stresses. During investigations it was found that at flexibility $\lambda = 80$, the load carrying capacity of the rolled samples was 145 tons, and in welded samples with the same cross-sectional area, it was 95 tons. In samples with deposited welds, the load-carrying capacity was 135 tons.

Study [4] gives the results of testing the columns made to determine the residual stress influence on their load-carrying capacity. Riveted and welded columns with the same cross-sectional area were tested. It was found that the load-carrying capacity of welded columns is lower than that of the riveted columns. This is attributable to the presence of high-level residual compressive stresses on the flange edges. As was anticipated, the values of tensile stresses in the region immediately adjacent to the weld, are close to the steel yield point, while the stresses at the flange ends reach the level of 1400 MPa.

The above research results allowed determination of the residual stress influence on the load-carrying capacity of columns loaded by compression, that are deformed in the plane of lower rigidity. Study [5] gives experimental data on the influence of residual stresses on the stability of columns of the I-beam and box profile at off-center compression. It was found that the columns with a weld of a smaller cross-section, are less susceptible to deformation. Lowering of the deformation susceptibility can be achieved by depositing beads on the column edges. Bead deposition can be replaced by heating the edges to the temperature higher than A_{c_3}.

The derived experimental data (this paper does not give the results of other studies) were the basis for developing in the Donbass Mining-Metallurgical Institute a procedure for determination of the stress-strain state in the sections of composite and rolled I-shaped columns, having residual stress fields, as well as a procedure of evaluation of the load-carrying capacity and deformation susceptibility of columns compressed with different eccentricity, allowing for the fields of residual stresses in their cross-sections. These procedures are based on the common principles and assumptions of the mechanics of deformable bodies, and allow determination of the parameters of the deformed column (reference points of the load–deflection diagram) at all the stages of the load application, also in the hypercritical (after achievement of the maximum on the state curve) region.

Solution of the problem of determination of the stress-strain state of the column in the explicit form is impossible, because of the presence of a greater number of the unknowns, than in the equilibrium equation. It is solved by the iteration method using a specially developed algorithm [6].

The procedure of evaluation of the load-carrying capacity of compressed I-shaped columns allowing for the presence of residual stresses of different kind was used in design of experimental samples [1 – 4].

Experimental data (absolute or relative values of critical forces) were compared with similar data, derived through computation. The ratios of theoretical values of the load-carrying capacity to experimental data, expressed by coefficient K_p, were subjected to statistical processing. A satisfactory fit of the magnitudes of the compared values was achieved. So, mathematical expectation of coefficient K_p in processing 75 results, turned out to be equal to 1.011, while the mean root square deviation was $\sigma = 0.05$. The given results are indicative of a sufficient reliability of the design procedure.

The above procedure was used to conduct a mathematical experiment, that allowed solving the following problems.

1. Determine the area of a rational application of the developed analytical equations.

2. Determine the extent of influence of different factors (strength properties of the material R_s, flexibility λ, kind and width d of the zones of the residual tensile stresses), developing in the cross-sections of I-shaped columns in welding or local heat treatment, on the values of the critical forces at eccentricities e of load application close to the random values.

3. Derive dependencies of the change of the coefficient of longitudinal bending $\varphi = f(\lambda, e, d, R_s)$ and using the procedures recommended by the standards, prepare the proposals on design of columns loaded by compression and having the residual stress fields.

When the first two problems were solved, more than 400 models of the columns were computed to find that:

1) influence of the stress fields on behaviour of columns under load for the entire range of variation of the material strength properties, is characterized by similar dependencies, namely the zones of residual tensile stresses, located at the chord edges, increase, and those located in the area of chord welds decrease the values of the critical forces;

2) significant discrepancies in the values of critical forces for the columns loaded by compression with chord welds are observed in the flexibility range from 40 to 100 (at columns flexibility below 40 and above 100, these discrepancies are minor). In the columns with the zones of tensile stresses on chord edges, the discrepancies in the values of critical forces begin at the flexibility higher than 40;

3) in the columns, in which the width of the zone of heating the chord edges up to the temperature, exceeding A_{c_3}, is more than 1.5 cm, the discrepancies in the values of critical forces, are negligible;

4) for the determined flexibility range ($60 < \lambda < 120$) the dependencies of variation of the longitudinal bending coefficient φ (λ, e, d, R_s) are nonlinear.

The scope of mathematical experiment for solving the third problem was determined proceeding from the results of the performed computations, as well as allowing for the format of presentation of the longitudinal bending coefficient variation in SNiP II-23–81*. Altogether 504 column models were computed, for which the relative values of critical forces were determined. The derived data were subjected to successive approximation by the least squares method. First an approximation function was derived, allowing for the change of the longitudinal bending coefficient φ_0, provided the residual stress zones were absent. For the slenderness ratios $60 < \lambda < 120$ and design values of resistance of steel $200 < R_s < 400$ MPa, this function has the form of

$$\varphi_0 = (0.162\overline{R} - 0.254)\,\lambda_s^2 + (0.578 - 0.617\overline{R})\,\lambda_s + (0.36\overline{R} + 0.596), \quad (1)$$

where $\overline{R} = R_s/200$ is the relative resistance of steel (R_s is the design resistance of steel in megapascals); λ_s is the relative slenderness ratio of the column, equal to $\lambda/60$.

This was followed by successive approximation of additional summands in the equation of the longitudinal bending coefficient, derived as the difference between the relative values of load-carrying capacity at $d_k(d_p) \neq 0$ and $d_k(d_p) = 0$ (d_k and d_p are interpreted in explications to the equations given below). Additional functions were derived that have the following form:

for zones of tensile stresses at chord edges

$$\varphi_{d,\,1} = [(0.776\overline{R} - 2.651)\lambda_s^2 + (9.44 - 2.993\overline{R})\lambda_s + (2.813\overline{R} - 7.38)]d_k^2 + [(0.375 + 0.0933\overline{R})\lambda_s^2 - (1.577 + 0.105\overline{R})\lambda_s + (1.592 - 0.126\overline{R})]d_k, \quad (2)$$

where $d_k = 2d_t/b_f$ (here d_t is the width of the HAZ, determined by a specially developed algorithm [6]; b_f is the flange width);

for chord welds

$$\varphi_{d,2} = [(0.0207\overline{R} - 0.0176)\lambda_s - (0.0221\overline{R} + 0.0024)]d_p^2 + \\ + [(0.015 - 0.041\overline{R})\lambda_s^2 - \\ - (0.0904\overline{R} + 0.0806)\lambda_s - (0.249 + 0.00454\overline{R})]d_p , \quad (3)$$

where $d_p = (k_f + \delta)/t_w$ (k_f is the weld leg; δ is the base metal penetration depth; t_w is the thickness of the I-beam wall).

Then, the relative load-carrying capacity (longitudinal bending coefficient) is

$$\varphi_f = \varphi_0 + \varphi_d, \quad (4)$$

where φ_d is determined by substituting the values of $\varphi_{d,1}$ or $\varphi_{d,2}$, found from equation (2) or (3), respectively, depending on the kind of the residual stress field.

The derived approximation functions were subjected to subsequent statistical processing to determine the mathematical expectation of coefficient $K = \varphi_f/\varphi_m$ (φ_f, φ_m are the relative values of load-carrying capacity of the columns, derived from equation (4), respectively. and during the mathematical experiment) and its mean root square deviation. As shown by the performed computations (a sampling of 504 values of φ_f and φ_m was processed), mathematical expectation of the coefficient was $K = 1.000845$, while its mean root square deviation $\sigma = 0.0153$. Considering, that at probability $P = 0.99$, the values of mean root square deviation σ are in the range of $\pm 2.6 \cdot 0.0153 = \pm 0.0398$, the recommendation was to assign the values of the longitudinal bending coefficients φ, allowing for correction factor $\gamma_d = 1.000845 + 0.0398 \cong 1.04$, i.e.

$$\varphi = \varphi_f/\gamma_d = 0.962\varphi_f. \quad (5)$$

Thus, the influence of the residual stress fields on the load-carrying capacity of compressed I-shaped columns, deformed in the lower rigidity plane, can be taken into account by multiplying the values of design resistance of steel R_s by the longitudinal bending coefficient, calculated by (2) – (5). For some values of variables $\overline{R}$, λ_s, d_k, d_p, the values of coefficients have been computed and tabulated [6]. Computations by the proposed equations can be performed in two variants, namely the specified geometrical parameters, strength properties of materials and patterns of the residual stress zones are used to determine the load-carrying capacity of the column (Tcentr-3 algorithm); assigned values of longitudinal force, strength properties of the material and patterns of residual stress zones are used to select the cross-sectional dimensions of a welded I-shaped element (Tzentr-4 algorithm).

REFERENCES

1. Shelestenko, L.P. (1954) Influence of inherent residual stresses on the overall stability of compressed welded H-shaped elements. *Zheleznodorozhnoye Stroitelstvo*, **2**, 22 – 24.
2. Kihara, H., Fujita, Yu. (1962) The influence of residual stresses on the instability problems. In: *Proc. of XIII Congress of the IIW*, Liege, June 13 – 19. Moscow: Mashgiz.
3. Lui, Kh., Massone, Ch. (1962) Influence of residual stresses on the phenomena of metal structure instability. *Ibid*.
4. Toll, L., Hubert, A., Bidle, L. (1962) Residual stresses and instability of columns at axial loads of columns. *Ibid*.
5. Ignatieva, V.S. (1979) Method of «fictitious» temperatures as the basis for investigations into the stress-strain state of welded joints. In: *Transact. of MISI*. Moscow.
6. Golodnov, A.I., Khvortova, M.Yu. (1997) *Analysis and design of elements of metal structures based on I-shaped beams with specified fields of initial stresses*. Manual. Alchevsk: DGMI.

EFFECT OF CARBON-CONTAINING MATERIALS OF FLUX-CORED WIRE ON TRANSFER OF CARBON INTO THE MOLTEN POOL DURING SURFACING

S.Yu. KRIVCHIKOV and **A.P. ZHUDRA**
The E.O. Paton Electric Welding Institute, NASU, Kyiv, Ukraine

ABSTRACT

Results of investigations of transfer of carbon into the molten pool during surfacing using self-shielded flux-cored wire are given. The effect of the type of a C-containing material of the core of a flux-cored wire on peculiarities of its melting, values of the coefficient of transfer of carbon into the deposited metal and its concentration in the latter has been established.

Key words: *surfacing, self-shielded flux-cored wire, carbon-containing material, deposited metal, transfer of carbon*

Carbon is one of the main alloying elements which determine type, structure and other properties of the deposited metal. In this connection, of practical interest are the data on the kinetics of its transfer from a flux-cored wire into the molten pool during surfacing.

This article gives results of investigations of the effect of the type and amount of C-containing materials of the core of a self-shielded flux-cored wire on the carbon content of the deposited metal.

Surfacing was performed using experimental flux-cored wires (Table) in which the carbon content was varied by adding to the wire core the following C-containing materials: graphite (Gr) of the electrode (99.6 % C) or silver (99 % C) type, silicon carbide SiC (29.5 % C) and carbon ferrochromium FKh800 (8.2 % C).

Flux-cored wires of the first series contained different amounts of electrode graphite and silicon carbide. Their ratio was varied so that a carbon content of all wires of this series remained equal to 2 wt.%. In flux-cored wires of the second series electrode graphite contained in mixtures was replaced by silver one. Flux-cored wires of the third series contained a mixture of electrode graphite and FKh800, and their ratio provided a carbon content of 1 %.

Wide-layer surfacing [1] was performed at a DCRP under the following conditions: I_w = 220 – 240 A, U_a = 24 – 25 V, amplitude of oscillations of the flux-cored wire tip was 30 mm.

Figure 1 shows that the degree of oxidation (reactivity) of silver graphite is higher than that of electrode graphite. This is attributable to the fact that, on the one hand, silver graphite contains a higher amount of ash impurities [2], and on the other hand, particles of electrode graphite are a bit elongated bulky grains, whereas particles of silver graphite are plate-like and flaky. A more developed surface of the silver graphite particles favours an increase in the amount of the elementary events of chemical interaction taking place between carbon and air oxygen at the particle–gas interface, which leads to a more complete occurrence of the reaction of oxidation of silver graphite carbon and decrease in its content of the deposited metal.

Replacement of graphite by carbon in a fixed condition is accompanied by an increase in a weight fraction of carbon in the deposited metal, $[C]_d$, and values of the coefficient of its transfer into the deposited metal, η_C^d. These values reach maximum in the case of use of a mixture containing 100 % SiC.

Composition of experimental self-shielded flux-cored wire for determination of reactivity of carbon in C-containing materials of the flux-cored wire core during surfacing

Core component	*Estimated composition of flux-cored wire, wt.%*														
	Series 1					*Series 2*					*Series 3*				
Electrode graphite	0	0.5	1.0	1.5	2.0	–	–	–	–	–	0	0.25	0.5	0.75	1.0
Silver graphite	–	–	–	–	–	0	0.5	1.0	1.5	2.0	–	–	–	–	–
Silicon carbide	6.7	5.0	3.3	1.6	0	6.7	5.0	3.3	1.6	0	–	–	–	–	–
Ferrochromium FKh800	–	–	–	–	–	–	–	–	–	–	12.5	9.4	6.25	3.1	0
Iron powder	10.7	11.9	13.1	14.3	15.4	4.9	7.8	10.6	13.6	16.4	10.7	11.9	13.1	14.3	15.4

Notes: 1. Flux-cored wire diameter — 2.4 mm; its filling coefficient K_a = 25 %. 2. Content of the rest of the components, wt.%: ferromanganese — 1.5; ferrosilicium — 2. 0; ferrotitanium — 2.0; aluminium powder — 0.6; marble — 1.2; silicon-fluoride sodium — 0.3; low-carbon strip 0.4 × 12 mm — 75.0.

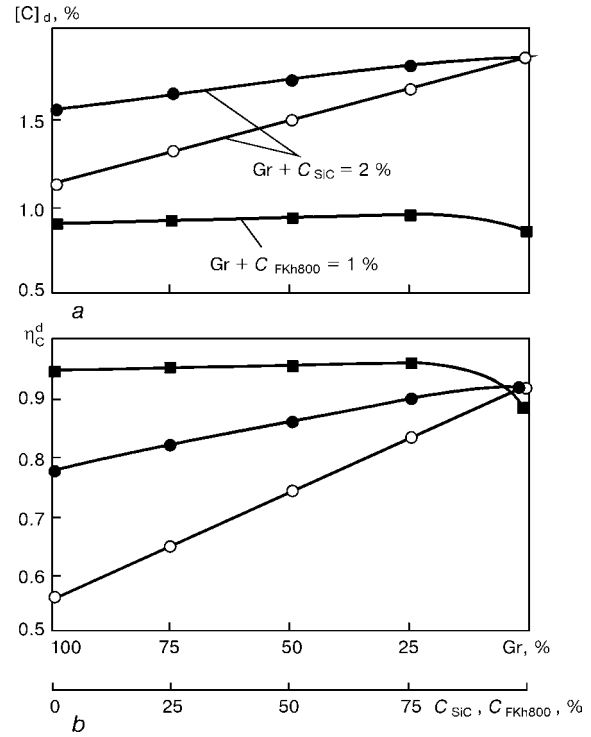

Figure 1. Effect of C-containing materials in the core of flux-cored wire on the carbon content of the deposited metal, $[C]_d$, (*a*) and on the carbon transfer coefficient, η^d_C, (*b*): ●, ■ — electrode graphite; ○ — silver graphite

Figure 2. Pictures obtained by high-speed filming of melting of flux-cored wires with a carbon fibre UN-2 content of the wire core equal to 2 (*a*) and 4 (*b*) wt.% (frequency of filming was 2200 frame/s)

Mixtures consisting of electrode graphite and carbon ferrochromium are characterized by the fact that at a selected level of the total carbon content of a flux-cored wire the Gr/C (FKh800) ratio has no effect on a weight fraction of $[C]_d$. The η^d_C values of FKh800 and SiC are almost equal to each other and do not depends upon the weight fraction of fixed carbon in mixtures of the flux-cored wire core materials. An increase in the electrode graphite content of the core from 1 to 2 % is accompanied by a decrease in the η^d_C values. This is attributable to the effect of graphite on the uniformity of melting of the flux-cored wire core and sheath.

The rates of melting of the core and sheath of a flux-cored wire containing 1 % of graphite are almost identical. The entire amount of graphite is dissolved at the stage of a droplet, and losses of carbon are caused primarily by its interaction with oxygen in the surface layer of the molten pool, and, according to the data obtained, they are not higher than 5 – 6 %.

Melting of a flux-cored wire containing 2 % of graphite is accompanied by formation of a protrusion at the core, part of graphite is transferred into the pool omitting the droplet stage. If we take into account that as a result of the oxidation reaction the carbon losses amount to 5 – 6 %, the total value of these losses caused by occurrence of the oxidation reaction and by particles of non-accommodated graphite (Figure 1) is 16 – 17 % in the case of using electrode graphite and 37 – 38 % in the case of using silver graphite.

The carbon content of droplets, $[C]_{dr}$, and molten pool, $[C]_d$, depends upon how complete the electrode droplet and C-containing core interaction is. To prove this assumption, a hydrate-cellulose carbon fibre of the UN-2 grade (90 % C) was added instead of graphite to the flux-cored wire core. Compared with electrode graphite, it has a lower wettability when wetted with a liquid metal and a close temperature of destruction of the crystalline lattice (3600 and about 4000 °C for UN-2 and graphite, respectively). It can be seen from the pictures produced by high-speed filming (Figure 2) that the UN-2 fibre becomes an independent component of the flux-cored wire core, which hardly participates in the melting process, and its interaction with liquid droplets is of an explosion-like character. Therefore, using a C-containing material in the core, which is poorly wetted by molten metal, results in low values of $[C]_d$, $[C]_{dr}$ and η^d_C. An improved wettability in the case of using electrode graphite favours a more complete accommodation of carbon both at the pool and droplet stages. A decrease in the values of the coefficients of transfer of carbon into a droplet, η^{dr}_C, and deposited metal, η^d_C, with an increase in mass fraction of graphite in a flux-cored wire is attributable to an increase in the non-uniformity of melting of a powdered core and metal sheath, which is accompanied by an increase in the length of an unmelted part of the core and frequency of its destruction.

REFERENCES

1. Krivchikov, S.Yu., Zhudra, A.P., Petrov, V.V. (1994) Modern technologies for arc surfacing of crankshafts. *Svarochnoye Proizvodstvo*, **5**, 4 – 6.
2. Ostrovsky, V.S., Virgiliev, Yu.S., Kostikov, V.I. *et al.* (1986) *Synthetic graphite*. Moscow: Metallurgia.

PECULIARITIES OF STRUCTURE OF QUASICRYSTALLINE Al–Cu–Fe SYSTEM COATINGS PRODUCED BY THERMAL SPRAYING METHODS

Yu.S. BORISOV, A.L. BORISOVA, M.T. PANKO, L.I. ADEEVA, M.V. KOLOMYTSEV, A.A. SHAKHRAJ and **V.N. SLADKOVA**
The E.O. Paton Electric Welding Institute, NASU, Kyiv, Ukraine

ABSTRACT

The effect of methods and conditions of thermal spraying on structure and phase composition of coatings of the Al–Cu–Fe system alloy powders has been investigated. It is shown that the maximum ψ-phase content of the coatings can be produced by the method of air-gas plasma spraying. In this case the thermal spray coatings inherit the multi-phase nature of initial powders. Preheating of the substrate prior to spraying allows the ψ-phase content of the coatings to be increased.

Key words: *thermal spraying, powders, coatings, structure, quasicrystalline phase, Al-Cu-Fe alloy*

As proved by numerous studies, alloys of the Al–Cu–Fe system with a quasicrystalline structure are characterized by a combination of unique properties, such as high hardness (6 – 10 GPa), capability of being elastically restored ($H/E > 0.08$) [1], decreased thermal diffusivity (0.5 mm^2/s) [2], high level of specific electrical resistance (7.8 – 10.5 μOhm·cm) [3], low specific mass (4 – 5 g/cm^3), increased corrosion resistance, low friction coefficient and high wear resistance [4, 5]. However, alloys of this system failed to find proper application in the form of products because of high brittleness and technological difficulties encountered in their fabrication, which in many cases required high cooling rates ($10^4 – 10^6$ K/s) in melt solidification. Therefore, a direction which holds more promise in terms of solving this problem is to coat products with materials with a quasicrystalline structure, primarily by the thermal spraying (TS) methods, as the latter are characterized by super high cooling rates ($10^4 – 10^6$ K/s).

It was shown in [6] that the quasicrystalline ψ-phase content of an initial powder could vary from 20 to 100 %, depending upon the technology of fabrication of the Al–Cu–Fe powders for TS (atomization of the melt with high-pressure water or compressed air, crushing of granules) and subsequent homogenizing annealing. Chemical composition of the spraying material can change during TS, which is caused primarily by evaporation of aluminium. However, the spray coatings can inherit to a certain degree (depending upon the method and technological parameters of the process) the structure of an initial powder.

Purpose of this study was to investigate the effect of methods and conditions of TS on structure and phase composition of coatings of the Al–Cu–Fe system alloy powders with a different content of the quasicrystalline ψ-phase in the initial condition.

Methods used for the fabrication of initial powders, their properties and investigation results are described in detail in [6]. Therefore, only their phase composition is given in this article (Table).

Thermal spray coatings were deposited by the methods of air-gas plasma spraying (AGPS) using the «Kyiv-7» unit, supersonic air-gas plasma spraying (SAGPS) using the «Kyiv-S» unit, flame spraying (FS) using the UGPN-5 unit and detonation spraying (DS) using the «Perun-S» unit. Coatings were sprayed on the substrate of St.3 (C — 0.14 – 0.22; Mn — 0.3 – 0.6 wt.%; Fe — balance). To activate the surface prior to deposition of coatings, the samples were subjected to abrasive-jet blasting using normal synthetic corundum of the 14A grade, in accordance with OST 2MT 793–80, with a grain size of 63 N. The TS conditions are given in the Table.

Powders with a particle size of 50 – 100 (for AGPS) and 20 – 50 μm (for DS and SAGPS) were used for TS of the coatings. To investigate the particle size effect on the coating quality, powders of four fractions with particle size from 20 to 160 μm (see Table, No.3 – 6) were used for FS.

Phase composition and structure of the coatings were investigated by metallography, microdurometry and X-ray phase analysis (XPA).

Metallography was done using the «Neophot-32» optical microscope on polished samples and samples after electrolytic etching in a reactive of the following composition: 1000 ml of 20 % aqueous solution of chromic acid, 20 ml of hydrofluoric acid and 15 ml of sulphuric acid.

Microhardness of thermal spray coatings was determined under a load of 0.49 N using the LECO instrument M-400.

Phase composition of the coatings was investigated using the DRON-UM1 diffractometer in a monochromatized radiation of CuK_α. To determine the amount of the ψ-phase, the X-ray patterns were recorded in

Conditions of thermal spraying and characteristics of thermal spray coatings of Al–Cu–Fe alloy powder

No.	Spraying method	Spraying conditions				Characteristics of powder*		Substrate temperature, °C	Characteristics of coatings			
		U, V	I, A	P_{air}, MPa	L mm	Particle size, μm	Content of ψ-phase, ($Z_ψ$), wt.%		Coating thickness, μm	HV, GPa	Phase composition	$Z_ψ$, wt.%
1	AGPS	340	180	0.24	200	80 – 100	75	20	200	5.1 – 7.7	ψ, β, traces $CuAl_2O_4$	70
2	SAGPS	300	135	0.40	180	20 – 50	70	20	280	2.5 – 4.1	β, ψ	30
3	FS	P_{oxygen} = 0.35 MPa; $P_{propane-butane}$ = 0.16 MPa; Transporting gas — air				125 – 160	75	20	650	–	β, ψ, traces λ	45
4	FS					80 – 100	75	20	650	4.2 – 5.7	ψ, β, traces λ	55
5	FS					50 – 80	70	20	1000	4.0 – 6.0	ψ, β, traces λ	60
6	FS					20 – 50	70	20	1600	–	ψ, β, traces λ	55
7	DS	Gas flow rate, m^3/h: propane-butane — 0.5; oxygen — 1.2; air — 0.4; Distance — 100 mm				20 – 50	70	20	200	2.3 – 6.1	ψ, β, traces λ, $CuAl_2O_4$	15
8	AGPS	340	180	0.24	200	80 – 100	55	20	350	4.7 – 5.1	ψ, β, traces $CuAl_2O_4$	50
9	AGPS	340	180	0.24	200	80 – 100	45	20	470	5.1 – 7.4	β, ψ, λ, traces $CuAl_2O_4$	20
10	AGPS	340	180	0.24	200	80 – 100	30	20	400	5.1 – 9.1	β, ψ, λ, traces $CuAl_2O_4$	20
11	AGPS	320	180	0.24	220	50 – 80	70	10	300	2.5 – 5.1	β, ψ, traces $CuAl_2O_4$	45
12	AGPS	320	180	0.24	220	20 – 50	55	10	300	2.4 – 4.6	β, ψ, traces $CuAl_2O_4$	20
13	AGPS	300	140	0.24	200	50 – 100	50	10	400	2.4 – 4.0	β, ψ, traces θ, $CuAl_2O_4$	25
14	SAGPS	370	180	0.40	220	20 – 50	70	10	100	2.4 – 3.8	β, ψ	30
15	SAGPS	380	180	0.40	200	20 – 50	55	10	100	3.2 – 5.7	β, ψ, traces θ	10
16	SAGPS	360	180	0.40	200	50 – 100	50	10	500	3.0 – 5.0	β, ψ, traces θ	40
17	AGPS	340	180	0.24	160	50 – 100	50	20	200	2.7 – 5.4	β, ψ, traces $CuAl_2O_4$	40
18	AGPS	340	180	0.24	160	50 – 100	50	400	200	3.0 – 6.4	ψ, β, traces $CuAl_2O_4$	55

*Initial powders with the ψ-phase content of more than 50 wt.% — two-phase (ψ + β); 30 – 50 wt.% — three-phase (β + ψ + λ); less than 30 wt.% — four-phase (β + ψ + λ + θ)

an angle range of location of the strongest diffraction maxima of the basic phases: $40° < 2\theta < 50°$ [7].

According to the constitutional diagram of the Al–Cu–Fe system, the quasicrystalline icosahedral ψ-phase ($Al_{63}Cu_{25}Fe_{12}$) can be in equilibrium with the crystalline phases. At a temperature below 900 °C, the ψ-phase, whose formation temperature is 880 °C, is in equilibrium with the monoclinic λ-phase ($Al_{73}Cu_5Fe_{22}$) and the melt. At a temperature of 800 °C the ψ-, λ- and β-phases and the liquid are in equilibrium. The cubic β-phase (Al(Fe, Cu)) has a wide range of homogeneity. At a temperature of 680 °C three crystalline phases surround the icosahedral region [8, 9]: λ-, β-phases and ordered trigonal ω-phase with a formation temperature of 700 – 720 °C; the latter corresponds to the Al_7Cu_2Fe composition. Solidification of the melt ends with the formation of a tetragonal θ-phase Al_2Cu.

The said crystalline phases can be formed both in initial powders and in structure of the thermal spray coatings in the case when their chemical composition deviates from the preset range.

The effect of the TS methods on the structure formation was investigated by applying coatings to an uncooled substrate with an initial temperature of 20 °C (see Table, No.1 – 7).

Technological conditions of plasma spraying (see Table, No.1, 2) were selected on the basis of:

- analysis of results of computer modelling of the processes of motion and heating of the dispersed $Al_{63}Cu_{25}Fe_{12}$ alloy particles in plasma jets using the CASPSP software [10];
- subsequent experimental optimization of the process parameters, at which the spraying material utilization factor tending to maximum, which characterizes the highest degree of melting, was chosen as the criterion of the process efficiency.

The produced plasma coatings have a lamellar structure, and the light lamelae are separated by oxide interlayers which are well seen on the unetched sections (Figure 1, *a, b*). In SAGPS the oxide interlayers are very thin. Therefore, the XPA method fails to detect oxide phases in these coatings. In AGPS oxidation occurs more intensively to form complex oxide $CuAl_2O_4$, the traces of which were detected by the XPA method. It should be noted that conditions of plasma spraying, optimal from the standpoint of a maximum material utilization factor, provide forma-

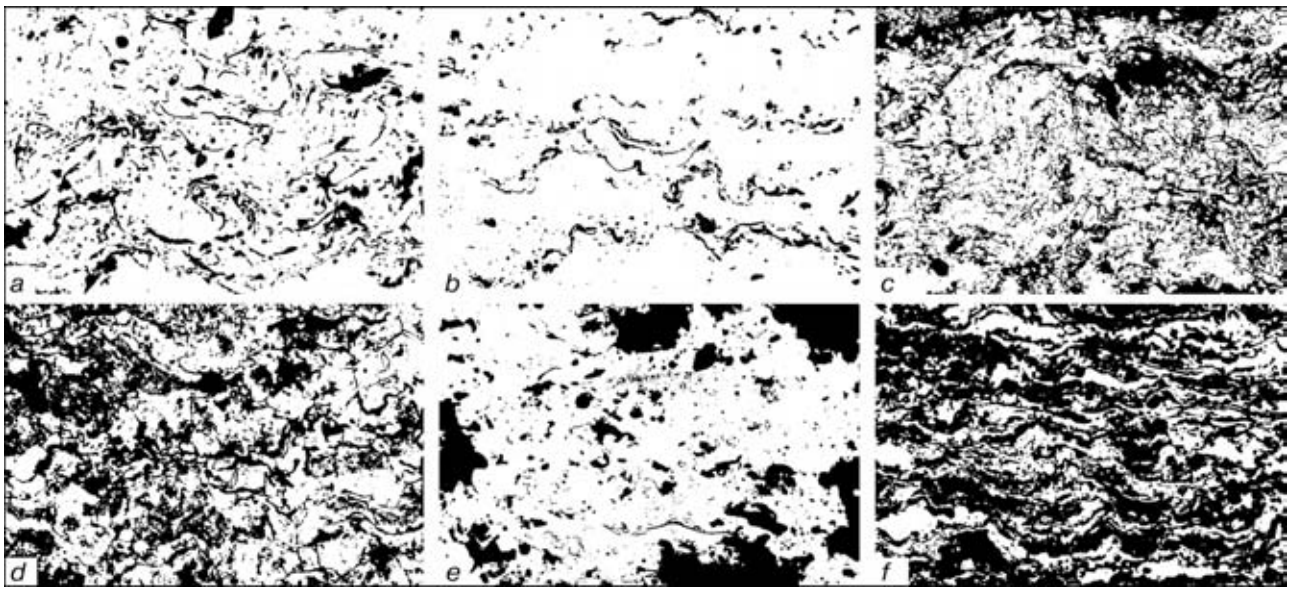

Figure 1. Microstructure of coatings deposited by the AGPS (*a, c*), SAGPS (*b, d*), FS (*e*) and DS (*f*) methods on the substrate of St.3 at a substrate temperature of 20 °C: *a, b, e, f* — unetched; *c, d* — etched (×400) (reduced by 4/5)

tion of a denser structure of the coatings with a higher degree of deformation of the sprayed layers, lower fraction of spherical particles, solidified in the jet or unmelted, and an insignificant amount of oxide interlayers.

Plasma coatings, like initial powders, contain the crystalline β- and quasicrystalline ψ-phases. The latter is revealed in the crystalline matrix in the form of hard and brittle inclusions by etching (Figure 1, *c, d*).

Despite the fact that the ψ-phase content of the initial powders differed but insignificantly (75 and 70 wt.%), in the AGPS coatings it decreased only by 7 %, whereas in the SAGPS coatings this decrease was 57 %. This difference is probably associated not so much with a difference in the spraying conditions, as with larger losses of aluminium, because powders used in the case of SAGPS have smaller particles with a larger amount of the active surface in contact with the oxidizing gas atmosphere.

Coatings produced by the FS method (see Table, No.3 – 6) were not sound, independently of the size of the powder particles. The coatings were characterized by a low cohesion strength, which led to spalling of individual particles in making a section (Figure 1, *e*). In addition to the ψ- and β-phases, the XPA method revealed in the coatings the presence of traces of the λ-phase, which was absent in the initial powder. The maximum ψ-phase content (60 wt.%) was obtained in using powders with particles 50 – 80 μm in size, which corresponded to a decrease of about 14 % in its content, as compared with the initial one. In some cases it was 20 to 40 %.

In DS (see Table, No.7) the structure formed is fine-grained with a high content of oxides, similar in structure to the SAGPS coatings but differing in a larger thickness of oxide interlayers along the boundaries of the lamelae (Figure 1, *f*). The oxide phase $CuAl_2O_4$ is clearly revealed by the XPA method, unlike the SAGPS coatings where only its traces were detected. The amount of the quasicrystalline ψ-phase in the coatings is not high (~15 %).

Therefore, investigations of the effect of the TS methods on phase composition of the Al–Cu–Fe alloy coatings proved that the maximum content of the quasicrystalline ψ-phase could be obtained by using the AGPS method.

The effect of phase composition of an initial powder on structure and phase composition of the sprayed coatings was investigated by an example of the AGPS method. The coatings were sprayed under the same conditions (see Table, No.1, 8 – 10), but powders used had different content of the quasicrystalline ψ-phase. It was found that coatings inherited the multiphase nature of the initial powders: ψ + β (see Table, No.1, 8) or β + ψ + λ (see Table, No.9, 10). In the first case the ψ-phase content of the coatings was decreased by 7 – 10 %, and in the second case it decreased by 30 – 50 %. In all the cases the XPA method revealed traces of $CuAl_2O_4$ oxides in the coatings.

A series of experiments on spraying powders on a cooled substrate by periodically feeding water onto its surface and by preheating the substrate was conducted to investigate the effect of temperature on the coating formation. The coatings were deposited on the cooled substrate by the AGPS (see Table, No.11 – 13) and SAGPS (see Table, No.14 – 16) methods using powders with a different content of the ψ-phase (70, 55 and 50 %).

It was found that an intensive cooling of the substrate led not to an increase, but on the contrary, to a decrease in the quasicrystalline ψ-phase content of the coatings. Thus, in AGPS, in the case of cooling the substrate the amount of the ψ-phase in a coating is approximately 35 % lower than in the initial powder (see Table, No.11), whereas without cooling it is only 7 % lower (see Table, No.1). The maximum decrease in the ψ-phase content (almost by 80 %) was noted in SAGPS by depositing powders with particles 20 –

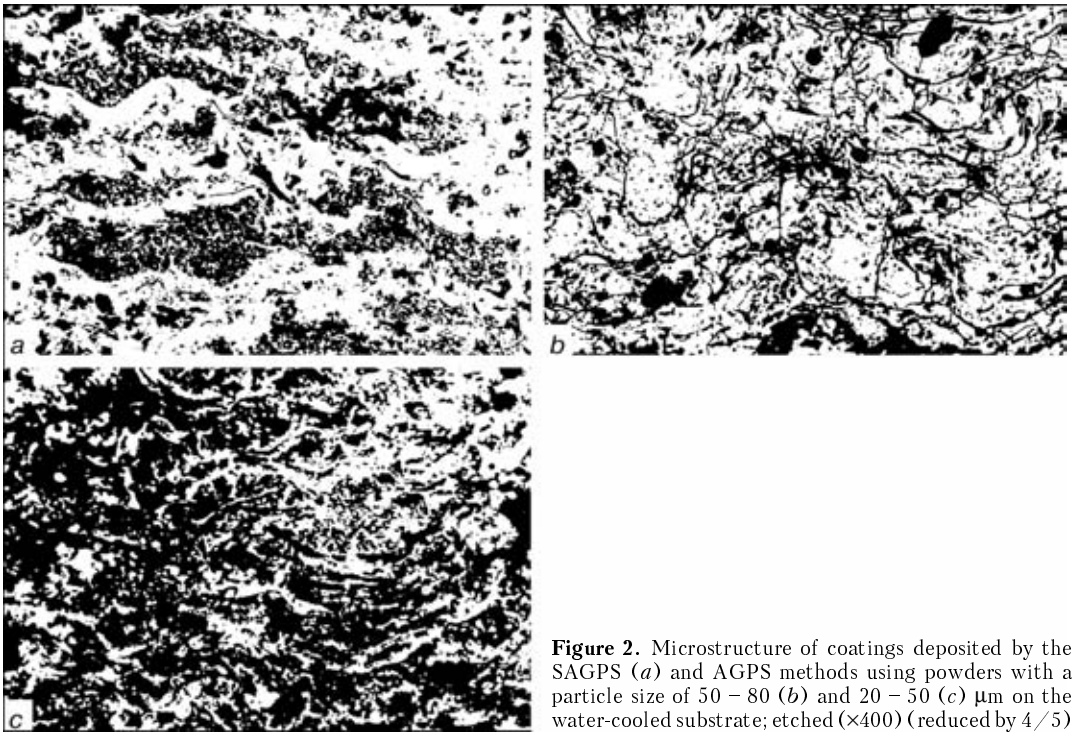

Figure 2. Microstructure of coatings deposited by the SAGPS (*a*) and AGPS methods using powders with a particle size of 50 – 80 (*b*) and 20 – 50 (*c*) μm on the water-cooled substrate; etched (×400) (reduced by 4/5)

50 μm in size on the cooled substrate (see Table, No.15). The use of powders with larger particles (50 – 100 μm) in SAGPS allows an increase in both thickness of the coating — to 500 μm (see Table, No.16), and ψ-phase content of the coating — from 10 to 40 %. It is characteristic that in this case no cracks were detected in the coatings (Figure 2, *a*).

A different picture was observed in subsonic plasma spraying. At a coating thickness of ≥ 300 μm and brittle ψ-phase content of 45 wt.% (see Table, No.11) the coating had cracks (Figure 2, *b*), although at a lower (≈ 20 %) ψ-phase content (see Table, No.12) and the same thickness the coating had no cracks (Figure 2, *c*).

Preheating of the substrate allows the ψ-phase content of the coating to be increased. In AGPS without preheating of the substrate (see Table, No.17) the ψ-phase content of the coating decreased from 50 to 40 %, as compared with the powder, whereas with preheating to 400 °C it increased from 50 to 55 % (see Table, No.18). In addition, preheating of the substrate promotes formation of a higher-quality homogeneous structure, having no pores and no cracks (Figure 3). It is highly probable that preheating of the substrate favours transformation of a metastable β-phase to a stable ψ-phase. The similar phenomenon was observed by the authors of [8] in deposition of the Al–Cu–Fe alloy coatings at a small spraying distance (76 mm), providing that the coating loosed not more than 8 at.% Al as a result of spraying.

Comparing phase composition of the initial powders and thermal spray coatings showed the following. In spraying two- (ψ + β) or three-phase (ψ + β + λ) powders the resulting coatings inherit in the main their qualitative composition. The quantitative ratio of individual phases depends mainly upon the temperature conditions of formation of the structure, and in a number of cases (e.g. in detonation spraying) — formation of oxide phases. In spraying a four-phase powder (see Table, No.10), no low-temperature θ-phase (Al_2Cu) was detected in the coating. It is very likely that it was fully oxidized to form $CuAl_2O_4$. At the same time, the θ-phase, which was absent in the initial two-phase (ψ + β) powder, is formed in a SAGPS coating deposited on a water-cooled substrate.

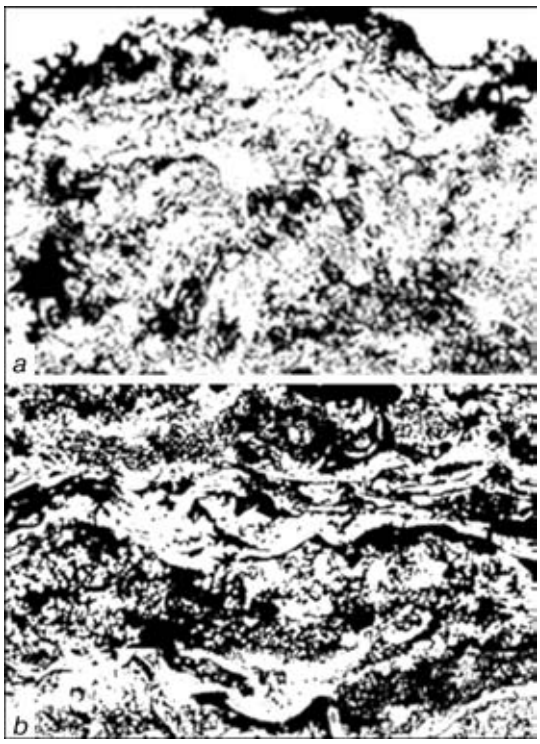

Figure 3. Microstructure of coatings deposited by the AGPS methods on the substrate of St.3 at a substrate temperature of 20 (*a*) and 400 (*b*) °C; etched (×400) (reduced by 4/5)

Hardness of the sprayed coatings is determined by their structure and phase composition. The maximum hardness was detected in plasma coatings with a high content of the ψ-phase (see Table, No.1) or λ-phase (see Table, No.9, 10), produced by the AGPS method.

Detonation coatings (see Table, No.7) exhibited a wide spread of the microhardness values, the maximum values being rather high, despite a low content (15 %) of the ψ-phase. This probably is attributable to a dense finely dispersed structure and a high oxide phase content of the coating.

CONCLUSIONS

1. Thermal spray coatings of Al–Cu–Fe alloy inherit to a considerable degree the initial powder phase composition. To produce coatings with a high content of the quasicrystalline ψ-phase, it is necessary to use powders with a dominant phase of this type.

2. The subsonic air-gas plasma spraying method, which allows formation of coatings of powders with rather large particles (80 – 100 μm), provides minimum losses of the ψ-phase in spraying. However, in this case traces of oxides emerge in the coatings. The powders used in SAGPS have smaller particles (20 – 50 μm). Therefore, losses of low-melting point aluminium and decrease in the ψ-phase content of the coating are more substantial. On the other hand, oxidation of the coating with this method hardly occurs.

3. Conditions of FS and DS used in this study did not allow coatings of a sufficiently high quality to be produced from the Al–Cu–Fe alloy. In the first case a high porosity and low cohesion strength are observed, and in the second case the coatings have a high content of oxides.

4. Preheating of the substrate to 400 °C allows an increase of 10 % in the ψ-phase content of the AGPS coatings, as compared with that of the initial powder.

REFERENCES

1. Koeaster, U., Liu, W., Liebertz, H. *et al.* (1993) Mechanical properties of quasicrystalline and crystalline phase in Al–Cu–Fe alloys. *J. of Non-Crystalline Solids*, **153, 154**, 446 – 452.
2. Dong, C., Perrot, A., Dubois, J.M. *et al.* (1994) Humerothery phase with constant e/a value and their related electronic properties in Al–Cu–Fe (–Cr) quasicrystalline systems. *Mater. Sci. Forum*. Vol. 150/151, 403 – 416.
3. Klein, T., Berger, C., Mayou, D. *et al.* (1991) Proximity of a metal-insulator transition in icosahedral phases of high structural quality. *Phys. Rev. Let.*, **22**, 2907 – 2910.
4. Dubois, J.M., Kang, S.S., Massuni, Y. (1993) Application of quasicrystalline alloys to surface coating of soft metals. *J. of Non-Crystalline Solids*, **153, 154**, 443 – 445.
5. Palo, S., Usmani, S., Sampath, S. *et al.* (1997) Friction and wear behaviour of thermal sprayed Al–Cu–Fe quasicrystal coatings. In: *Proc. of United Forum for Scientific and Technological Advances on Thermal Spray*. Ohio: Materials Park.
6. Borisov, Yu.S., Panko, M.T., Adeeva, L.I. *et al.* (2001) Production of powders of the Al–Cu–Fe system for thermal spraying of coatings with quasicrystalline structure and investigation of their properties. *Avtomaticheskaya Svarka*, **1**, 45 – 50.
7. Sordelet, D.J., Besser, M.F., Anderson, I.E. (1996) Particle size effect on chemistry and structure of Al–Cu–Fe quasicrystalline coatings. *J. of Thermal Spray Technology*, **2**, 161 – 174.
8. Sordelet, D.J., Krotz, P.D., Daniel, R.L. *et al.* (1995) Microstructure and wear behaviour of quasicrystalline thermal spray coatings. In: *Proc. of the 8th National Thermal Spray Conf.*, Sept. 11 – 15. Houston, Texas.
9. Gratias, D., Calvayrac, Y., Devaud-Rzepski, J. *et al.* (1993) The phase diagram and structures of the ternary Al–Cu–Fe system in the vicinity of the icosahedral region. *J. of Non-Crystalline Solids*, **153, 154**, 482 – 488.
10. Borisov, Yu.S., Krivtsun, I.V., Muzhichenko, A.F. (1998) Software CASPSP (Version 2.0) for simulation of the plasma spraying process. *Avtomaticheskaya Svarka*, **12**, 73.

EXPERIMENTAL EVALUATION OF THE STATE OF METAL OF LONG-SERVICED WELDED OIL PIPELINES

S.E. SEMENOV[1], A.A. RYBAKOV[1], V.I. KIRIAN[1], T.N. FILIPCHUK[1], L.V. GONCHARENKO[1], V.M. VASILYUK[2], R.V. KLIMONCHUK[2], M.V. STETSKIV[3] and F.S. VLASYUK[3]

[1]The E.O. Paton Electric Welding Institute, NASU, Kyiv, Ukraine

[2]State Joint Stock Company «Main Oil Pipelines «Druzhba», Lviv, Ukraine

[3]State Joint Stock Company «Pridneprovskiye Main Oil Pipelines», Kremenchug, Ukraine

ABSTRACT

Results of comprehensive investigations of samples of pipes cut out from oil pipelines, including hydraulic tests of a pipe section to fracture, are given. Factors of long-time force loading were found to have a low effect on mechanical properties and safety factor for ductility of materials, as well as on preservation of a high structural strength of pipelines after a long-time operation.

Key words: *pipeline, operation, material, state, ageing, investigation, hydraulic tests, mechanical properties*

Accumulation of the information on an actual state of metal of long-serviced main oil pipelines is very important for correct estimation of a risk associated with the ageing phenomena. In this connection, investigations were conducted on samples of base metal and welded joints taken from oil pipelines in operation in the territory of Ukraine. Analysis of results of the investigations is given in [1]. As other similar studies [2 – 4] give different estimates of the consequences of ageing of the pipeline materials, we think it would be appropriate to consider in more detail individual aspects of the problem investigated.

This article gives information mostly on mechanical properties of the investigated material samples. The investigation results concerning other properties of the materials will be presented in other studies.

Base metal of hot-rolled seamless and straight-welded pipes with a diameter of 377 – 720 mm, manufactured by enterprises of the former USSR, Czechoslovakia and France, as well as factory and field welded joints in these pipes were investigated. Seamless pipes were represented by samples of steel 20 (C — 0.2 wt.%; Fe — balance) (produced by ChTPZ) and 19G type (produced by a pipe plant in Czechoslovakia). Also investigated were samples cut out from hot-straightened and expanded welded pipes made by Chelyabinsk and Khartzyzsk factories, as well as by a French pipe plant, of steels of 19G (C — 0.19; Mn — 1.0 wt.%), 17GS (C — 0.17; Mn — 1.0; Si — 1.0 wt.%), 14GN (C — 0.14; Mn — 1.0; Ni — 1.0 wt.%), 14KhGS (C — 0.14; Cr — 1.0; Mn — 1.0; Si — 1.0 wt.%) grades and 16G2B (C — 0.16; Mn — 2.0; Nb — 1.0 wt.%) type. All the oil pipelines from which the samples were taken had been in operation for a long time, i.e. from 20 to more than 35 years.

Compliance of mechanical properties of metal of an oil pipeline after a long period of operation (and emergency stock pipes) with the specification requirements imposed on pipes in the initial condition and, accordingly, variations in different properties of metal under the effect of long-time service loads were evaluated.

Characteristics of pipes in the initial condition, depending upon the availability of the data, were determined from analysis of requirements of the regulatory-technical documents (RTD), statistical processing of certificates, literature data and archive materials.

The investigations conducted showed that the controlled parameters (chemical composition of steel, mechanical properties and microstructure of base metal and metal of longitudinal and circumferential field welded joints) complied with the specification requirements and differed but slightly from or were predetermined by the initial condition of metal.

The tests results showed (Figure 1) that mechanical properties of samples of the base metal of the investigated pipes made from different steel grades after a long-time operation were within the range of scatter of similar properties of the pipe metal in the initial condition (mostly within the standard deviation of $\pm\sigma$ of a given property mean value). As a rule, all the controlled parameters of the pipe metal after a long-time operation met the specification requirements. A similar conclusion can be made also for the emergency stock pipe metal subjected to natural ageing during a long shelf life. The exception were the 720 mm seamless pipes of steel of the 19G type produsedin Czechoslovakia, whose metal had decreased values of yield and tensile strength, as compared with

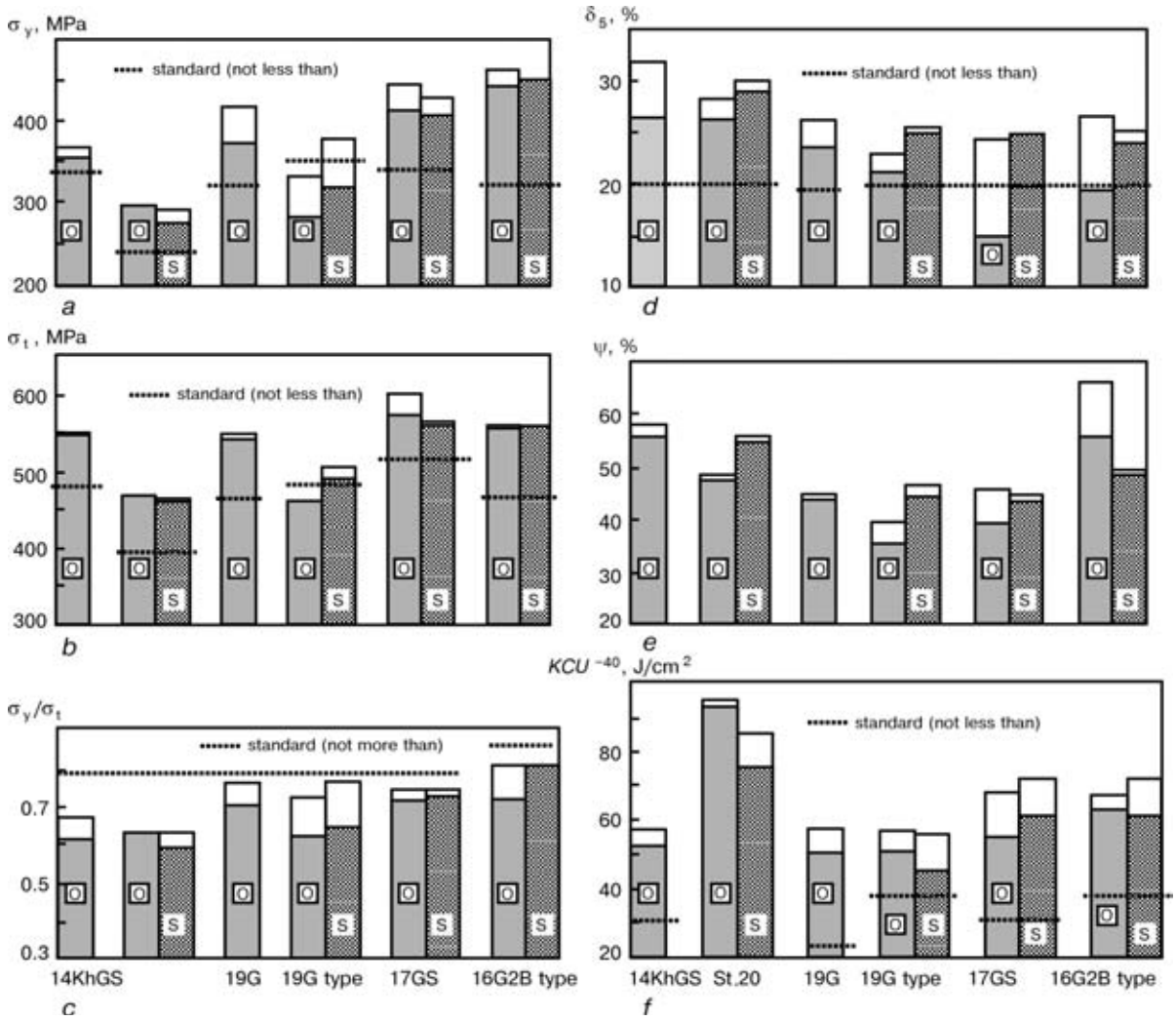

Figure 1. Mechanical properties of base metal of pipes investigated (*a* – *f*): O — pipes after operation; S — emergency stock pipes; light zone — range of scatter of values

the RTD and certificate data, as well as one of the tested welded pipes 720 mm in diameter, produced by ChTPZ from steel 17GS with a base metal elongation of less than 20 %. However, these deviations can be explained by violations in the technology of manufacture of steel, which led to formation of an abnormal structure of steel 17GS, or by insufficient basic alloying of steel of the 19G type. Besides, metal of pipes of steel of the 16G2B type had an increased ratio of σ_y/σ_t, as compared with the certificate data. It should be borne in mind that this steel was made during a period of mastering of the commercial technology of controlled rolling. Therefore, it is impossible to rule out the probability of excessive hardening of metal of individual batches during rolling with an intensive reduction in the γ–α temperature region. At the same time, issues associated with the probability of variations in mechanical properties of the pipe steel hardened by thermomechanical treatment under the effect of factors promoting ageing of the metal are worthy of a deeper insight.

Temperature dependencies of impact toughness of metal of the investigated pipe samples (Figure 2) are characterized by a gradual decrease in its value with a decrease in temperature, which is rather typical also for pipes of similar steels in the initial condition. Electron fractography of fracture surfaces revealed no signs of intergranular fracture, which could have been indicative of development of the very dangerous phenomena of metal ageing. Metal of all of the investigated welded joints, both longitudinal and circumferential, is characterized by rather high strength, ductile and tough properties (Table 1, Figure 2), which are typical in general for the welding technologies used for the manufacture of pipes and construction of pipelines.

Therefore, the data obtained are indicative of a comparatively low effect of factors of a long-time force loading or natural ageing on the oil pipeline metal.

NDT and analysis of macrosections of circumferential welded joints showed, in particular, that the weld metal contained a considerable amount of technological defects in the form of edge displacement, lack of penetration, clusters of slag inclusions and pores. However, as proved by metallography, no further development of defects under service loading took place. Nor was fixed any hardening of metal near the weld defects, which would have been indicative of an accumulation of local plastic strains.

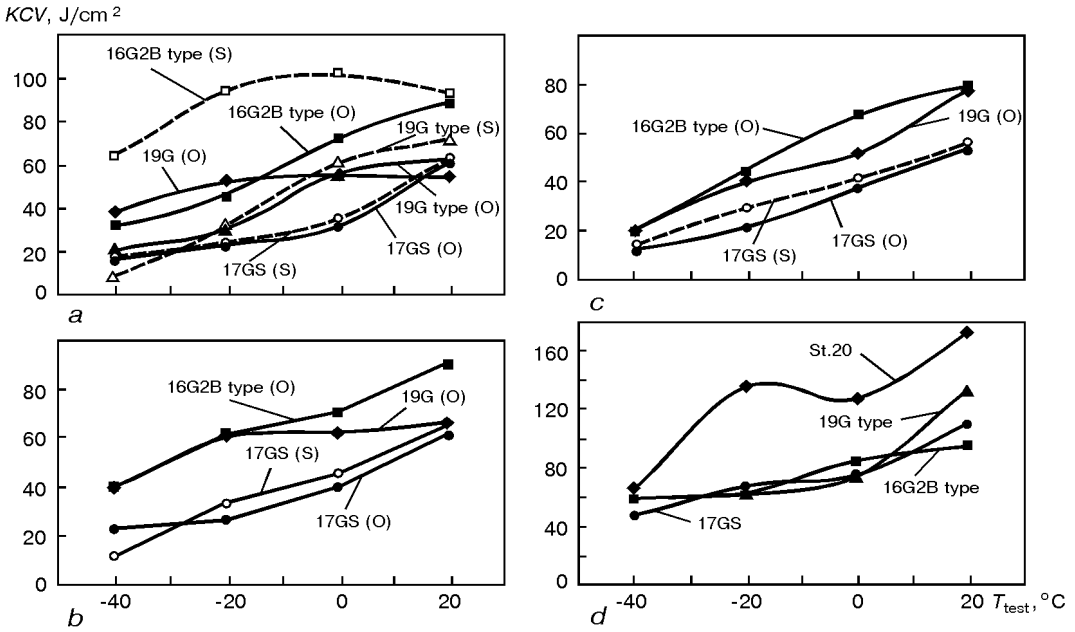

Figure 2. Impact toughness of metal of the investigated pipe samples (*a* – *c*) (*a* — base metal; *b* — weld metal, *c* — HAZ metal) and weld metal of circumferential field joints (*d*)

Therefore, during a long-time operation none of the investigated mechanical properties (σ_y, σ_t, δ_5, ψ, KCU^{-40}, KCV^0) of the oil pipeline materials underwent any substantial changes under the effect of operational loads or long-time shelf life without force loading. All the properties met the RTD requirements, whereas the deviations observed in σ_y, σ_t and δ_5 of the base metal of some pipes were caused by the corresponding peculiarities of structural characteristics of initial steels and imperfection of the technologies at the stage of their manufacture.

Of interest are the results of the hydraulic tests of samples of the pipes of steels 19G and 14GN cut out from active pipelines after a long-time operation.

During the tests the section composed of branch pipes with dents of different sizes and configurations fractured in the body of a branch pipe of steel 14GN outside the dent and weld zones under a pressure of 10.69 MPa, which was much in excess of a design working pressure in the pipeline. Under this pressure the value of stress in the branch pipe was 511.1 MPa, which corresponded to a rated tensile strength of steel. It means that, except for the fracture zone proper, the state of pre-fracture was achieved only in the fractured branch pipe of the test section. A critical strain of the pipe body by the moment of loss of plastic stability (formation of the fracture zone), as estimated by an increase in the perimeter outside the fracture zone, was ≈ 3 %, which in general was close to a similar property of pipes produced during a period under consideration.

During the hydraulic tests the metal of other branch pipes of the section was also subjected to a rather high cold plastic deformation. Investigation of properties of metal of the loaded test section provides an idea of the safety factor for serviceability of metal of the long-service pipelines. As shown by later tests (Table 2), an additional cold plastic deformation, the value of which (estimated by an increase in the pipe perimeter) was 1.24 – 2.98 %, led to a natural increase in the values of σ_y and σ_y/σ_t and some decrease in the values of δ_5 and ψ of the base metal. Thus, if the pipes after a long-time operation had the σ_y/σ_t ratio, as estimated by the mean values for different steel grades, except for steel of the 16G2B type, equal to 0.63 – 0.76, after deformation during the hydraulic tests this ratio increased to 0.83 – 0.87. Comparative values of elongation were 20.6 – 28.8 and 18.5 –

Table 1. Mechanical properties of weld metal of investigated pipes

Material tested	*Pipe size, mm, and steel grade*	σ_y, *MPa*	σ_t, *MPa*	σ_y/σ_t	δ_5, %	ψ, %	KCU^{-40}, *J/cm*^{2}
Weld metal of longitudinal factory welded joints	720 × 9, 17GS	441.2	560.8	0.78	23.0	54.0	60.4
	720 × 8, 16G2B type	523.7	652.7	0.80	26.7	63.7	74.3
	720 × 8, 19G	422.5	544.5	0.80	20.9	54.5	72.5
Weld metal of circumferential field welded joints	720 × 9, 17GS	474.7	602.5	0.78	29.0	54.2	101.7
	377 × 9, St.20	–	–	–	–	–	110.0
	720 × 8, 16G2B type	443.4	548.1	0.81	25.7	61.5	62.8
	720 × 9, 19G type	400.7	555.3	0.72	27.4	70.3	101.7
	720 × 8, 19G	383.7	541.5	0.70	22.1	61.8	50.4

Table 2. Mechanical properties of base metal of some branch pipes in a section subjected to hydraulic tests

Pipe size, mm, and steel grade	*Degree of branch pipe expansion, %*	σ_y, *MPa*	σ_t, *MPa*	σ_y/σ_t	δ_5, %	ψ, %	KCU^{-40}, *J/cm*^{2}	KCV^{20}, *J/cm*^{2}
720 × 8, 19G	1.24	430.3	515.8	0.83	20.17	44.9	84.2	79.5
	1.72	428.2	505.7	0.85	18.6	44.2	58.7	67.8
	1.98	453.3	519.6	0.86	23.6	39.9	56.7	48.0
720 × 8, 14GN	1.63	438.3	500.6	0.87	24.2	42.4	48.3	38.8
	2.98	453.3	519.6	0.87	18.5	40.6	42.3	35.0

24.2 % and those of reduction in area were 45.5 – 55.5 and 39.9 – 44.9 %, respectively.

The values of impact toughness of metal of the tested section were in excess of the specification requirements. However, there was a decrease in the level of impact toughness at «an upper shelf» of its temperature dependence. Also, as the temperature decreased, the material exhibited a more drastic tough-brittle transition.

There is a common opinion that the cast metal, which is characterized by an increased heterogeneity and non-equilibrium of the structural state, is more susceptible to ageing than the metal subjected to subsequent hot deformation or improving heat treatment. As noted above, mechanical properties of the weld metal of the investigated pipeline underwent no substantial changes under impacts of a long-time operation. In addition, extra loading with a residual strain of branch pipes had no substantial effect either on mechanical properties of the weld metal of the longitudinal welded joints in pipes (Table 3). Besides, there is a trend to hardening and increase in such properties of the weld metal as elongation and reduction in area. Nevertheless, the elongation values remain almost at a level of requirements imposed on the base metal. A relatively low reaction of the weld metal to expansion of pipes in the elasto-plastic region of loading by an internal pressure is likely to be associated with an increased local rigidity and, therefore, is caused by a lower deformation of the weld metal, as compared with the pipe body metal.

At the same time, noted was a more appreciable effect of the value of deformation of a branch pipe on a decrease in impact toughness of the HAZ metal of the longitudinal welded joints. Thus, an increase in residual strain along the perimeter of the 14GN pipe from 1.63 to 2.98 % was accompanied by a decrease of 1.5 – 2.0 times in impact toughness of the HAZ metal. Even in the state of pre-fracture of the base metal, impact toughness of the HAZ metal at a temperature of 0 °C and higher had a value of more than 40.0 J/cm^2.

The investigations conducted allow a conclusion that material of the examined pipes and welded joints after a long-time operation preserved the values of the safety factors for ductility and toughness close to the initial ones. This is rather convincingly proved by the results of the hydraulic tests and estimation on their basis of mechanical properties of the metal in the ultimate state. To achieve the pre-fracture state, it was necessary to subject the material of the long-serviced pipes to substantial cold plastic deformation, which was accompanied by a natural hardening of the metal. Supposedly, the factor of the intensity of the effects, deformational in particular, if we mean the effect of strain ageing, has the most critical importance for development of the phenomena of degradation of performance of the pipe metal.

Therefore, ensuring a long-time reliable operation of main oil pipelines, implying retention of performance of the basic load-carrying structural elements of their linear part, i.e. metal of the pipes and welded joints, is feasible. However, this requires keeping strictly to the specified loading conditions of pipelines, elimination of emergency situations that lead to overloading, intensive cyclic and other effects, which eventually can be accompanied by formation of the strained zones and fracture centres.

Table 3. Mechanical properties of weld metal of welded joints in pipes subjected to hydraulic tests

Material tested	*Pipe size, mm, and steel grade*	*Degree of branch pipe expansion, %*	σ_y, *MPa*	σ_t, *MPa*	σ_y/σ_t	δ_5, %	ψ, %	KCU^{-40}, *J/cm*^{2}
Weld metal of longitudinal welded joints	720 × 8, 19G	1.24	407.5	521.5	0.78	21.8	51.9	60.6
		1.98	419.8	536.0	0.79	20.0	49.0	62.0
		1.63	395.0	517.8	0.77	21.8	53.0	66.6
		2.98	420.3	537.0	0.79	20.0	50.9	70.8
Weld metal of field circumferential welded joints	720 × 8, 19G	1.98	497.3	577.7	0.83	19.3	54.4	59.6

Also, it is important to bear in mind that the probable pre-service intensive technological conditions may have a dangerous effect on a material, which is characteristic mostly of the local zones of shape distortions, surface dents, expansion, deviations from the specified welding conditions, etc. As was noted in [1], of special importance for ensuring the reliable operation of pipelines is prevention of formation, timely detection and repair of various dangerous defects and damages, within the zones of which the considerable changes in a material, leading to fracture, might occur under the affect of applied loads and aggressive environments.

The results obtained are of a certain interest also from the standpoint of the methodology used for evaluation of the state of a material of active pipelines. The appropriate evaluation criteria are required to trace a decrease in performance or occurrence of the pre-accident situations. Characteristics of fracture resistance, including indicators of crack resistance, are considered the most reliable of the above criteria. The useful information can also be derived in the course of investigation of deformational (geometrical) and structural characteristics, behaviour of defects, etc. The results of tests of standard mechanical properties, estimated in terms of their correspondence to specification requirements, should be treated with a certain care.

Investigations of the pipe metal after the hydraulic tests indicate that the low threshold design levels of impact toughness (this is especially typical for pipes with a nominal diameter of up to 1000 mm) do not allow a satisfactory state of the pipe metal after a long-time operation to be reliably guaranteed. Additional investigations are required for detection of the actual metal state.

REFERENCES

1. Paton, B.E., Semenov, S.E., Rybakov, A.A. *et al.* (2000) Ageing and methodology of evaluation of the state of metal of active main pipelines. *Avtomaticheskaya Svarka*, **7**, 3 – 12.
2. Pashkov, Yu.I., Anisimov, Yu.I., Lanchakov, G.A. *et al.* (1996) Prediction of the residual strength of main gas and oil pipelines, allowing for the time of their operation. *Stroitelstvo Truboprovodov*, **2**, 2 – 5.
3. Lanchakov, G.A., Stepanenko, A.I., Pashkov, Yu.I. (1994) Effect of time of operation on residual strength of pipelines. *Gaz. Promyshlennost*, **3**, 11 – 12.
4. Gumerov, A.G., Zajnulin, R.S., Yamaleev, K.N. *et al.* (1995) *Ageing of pipes in oil pipelines*. Moscow: Nedra.

DEVELOPMENT OF MATERIALS AND TECHNOLOGY OF MANUFACTURE OF SINGLE-ROLLER SUPPORTING MEMBERS OF BRIDGES USING SURFACING

V.K. KALENSKY, V.I. DVORETSKY, V.M. BUGA and **A.V. SEMENIKHIN**
The E.O. Paton Electric Welding Institute, NASU, Kyiv, Ukraine

ABSTRACT

The flux-cored wires have been developed for submerged arc surfacing of working surfaces of rollers and plates of single-roller supporting members (SRSM) of bridges with a layer of high-strength steel of the 30Kh13MN grade, which is resistant to the atmospheric corrosion. The technology of manufacture of SRSM using surfacing allows their life to be extended 3 times to make it equal to the life of the bridge. Plants of the E.O. Paton Electric Welding Institute are manufacturing SRSM on the commercial scale.

Key words: *surfacing, materials, bridges, single-roller supporting members, corrosion-resistant high-strength contact surfaces, technology, manufacturing*

In accordance with the data of domestic and foreign statistics, the average service life of the bridges is about 100 years, while that of their supporting members (SM) does not exceed 30 years. The latter had to be replaced not less than 3 times that is expensive and very labour-consuming operation taking into account the large mass of the bridge spans.

Until now, in construction of large-span bridges the multi-roller SM were used mainly, for which a coefficient of rolling friction, technological strength, hardness and corrosion resistance of contact surfaces were not guaranteed. During long-time service the mode of span supporting on the SM changed, the movable SM jammed, the design configuration of the construction changed and defects appeared on the supporting members and in spans.

The single-roller supporting members (SRSM) consisting of two supporting plates and a roller between them are simplest in design and most advanced by functionality (Figure 1). However, the application of SRSM in CIS was limited due to a low load-bearing capacity of carbon and low-alloyed steels recommended by SNiP 2.05.03–84 for their manufacture.

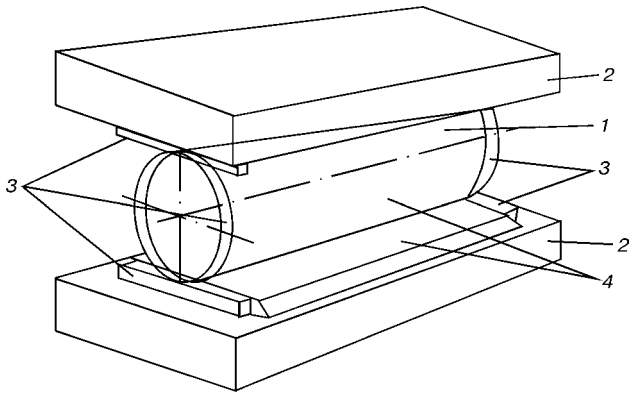

Figure 1. Sketch of SRSM: *1* — roller; *2* — supporting plates; *3* — rest devices; *4* — working rolling surfaces

The present development is based on the idea of producing working contact surfaces of SRSM using surfacing with a high-strength steel which provides high values of hardness and possesses a sufficient resistance to the atmospheric corrosion. Use of these SRSM, characterized by a high reliability, low coefficient of friction, low metal consumption and minimum-possible overall height, will make it possible to increase their service life almost by 3 times and to level it with the term of the bridge service.

This idea was first realized in Germany where the prefabrications of SRSM rollers and plates made from the low-carbon steel were subjected to surfacing in argon with electrode wires containing 12 – 17 % Cr [1].

When developing the domestic variant of the technology, it was decided to manufacture the SRSM prefabrications from steel 09G2S (C — 0.09 – 0.1; Mn — 1.5; Si — 0.4 wt.%), and to perform submerged arc surfacing with chromium steel flux-cored wires in 2 layers: ductile (intermediate) and high-strength (working).

To reduce to minimum the burning out of the alloying elements during surfacing, a low-active low-silicon flux AN-72 (SiO_2 — 16 – 18; CaO — 18 – 20; Al_2O_3 — 18 – 23; CaF_2 — 40 – 45 wt.%) was used [2], providing a good formation of deposited beads and excellent removal of the slag crust. Experiments on surfacing were performed in the A-874N type machine with an independent feeding of wire at DCRP. The power source with a rigid external characteristic was used. The surfacing conditions were as follows: $I = 300 – 380$ A, $U = 30 – 32$ V, $v_s = 30$ m/h.

The intermediate layer was deposited in 3 passes with an experimental flux-cored wire 07Kh15 (C — 0.7; Cr — 15.0 wt.%; Fe — balance) on the narrow faces of the plates of $90 \times 300 \times 400$ mm size, heated to 280 °C. Hardness of the deposited metal was *HRC* 25, and the impact strength — 27 J/cm^2.

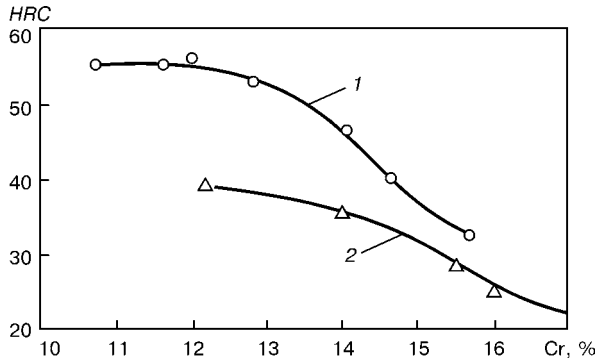

Figure 2. Effect of chromium on hardness of steels: *1* — deposited metal (0.3 % C); *2* — hardened rolled metal (0.1 % C)

The task was to develop the flux-cored wire for surfacing of the corrosion-resistant layer having a high hardness (*HRC* 48 – 52) and strength (σ_y = 1200 – 1500 MPa). These characteristics are provided by martensitic chromium steels, subjected to the air hardening [3, 4]. To specify the nature of chromium and carbon effect on the hardness of the deposited metal a series of experimental flux-cored wires with 11 – 16 % Cr and 0.1 – 0.4 % C was manufactured and used for surfacing. From the results of hardness measurements (Figures 2 and 3) the deposited metal of the 30Kh13 (C — 0.3; Cr — 13.0 wt.%; Fe — balance) type was taken as a base for the working layer composition.

Steels of this type are susceptible to crack formation during hardening, welding and surfacing [5, 6]. Therefore, the chemical composition of the working layer was optimized using the method of a mathematical planning of experiment, during which two its criteria were evaluated: hardness and crack resistance. The flux-cored wires were manufactured providing the deposited metal within the ranges of compositions, which were preset in the plan, %: C — 0.15 – 0.30; Cr — 11 – 15; Ni — 0.2 – 0.5; Ti — 0 – 0.2 at Mn — 0.45; Si — 0.5; Mo — 1.0.

To determine hardness and crack resistance, the beads were deposited by 2 passes in width and 5 passes in height on the 07Kh15 steel intermediate layer on the narrow faces of the above-mentioned plates. The crack resistance was evaluated by 12-point scale system visually (depending on the quantity and length of cracks). As a result of searching of the optimum composition a global extremum of composition of the deposited metal was obtained in the computer, containing, %: C — 0.24; Cr — 12.5; Ni — 0.35; Ti — 0.018 at Mn — 0.45; Si — 0.5; Mo — 1.0 and providing hardness of approximately *HRC* 50 at a complete absence of the cracks. The obtained data helped to develop the flux-cored wire of PP-AN 165 (PP-Np-30Kh13MN) grade, providing deposited metal whose composition is close to optimum. The wire for surfacing of the intermediate (buffering) layer was designated PP-AN 166 (PP-Np-07Kh15). The mentioned wires were manufactured and used for the next experiments.

Table 1. Mechanical properties of 30Kh13MN deposited metal depending on the tempering temperature

Tempering temperature, °C	*Impact strength, J/cm²*	*Yield strength, MPa*	*Ultimate strength, MPa*	*Elongation, %*	*Reduction in area, %*	*Hardness HRC of upper layer*
300	17	1292	1397	2.6	5.9	48
350	30	1301	1336	5.3	23.3	48
400	41	1364	1463	5.8	16.0	49
490	12	1186	1366	4.0	8.0	49

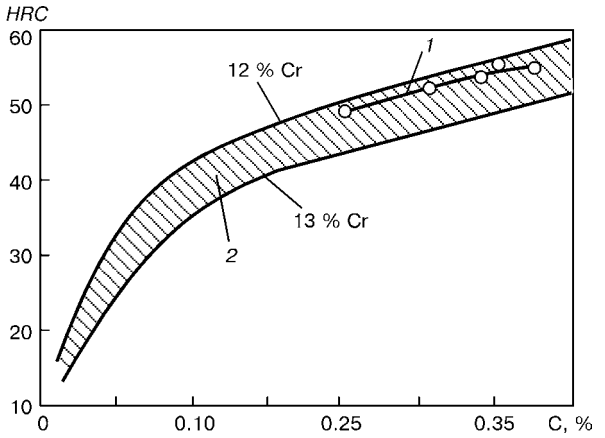

Figure 3. Effect of carbon on hardness of chromium steels: *1* — deposited metal; *2* — hardened rolled metal

The surfacing was made at the mentioned conditions by 6 passes (with three wires of PP-Np-07Kh15 grade and PP-Np-30Kh13MN grade) using the flux AN-72. Samples for examinations were cut from the working layer. The chemical composition of the working layer was the following, %: C — 0.26; Si — 0.59; Mn — 0.46; Cr — 12.53; Ni — 0.52; Mo — 0.81; Ti — 0.015; S — 0.016; P — 0.018.

The part of samples was subjected to tempering within the range of 250 – 650 °C temperatures. The tempering duration was 1 h, furnace cooling. Results of hardness measurement of tempered samples are given in Figure 4, which shows that the deposited metal is characterized by an increased stability to the hardness decrease. At 500 °C a little secondary increase in hardness was observed due to precipitation of special carbides. For comparison the hardness of a

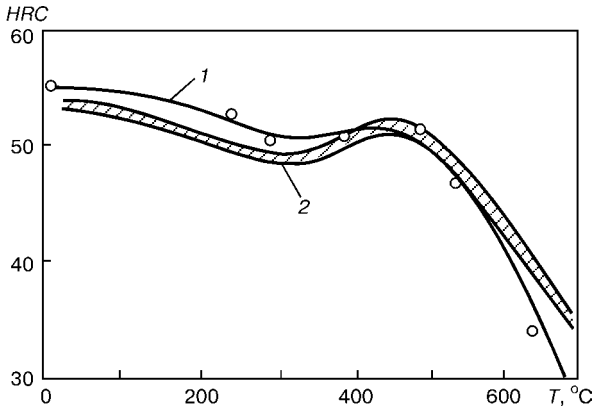

Figure 4. Effect of tempering temperature on hardness of chromium steels: *1* — deposited metal 30Kh13MN; *2* — rolled metal of steel 30Kh13

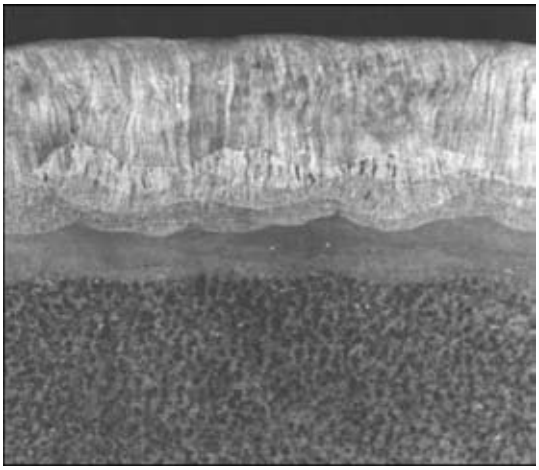

Figure 5. Macrostructure of deposited sample

rolled steel close by the composition is shown in the diagram.

The results of mechanical tests of the working layer metal are given in Table 1. It follows from the Table that the best characteristics of hardness, impact strength, strength and ductility are attained in the deposited metal after tempering at 400 °C.

Figure 5 shows a macrosection of the deposited sample. Structure of metal, especially three upper passes, has a clearly expressed transcrystalline nature. No defects were revealed in the metal of the deposited layer and HAZ. Distribution of hardness across the thickness of the deposited layer is shown in Table 2.

Microstructure of the deposited metal is given in Figure 6. The fusion zone of the deposited metal 07Kh15 with parent metal (Figure 6, *a*) is characterized by the increased etching due to clustering of fine-dispersed carbides in it, forming a carbide row along the fusion boundary. From the side of the parent metal a decarburized band of ferrite is adjacent to the boundary, and below, a fine-grained ferritic-pearlitic structure is seen. The structure of the deposited metal 07Kh15 at the fusion boundary is ferritic with fine-dispersed precipitations of the chromium carbide.

Table 2. Hardness *HRC* of deposited metal

Deposited metal	*Distance from surface, mm*	*As-deposited state*	*After tempering at 400 °C*
30Kh13MN	1	50	50
	2	50	50
	3	51	49
	4	49	49
	5	48	48
	6	45	45
	7	45	44
Fusion zone	8	37	37
	9	30	30
	10	28	26
07Kh15	11	27	26
	12	26	25

Figure 6, *b* shows the fusion boundary of deposited metals 07Kh15 and 30Kh13MN. Structure 07Kh15 (at the bottom) consists of a ferritic matrix with dispersed chromium carbides and feathered precipitations of sorbite, while structure 30Kh13MN (top) consists of a tempered martensite, δ-ferrite and dispersed precipitations of carbides.

In the second and third passes of the deposited metal 30Kh13MN (Figure 6, *c*) the number of δ-ferrite regions is decreased, and the content of martensite is increased. The maximum microhardness (*HV* 0.5 – 4410 MPa) is typical of the upper layer of the deposit.

The resistance of the deposited metal 30Kh13MN to the general corrosion in atmospheric conditions was evaluated in comparison with the resistance of rolled metal of steels 20Kh13 (C — 0.2; Cr — 13.0 wt.%; Fe — balance), 40Kh13 (C — 0.4; Cr — 13.0 wt.%; Fe — balance) and steel 45 (C — 0.45 wt.%; Fe — balance)*. For examination, the samples of 2 × 10 × × 60 mm size were suspended in chambers of a salt fog (aerosol of 3 % solution of NaCl in water), in-

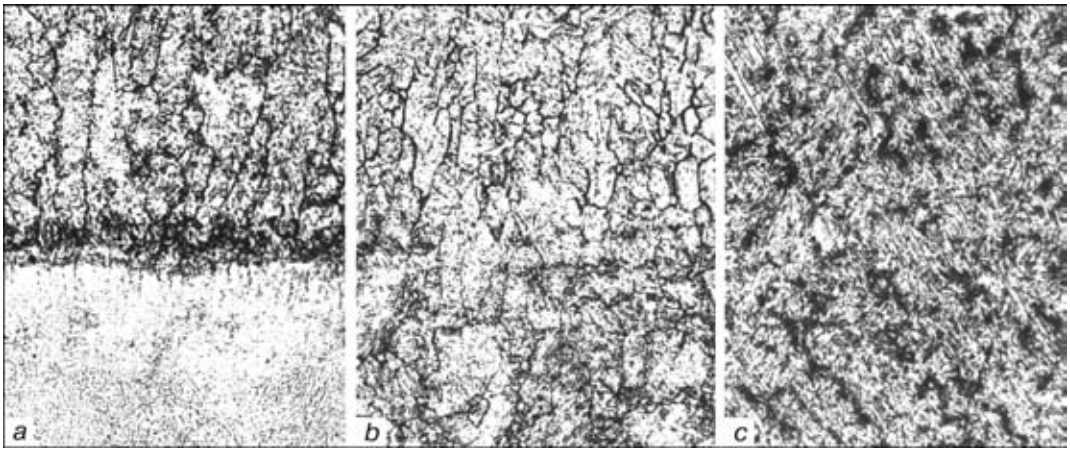

Figure 6. Microstructure of deposited sample: *a* — fusion boundary with parent metal (×200); *b* — fusion boundary of 07Kh15 and 30Kh13MN (×200); *c* — deposited metal 30Kh13MN (×400) (reduced by 4/5)

* Work on study of the corrosion resistance of the deposited metal was performed by G.E. Boeva, E.P. Los, V.A. Gorban.

Table 3. Rate of general corrosion of samples, mm/year

Metal examined	*In chamber of salt fog*	*In chamber of humidity*	*In chamber of SO_2*
30Kh13MN	0.033	0.0015	0.0011
20Kh13	0.348	0.0078	0.0168
40Kh13	0.200	0.0075	0.0165
St.45	1.280	0.2860	0.4300

creased humidity and with a sulphur dioxide. Tests were performed daily during 1000 h at temperature 35 – 40 °C with a change of medium each 15 days. It follows from Table 3 that the deposited metal 30Kh13MN in all three chambers was subjected to corrosion much slower than others. In accordance with the 10-point scale of the corrosion resistance (GOST 13819–86) the deposited metal can refer to the «very resistant».

To evaluate the probability of proceeding the electrochemical corrosion in the fusion zone of the deposited metal with the parent metal, the potentials of these metals were measured using the method of an accelerated determination of the electrochemical heterogeneity of metal under the drop of eletrolyte from the 3 % solution of NaCl [7]. The potentials were measured on the $3 \times 10 \times 60$ mm samples, cut normal to the surface deposited. The results of measurements are presented in Table 4. For comparison it has also the corrosion potential of steel 08Kh18N10T.

It is seen from the Table that the difference in potentials of metals 09G2S and 07Kh15 is –210 mV, and 09G2S and 30Kh13MN is –190 mV. In case of formation of defects in the zone of fusion this difference can become a cause of a progressing corrosion. Therefore, the zones of fusion of the parent and deposited metals should be covered with durable inhibitors.

The determination of deposited metal 30Kh13MN susceptibility to corrosion cracking was performed in a wheel of alternating wetting in 3 % solution of NaCl according to GOST 26294–84. Samples of $2 \times 10 \times \times 120$ mm size, cut from the upper layer, deposited at optimum condition and tempered at 300, 350, 400 and 490 °C, were tested. They were fixed in cramps and loaded in four points with a force of 5.0 and 7.5 kN. The test results are given in Table 5. It follows from the Table that the good characteristics are provided at the 400 °C tempering temperature.

Thus, the investigations carried out confirmed the correct selection of surfacing materials, surfacing conditions and heat treatment.

Table 4. Values of corrosion potentials of deposited and parent metals

Metal examined	*Value of potential E_c, mV*
09G2S	–580
07Kh15	–370
30Kh13MN	–390
08Kh18N10T	–240

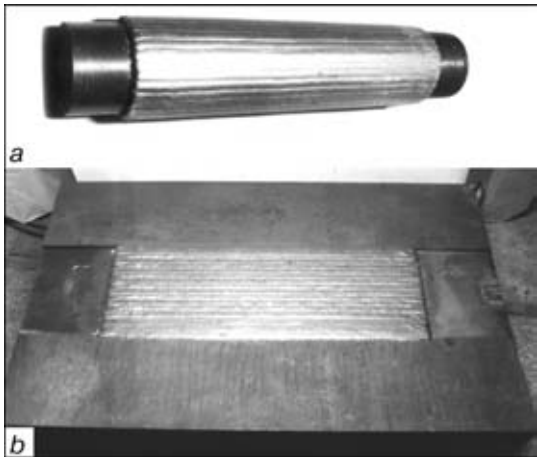

Figure 7. Prefabrication of SRSM after surfacing: *a* — roller of 212 mm diameter; *b* — plate

Technological diagram of manufacture of SRSM rollers and plates is as follows.

The preliminary machined prefabrications of rollers and plates, whose sizes depend on the loading on SRSM are heated to 200 – 220 °C. The intermediate layer is deposited with wire PP-Np-07Kh15 using flux AN-72 in 2 or 3 passes along the height with longitudinal beads at a shuttle displacement of the welding head. To deposit the working layer the prefabrications are heated to 250 – 300 °C. The surfacing is made, as a rule, in 3 passes along the height with wire PP-Np-30Kh13MN. The surfacing conditions were abovementioned.

Then, the prefabrications are subjected to tempering at 390 – 410 °C for 1 h with a furnace cooling. After cooling to 200 °C, they can be subjected to the air cooling.

As-deposited and tempered prefabrications for manufacture of SRSM at vertical loading 13 kN are shown in Figure 7.

Then, the machining is performed according to the drawing. The thickness of the deposited layer after machining should be not less than $0.1R - 2.0$ mm (R — roller radius).

The quality control is made after polishing the deposited surfaces of the rollers and plates using the methods of ultrasonic and magnetic particle flaw detection. Cracks are not admitted. The presence of pores and slag inclusions should not exceed the standards.

Table 5. Resistance of the deposited metal to corrosion cracking after tempering

Temperature of tempering, °C	*Loading, kN*	*Time before fracture, h*
300	5.0	595.0
	7.5	14.5
350	5.0	>1000.0
	7.5	>1000.0
400	5.0	>1000.0
	7.5	>1000.0
400	5.0	>1000.0
	7.5	860.0

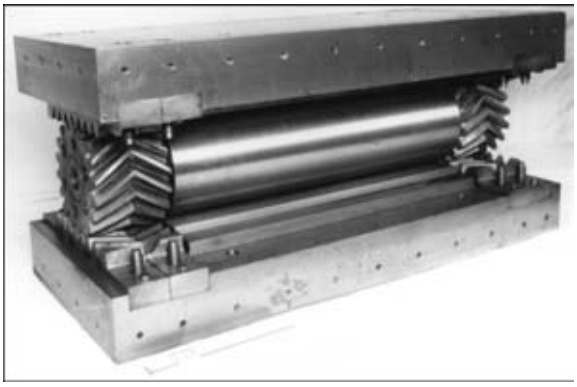

Figure 8. One of ready SRSM mounted in spans of the bridge across the Ural river

The ready surfaced rollers and plates are considered quality if the hardness of contact surfaces is *HRC* 48 – 53, and at the depth of 0.04*R* from the contact surfaces it is not less than *HRC* 45.

To test the developed materials, technology and structures the experimental SRSM with 90 mm diameter roller were manufactured. They were mounted into a span of the experimental grounds of Research Institute of Railway Transport for testing. A systematic inspection did not show any defects that confirmed the right technical solution of the problem and made it possible to start the SRSM manufacture with roller diameters of 212 – 250 mm.

The single-roller supporting members with deposited working surfaces were manufactured and mounted to the spans of the following objects:

- South Bridge transition across the Dnieper river in Kyiv;
- road bridge across the Chusovaya river in Perm;
- first two bridges across the Malaya and Bolshaya Kayukovka river of the bridge transition across the Bolshaya Volga in Saratov;
- road bridge across the Ural river in Uralsk (Figure 8).

At present the manufacture of SRSM is organized at the enterprises of the E.O. Paton Electric Welding Institute of NAS of Ukraine.

REFERENCES

1. Packeiser, W. (1973) Auftragschweissen von Brüackenlagern mit Chromstahl. *Industrie-Anzeiger*, **23**, 452 – 482.
2. Buga, V.M. (1980) Low-silicon flux for arc and electroslag surfacing. *Avtomaticheskaya Svarka*, **6**, 58 – 61.
3. Gudremon, E. (1959) *Special steels*. Moscow: Metallurgizdat.
4. Gulyaev, A.A. (1963) *Metals science*. Moscow: Oborongiz.
5. Kakhovsky, N.I. (1975) *Welding of high-alloyed steels*. Kyiv: Tekhnika.
6. Frumin, I.I. (1961) *Automatic electric arc surfacing*. Kharkov: Metallurgizdat.
7. Evans, Yu.R. (1962) *Corrosion and oxidation of metals*. Moscow: Mashgiz.

PULSED WIRE FEED MECHANISMS WITH PULSE PARAMETER CONTROL

V.A. LEBEDEV, V.G. PICHAK and **V.B. SMOLYARKO**
The E.O.Paton Electric Welding Institute, NASU, Kyiv, Ukraine

ABSTRACT

The paper analyses the features of design of pulsed wire feed mechanisms based on quasi-wave converters. It is shown that the maximal acceleration voltage achieved in the pulse can be essentially increased by cascade connection of several modulators or by changing the modulating pulse frequency. Conditions are determined under which the mechanism designs will be optimal in terms of both their manufacture and adjustment of the output parameters. The main principles of designing new types of pulsed feed mechanisms are defined that allow for the features of their mounting in the mechanised arc welding equipment.

Key words: *mechanised arc welding, surfacing, metal transfer, pulsed control, spatter, weld formation, feed mechanism, motion pulse, pulse parameters, motion conversion, design*

Mechanised processes of consumable electrode arc welding and surfacing, conducted in shielding gases using self-shielding flux-cored electrode wires, still remain to be the main processes in welding production, as well as in reconditioning and strengthening of components and parts. In this connection, their improvement is an urgent problem. The approaches used to solve the problem can be different and can be based on application of new materials, shielding atmospheres, as well as new methods of controlling the electrode metal transfer.

Control of electrode metal transfer is one of the most effective methods for improvement of mechanised arc welding processes, that can be implemented with the use of a pulsed impact of the arc power source and pulsed feed of the electrode wire. It should be noted that application of controlled pulsed feed of the electrode wire, carried out with special mechanisms, is simpler in technical terms, than when a pulsed arc source is used. This allows a considerable lowering of the levels of electrode metal spatter, widening the range of thicknesses of the welded or surfaced metal, as well as controlling weld formation, weld and HAZ metal quality. The main problem to be solved, is selection of a mechanism of rational design, having certain technical and technological capabilities. One of the most perfect mechanisms of this type, is the mechanism with conversion of the rotary motion of the driving electric motor shaft into pulsed rotation of the feed rollers, namely mechanism with a quasi-wave converter (QWC). This mechanism, unlike the earlier described ones [1], including those with one-sided grips, has a sufficient operating life, as well as specific features in formation of pulses with certain parameters that provide an accelerated motion of the electrode wire in the pulse for a forced transfer of the electrode metal drops into the pool.

However, the earlier considered designs of pulsed wire feed mechanisms of this type, have certain limitations as regards formation of pulses with specified parameters, related to the engineering solutions used in these mechanisms. A number of modifications of the pulsed feed mechanisms with QWC have been developed, manufactured and tested recently, that allow an essential expansion of their technical and technological capabilities for use in the mechanised arc welding equipment.

The aim of this paper is to consider new modifications of pulsed feed mechanisms based on QWC with pulse parameter control for further improvement of the mechanised arc welding and surfacing processes by providing a forced transfer of the electrode metal without any further technological cost.

Study [2] describes the design of a mechanism for pulsed feed of the electrode wire with QWC application, where the speed of pulsed rotation of feed roller ω_r is determined in the form of

$$\omega_r = \left[-\frac{e}{R} \pm \frac{e}{b} \frac{\cos(\varphi_1 - \alpha)}{\cos \alpha} \right] \omega_1, \qquad (1)$$

where e is the eccentricity; R is the radius of the central gear; b is the support lever length; α is the angle of inclination of the support plane; φ_1 is the current value of the angle of rotation of the eccentric; ω_1 is the frequency of rotation of the driving motor shaft.

Integrating expression (1), with the known value of the feed roller diameter D_r, it is possible to obtain the value of acceleration of the electrode wire movement in the feed pulse a_e in the following form:

$$a_e = \frac{D_r}{2} \left[\frac{e \sin(\varphi_1 - \alpha)}{b \cos \alpha} \right] \omega_1^2. \qquad (2)$$

Analysis of expressions (1) and (2) shows that the feed pulse shape can be adjusted by varying the values b and α with predesigned e, R parameters of the mechanism. The frequency of feed pulses in the considered mechanism is dependent on ω_1 parameter and its maximal level is determined by the certificate

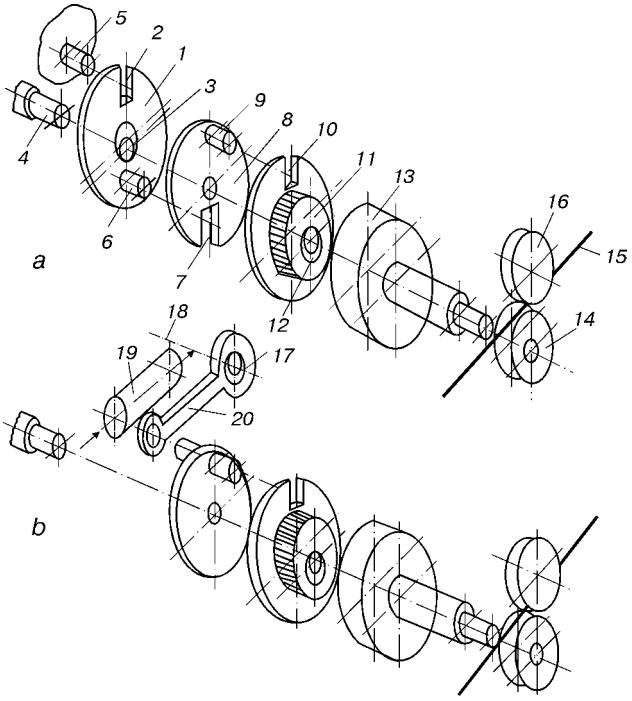

Figure 1. Pulsed wire feed mechanism based on QWC with two modulators, having the same (*a*) and different (*b*) rotation frequencies

nominal value of the rotation frequency of the driving motor shaft.

The experience of practical design and use of the pulsed wire feed mechanisms based on QWC, shows that there exist certain boundary conditions for selection of the parameters of the structural elements, as well as the conditions under which this mechanism can still be regarded as simple enough for fabrication and regulation of the parameters of the feed roller pulsed rotation.

Let us consider these conditions. First of all, note that eccentricity e and radius R of the central gear practically cannot be made adjustable. They are assigned proceeding from considerations of providing the required values of integral rate of electrode wire feed, as e/R ratio determines the gear ratio of the mechanism as a whole. In addition, the designers try to make the eccentricity minimal, that is determined by the conditions of providing minimal vibrations of the mechanism, dependent both on e value and weight-size characteristics of the satellite gear.

Length b of the lever can be designed to be adjustable, as this adjustment is not required to be performed during operation. Fine adjustment of length b can be performed after the first attempts at welding in the required modes with a certain hose holder.

Design of the regulator of angle of inclination α of the support plane is an engineering challenge. After a number of attempts at developing such a regulator with an acceptable adjustment range, we came to the conclusion that the most rational solution for the regulator design, is selection of a certain fixed value of the angle of inclination α, that cannot be greater than 45° by the conditions of functioning of the considered mechanism. The above adjustments present the entire capabilities of the above mechanisms based on QWC. In a number of cases, for instance, CO_2 welding with a long arc, overhead welding, use of long flexible guides (2 – 3 m), these adjustments can be insufficient to provide the acceleration of the electrode metal drop of a specified weight (size) to ensure its forced transfer into the pool.

Therefore, a search for and development of several new variants of pulsed wire feed mechanisms, based on QWC, have been performed.

The mechanical diagram of a new modification of pulsed wire feed mechanism with QWC and expanded capabilities for adjustment of the parameters of the above pulses, is given in Figure 1, *a*. Let us consider a variant of the mechanism design. First washer *1* with slot *2* is mounted on first eccentric *3*. In rotation of the shaft of motor *4*, slot *2* of washer *1* interacts with pin *5*, that is rigidly connected to the mechanism case. Washer *1* further contains pin *6*, interacting with slot *7*, made in additional washer *8*, mounted on the shaft of motor *4* with the capability of rotation about this axis. Additional washer *8* has one more pin *9*, interacting with slot *10*, made in the central (inner) gear *11*, that is mounted on eccentric *12* and transfers the torque to outer gear *13*. The latter is rigidly connected to feed roller *14*. Electrode wire is designated by number *15*, and press-down roller — by number *16*.

This mechanism operates as follows. When the shaft of motor *4* rotates, first eccentric *3* also starts turning, and first washer *1*, mounted on the bearing of the above eccentric and connected to the mechanism case by pin *5* and slot *2*, is imparted a certain angular displacement, the extent of which is dependent on eccentricity of eccentric *3* and radial distance of pin *5* relative to the path, described by eccentric *3* in its rotation. This angular displacement through pin *6*, mounted on washer *1*, is transferred to additional washer *8* by interaction of the above pin with slot *7*. Washer *8* rotates on the part of the motor axle that has no eccentric. Pin *9* of additional washer *8* enters the slot of inner gear *11* and also makes this inner gear turn through a certain angle. Considering that the inner gear is installed on a bearing, mounted on the eccentric of the driving motor shaft, the resultant angle of rotation of the inner gear, depends both on the parameters of the first washer eccentric and the lever (radial distance of pin *5* relative to the eccentric path), and on the inner gear eccentric and its lever (radial distance of pin *9* relative to the eccentric path). The total angle of rotation of the inner gear transfers, through the gearing, the torque to the outer gear, that is directly connected to feed roller *14*. Electrode wire is imparted periodical pulsed motion with the frequency, dependent on the frequency of rotation of the driving motor shaft, and with the step, determined by the gear ratio of the inner gear–outer gear pair at the described oscillatory motion of the inner gear and feed roller diameter.

Based on the procedure suggested in [2], and taking into account the fact that the values of eccentricity

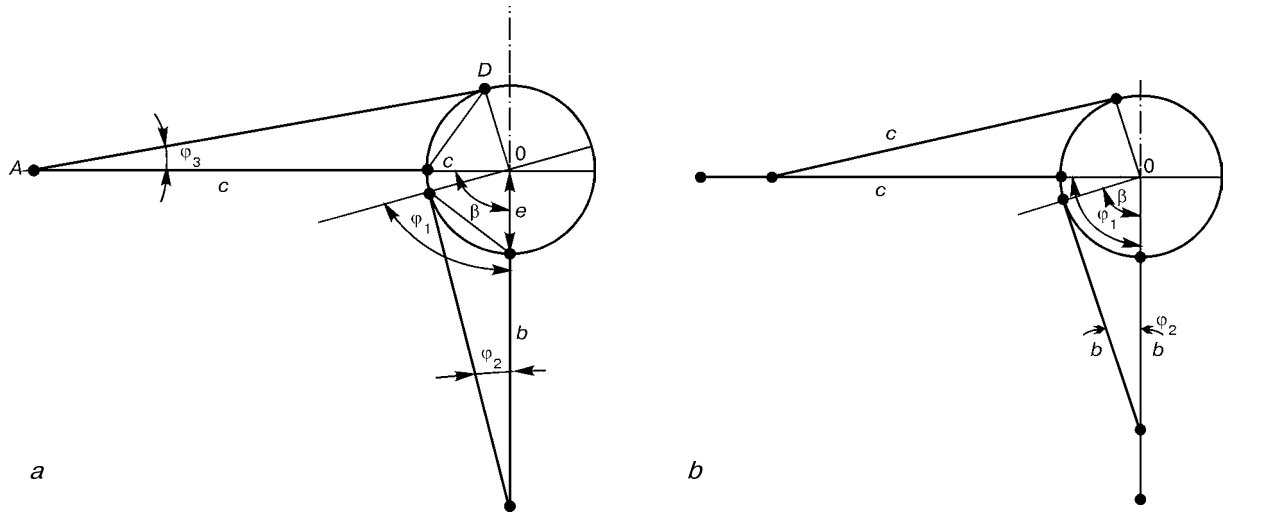

Figure 2. Design mechanical diagram of a two-modulator mechanism of pulsed feed with mobile pins (*a*) and with mobile slots (*b*)

of eccentrics *3* and *12* are the same and equal to e, let us consider the first variant of the design diagram, shown in Figure 2, *a*. The expressions for the roller rotation frequency and accelerations of electrode wire motion for this (first) modification of the mechanism, can be written as

$$\omega_{r1} = \left[-\frac{e}{R} \pm e \left(\frac{1}{b} + \frac{1}{c} \right) \cos \varphi_1 \right] \omega_1, \quad (3)$$

$$a_{e1} = \frac{eD_r}{2} \left[\left(\frac{1}{b} + \frac{1}{c} \right) \sin \varphi_1 \right] \omega_1^2, \quad (4)$$

where c is the distance from the eccentric motion path to pin *9* (length of lever, turning inner gear *11*).

Let us consider one more QWC variant, in which both pins are mobile (Figure 2, *b*). In keeping with the above procedure and proceeding from the geometrical constructions, it can be stated that for this variant, the expressions for the angular frequency of roller rotation and accelerations of electrode wire motion practically do not differ from expressions (3) and (4). Therefore, in terms of the effect achieved, the variants of the design with mobile slots and pins are practically identical, thus providing additional possibilities for searching for optimal designs, as regards the considered modifications of the pulsed wire feed mechanisms with QWC.

Let us further also use the above procedures to consider a general case of a possible mechanism design. Let us assume the following conditions:

- the device, similar to previous modifications, incorporates two modulators of pulsed motion of the outer gear (feed roller), namely the first modulator, including pin *5*, washer *1* with slot *2* and pin *6*, additional washer *8* with slot *7*, as well as the second modulator that consists of additional washer *8* with pin *9* and inner gear *11* with slot *10*;
- slots and pins of the second modulator are shifted relative to the slots and pins of the first modulator by a certain angle β;
- eccentricity of both eccentrics is made to be different with independent values e and e_1, while the eccentrics are shifted relative to each other in the direction of rotation by angle γ. The design schematic of the above modification of the pulsed wire feed mechanism is shown in Figure 3.

For the second case, based on the above procedures, we can write

$$\omega_{r2} = \left[-\frac{e}{R} \pm \left(\frac{e \cos \varphi_1}{b} + \frac{e_1 \cos [\beta - (\gamma + \varphi_1)]}{c} \right) \right] \omega_1, \quad (5)$$

$$a_{e2} = \left[\frac{D_r}{2} \left(\frac{e \sin \varphi_1}{b} + \frac{e_1 \sin [\beta - (\gamma + \varphi_1)]}{c} \right) \right] \omega_1^2. \quad (6)$$

In all of the above modifications of wire feed mechanisms, it was assumed, that all the slots were made in the radial direction. In order to derive the equation of roller motion in the most general case, let us consider the third variant by analogy with expression (1), when both slots are made at certain angles α and α_1 to the radial direction. In this case, the equations describing the frequency of the feed roller rotation and electrode wire acceleration in the general form, are similar to equations (5) and (6), allow for elements of equation (1) and have the form of

$$\omega_{r3} = \left[-\frac{e}{R} \pm \left(\frac{e (\cos \varphi_1 - \alpha)}{b \cos \alpha} + \frac{e_1 \cos [\beta - (\gamma + \varphi_1) - \alpha_1]}{c \cos \alpha_1} \right) \right] \omega_1, \quad (7)$$

$$a_{e3} = \left[\frac{D_r}{2} \left(\frac{e \sin (\varphi_1 - \alpha)}{b \cos \alpha} + \frac{e_1 \sin [\beta - (\gamma + \varphi_1) - \alpha_1]}{c \cos \alpha_1} \right) \right] \omega_1^2. \quad (8)$$

At pulsed feed of electrode wire, its maximal acceleration is of the greatest interest, that ensures a forced separation of the drop at the moment of the pulse running [3].

Let us analyse equations (4), (6), (8), in order to determine the possible maximal accelerations. Let us also take into account the simplest variant of the pulsed feed mechanism with one modulator, that was the basis for all subsequent development.

For demonstration purposes let us present equations (1), (4), (6), (8) in relative units, assuming that the gear ratio of the mechanism $e/R = 1$, and dividing all the addends by the above gear ratio. We will derive the following equations, describing the

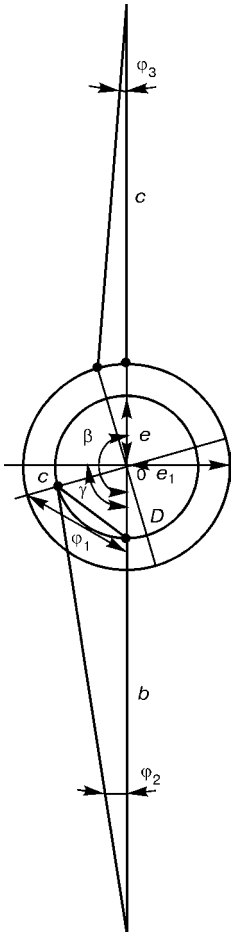

Figure 3. Design mechanical diagram of pulsed feed mechanism with two modulators, having broader capabilities of pulse parameter adjustment

changes of angular velocities for the considered modifications of the mechanisms:

$$\omega_r = \left[1 \pm \frac{R}{b}\frac{\cos(\varphi_1 - \alpha)}{\cos\alpha}\right]\omega_1, \quad (9)$$

$$\omega_{r1} = \left[1 \pm \left(\frac{R}{b} + \frac{R}{c}\right)\cos\varphi_1\right]\omega_1, \quad (10)$$

$$\omega_{r2} = \left[1 \pm \left(\frac{R\cos\varphi_1}{b} + \frac{e_1 R\cos[\beta - (\gamma + \varphi_1)]}{ec}\right)\right]\omega_1, \quad (11)$$

$$\omega_{r3} = \left[1 \pm \left(\frac{R\cos(\varphi_1 - \alpha)}{b\cos\alpha} + \frac{e_1 R\cos[\beta - (\gamma + \varphi_1) - \alpha_1]}{ec\cos\alpha_1}\right)\right]\omega_1. \quad (12)$$

It should be noted that, despite the fact that electrode wire motions in the pulsed feed mechanisms, differing in their complexity and capability of arranging them, were considered, the law of the change of the feed roller pulsed rotation speed can be described by one equation (12). The other equations mostly are particular cases. However, it should be borne in mind, that the mechanisms described by equations (11) and (12), can only yield the utmost effect, if their slots and eccentrics have relative displacements in the direction of rotation. Otherwise, the mechanism does not realise its potential in terms of additional control of the feed pulse acceleration.

Figure 4, *a* gives a number of dependencies of the angular frequency of rotation of the feed roller on the parameters of the pulsed feed mechanisms with one or two modulators, that can be regarded as direct laws of variation of the electrode wire feed rate.

Equations (9) – (11) and selected graphs show that the mechanisms with two modulators have much broader capabilities for feed pulse formation, as well as regulation of the amplitude value of speed and acceleration. In this case there are no design limitations on pulse formation, inherent to the one-modulator design mechanisms in terms of variation of the angle of inclination of the slot and the eccentricity. It should be specially noted that the shape of the pulse, as regards achievement of a particular value of acceleration of the electrode wire feed, can be adjusted by relative displacement of the slots and eccentrics, as well as the length of the levers and eccentricity. It is obvious that for design reasons, the second modulator in the two-modulator design of the pulsed feed mechanism has great capabilities for the above modulation. Adjustment of the pulse shape can be both stepwise and smooth with the range from smooth (no-pulse) motion up to increase (by several times) of the pulse amplitude compared to uniform feed with the appropriate acceleration values.

Let us also note another effect from the use of new modifications of the pulsed feed mechanisms. If in the systems that have no relative displacements of the slots and eccentrics, the shapes of feed pulses are symmetrical relative to their extremums, when the above displacement is made, the symmetry is disturbed with an appropriate change of the pulse curvature, and, hence, with the increase or decrease of acceleration. This fact can be also used to control the acceleration of electrode wire feed and electrode metal drop transfer.

The graphs in Figure 4 demonstrate that the greater reverse motion of the roller in the pulse is also recorded with the increase of the amplitude value of the pulsed rotation speed. This effect provides the maximal accelerations at feeding. However, with a sufficient length of the flexible guides, the above phenomenon can also lead to undesirable consequences, that consist in a partial elimination of the electrode wire surplus in the guide [4]. At subsequent feed pulse, a certain length of the feed step will be spent for creating a surplus of the wire, i.e. the anticipated (by the mechanism parameters) acceleration of the electrode wire motion will not be achieved, and it will even be somewhat decreased. For this case, it is expedient to consider the conditions for a pulsed rotation of the feed roller without its reversal. Let us define the condition of the above no-reverse motion for the modification of the mechanism that is described by general equation (12) in the following form:

$$\gamma - \beta \geq \arcsin[(ce)/(Re_1)]. \quad (13)$$

Let us consider some other quite interesting and useful capabilities for controlling the electrode metal

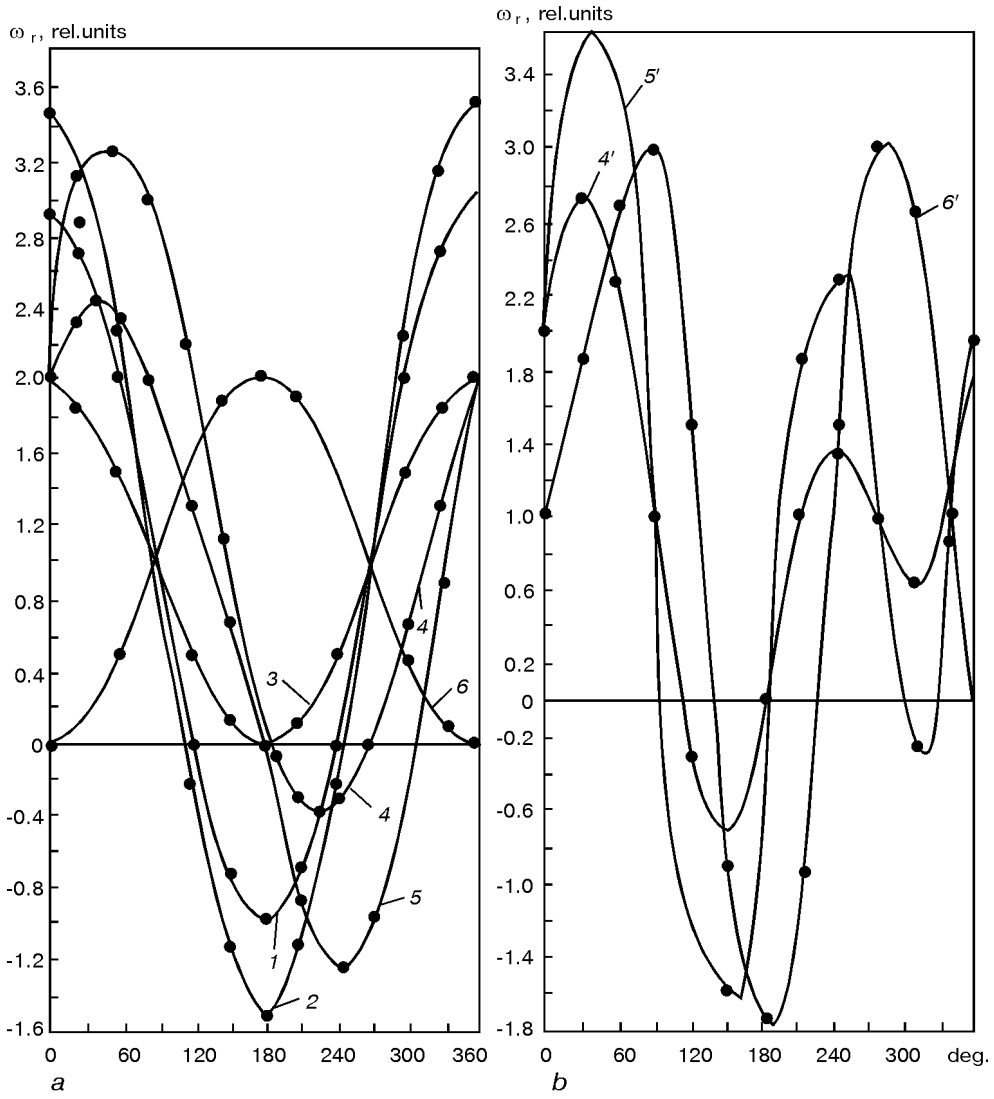

Figure 4. Plots of dependencies of variation of angular frequency of the feed roller rotation on the angle of rotation of driving motor shaft for pulsed wire feed mechanism based on QWC with two modulators, having the same (*a*) and different (*b*) rotation frequencies: *1* — $R/b = 1$; $R/c = 1$; *2* — $R/b = 1.25$; $R/c = 1.25$; *3* — $R/b = 1$; $R/c = 0$; *4*, *4′* — $R/b = 1$; $R/c = 1$; $e/e_1 = 1$; $\beta = \pi$; $\gamma = \pi/2$; *5*, *5′* — $R/b = 1$; $R/c = 1$; $e/e_1 = 2$; $\beta = \pi$; $\gamma = \pi/2$; *6*, *6′* — $R/b = 1$; $R/c = 1$; $e/e_1 = 2$; $\beta = 2\pi/3$; $\gamma = \pi/2$

transfer and adjustment of the heat input, achieved through further work on purposeful modification of the designs of the pulsed wire feed mechanisms based on QWC.

Sometimes, especially at small feed steps, this feed frequency can be insufficient to produce the required integral feed rate, and, therefore, to provide the required arc process current. This is also true in the case when motors with small nominal values of their shaft rotation frequency are used in the feed system. So, for instance, DPU87-75 type motor used in the series of semi-automatic machines of modular design with basic model PSh107V [5], has the nominal rotation frequency of 16.7 s^{-1} at the nominal supply voltage of 20 V, and 33.3 s^{-1} at the admissible supply voltage of 40 V, that can be sufficient for surfacing with self- shielding electrode wires of larger diameters with a pulsed feed, but is too low for some cases of gas-shielded welding with a pulsed feed of thin solid electrode wires. For the above cases, we have found and implemented several engineering solutions, given below:

- to increase the frequency of pulsed feed of electrode wire a multiplier was mounted on the driving motor shaft, with the capability of the multiplier connection into the system and direct action of the shaft on the pulsed feed mechanism;
- to vary the shape of the pulses and possibly increase their frequency, the relative frequency of rotation of the shaft of one of the modulators was changed, having first disengaged the preliminary kinematic connection between the first and second modulators;
- to change the shape of the pulses and possibly increase their frequency, one modulator was used, but it was modulated additionally, for instance, by an outer eccentric or cam mechanism with the frequency, differing from the frequency of rotation of the driving motor shaft. The latter variant, given in Figure 1, *b*, includes, in addition to the earlier known elements of the one-modulator design, additional eccentric *17*, mounted on shaft *18* and driven by the same driving motor through multiplier *19*. Modulator washer is connected to the eccentric via rocking lever *20*.

The law of variation of the angular frequency of rotation of the feed roller and feed acceleration in this (fourth) mechanism can be described by equations (12) and (13), assuming that the frequency of rotation of eccentric *2* differs from the frequency of rotation of the motor shaft. We will have

$$\omega_{r4} = \left[1 \pm \left(\frac{R\cos\varphi_1}{b} + \frac{e_1 R\cos[\beta - (\gamma + \varphi_2)]}{ec}\right)\right]\omega_1, \quad (14)$$

$$a_{e4} = \frac{D_r}{2}\left(\frac{e\sin\varphi_1}{b}\omega_{11}^2 + \frac{e_1\sin[\beta - (\gamma + \varphi_1)]}{c}\right)\omega_{12}^2, \quad (15)$$

where ω_{11}, ω_{12} are the frequencies of rotation of the shafts of the main and additional modulators, respectively.

To avoid addition of new parameters, let us assume in equations (14), (15), that values e_1 and c correspond to the characteristics of the added eccentric mechanism with angle of rotation φ_2, differing from φ_1. It was taken into account that $\varphi_1/\varphi_2 = \omega_1/\omega_{ad}$, where ω_{ad} is the frequency of rotation of an additional eccentric.

The graphs of dependencies $\omega_{r4} = f(\varphi_1)$ for a number of ratios R/b, e_1R/ec, β, γ, as well as the double frequency of the new eccentric modulator ($\varphi_2 = 2\varphi_1$) are given in Figure 4, *b*.

When this modification of the mechanism is used, it is possible to produce complex-shaped pulses. So, in one rotation of the driving motor shaft, it is possible to generate a pulse with two levels of amplitudes, namely a large one and then a small one, or, vice versa, a smaller one and then a larger one, this to a certain extent complying with the recommendations, given in [6], for the arc power sources designed for the gas-shielded pulsed-arc welding process. In this case the first pulse of a small amplitude melts the electrode wire, and the subsequent one of a larger amplitude, makes the drop separate from the electrode metal and transfers it to the metal pool. The advantage of producing the above combinations of pulses can consist in that, for instance, the first pulse runs through the guide channel (eliminating the gaps) of a considerable length and the second one makes a full impact on the electrode metal drop. It is important, that the mechanism parameters can be selected so as to produce in one rotation of the driving motor shaft, more than one wire feed pulse with close enough amplitudes, that are sufficient for controlling the electrode metal transfer. Such a capability somewhat changes the overall logic of pulsed feed mechanism operation, if in one cycle (rotation of the driving motor shaft) the electrode wire is fed with one, preselected displacement step, that is directly proportional to the feed roller diameter. The wish to provide small displacement steps, on the one hand, leads to reduction of the feed roller diameter, thus impairing the feeding conditions, and on the other — to increase of the frequency of rotation of the driving motor shaft, this being not always possible, because of the types and designs of the motors proper, that are used in mechanised arc welding equipment. The engineering solution proposed and substantiated by us, eliminates the above problem, by increasing the feed step per one rotation of the motor shaft, with superposition of several pulses on this step.

In order to make further quantitative assessment of the possibilities for modification of the mechanisms of the pulsed wire feed with QWC, let us perform their comparative analysis, taking the possible maximal accelerations of the rotary motion of the feed roller (electrode wire) in the pulse, as the criterion. Let us make the comparison relative to those values of acceleration, that are achieved with the use of pulsed feed mechanisms with one-sided grips and eccentric converters of motion [7], as some of the simplest technical means, providing a pulsed nature of electrode wire motion.

It is obvious that the acceleration a_{e0} of motion of a one-sided grip as electrode wire propeller, can be described by the following equation:

$$a_{e0} = e\omega_1^2 \sin(\varphi_1 t), \quad (16)$$

while the maximal value of acceleration, is written as follows:

$$a_{e0max} = e\omega_1^2. \quad (17)$$

It should noted that the maximal values of acceleration in equations (4), (6), (8), (15) are given by the following expressions:

$$a_{e1max} = \frac{eD_r}{2}\left(\frac{1}{b} + \frac{1}{c}\right)\omega_1^2, \quad (18)$$

$$a_{e2max} = \frac{D_r}{2}\left(\frac{e}{b} + \frac{e_1\sin(\beta - \gamma)}{c}\right)\omega_1^2, \quad (19)$$

$$a_{e2max} = a_{e3max} = \frac{D_r}{2}\left(\frac{e\sin[(\pi/2) - \alpha]}{b} + \frac{e_1\sin[\beta - (\gamma + \pi/2) - \alpha_1]}{c}\right)\omega_1^2, \quad (20)$$

$$a_{e4max} = \frac{D_r}{2}\left(\frac{e\sin\varphi_1}{b}\omega_{11}^2 + \frac{e_1\sin[\beta - (\gamma + \varphi_1)]}{c}\right)\omega_{12}^2. \quad (21)$$

Assuming the maximal possible acceleration of electrode wire feed for the mechanisms with one-sided grips to be a unit value, it is possible to calculate their relative effectiveness from maximal accelerations at the same values of the feed step and frequency. Such calculations made for a number of designs, are given in the Table.

Preliminary calculations demonstrate that mechanism designs with two modulators are exactly the designs where achievement of maximal accelerations (approximately 100 m/s^2 and more) is probable, that may be in excess of those accelerations required for electrode metal transfer in gas-shielded welding, that are defined in [3].

Development and investigation of the pulsed wire feed mechanisms based on QWC, considered in the paper, also included kinematic models of all their modifications. It should be noted, that study of the

Mechanism	*Ratio of maximal accelerations*	*Advantages*	*Disadvantages*
With one-sided grips	1	Simple design	Low reliability, intermittent operation, low accelerations
One-modulator QWC	1.0 – 1.7	Relative simplicity, reliability	Not noted
Same with introduction of angle of inclination α	Up to 2	Same	Complex regulation of angle of inclination α
Two-modulator QWC (19)	Up to 2.5	Possibility of pulse shape adjustment	Relatively complex design
Same (20)	Up to 3.5	Ability to control the pulse shape in a broad range	Much more complex design
Same (21)	3 – 4	Same	Relative complexity of design
Same (12)	Up to 6	Same, greater number of pulses per cycle	Relatively complex design and large overall dimensions

performance of the models and samples, completely confirms their theoretical description. In addition, the mock-up sample of the mechanism with a double modulator (Figure 3), was tested during CO_2 welding with 1.2 mm electrode wire at the welding current of 180 – 220 A. The frequency of feeding the pulses along the hose holder of 1.7 m length was 40 – 50 Hz. The process of welding in all positions, was stable, and the frequency of the electrode metal transfer precisely corresponded to the feed pulse frequency.

CONCLUSIONS

1. Integrated development of pulsed wire feed mechanisms based on QWC, allows selection of those of them that will provide the electrode wire motion from the smooth to the pulsed motion, also with a partial reversal of the feed roller. This entire range of motions can be used to solve various tasks from simple passage through the guide channel to lowering the feed resistance at small pulse amplitudes and controllable transfer of the electrode metal.

2. In order to expand the capabilities of the mechanism as regards maximal acceleration of the electrode wire, it is necessary to have the second modulator, in which the eccentricity is only limited by the conditions of the mechanism vibration and can be really increased by 2 to 3 times in relation to eccentricity of the inner gear.

3. Designs providing rotation of the shafts of both modulators with different frequencies, will allow a significant expansion of the capabilities of the pulsed wire feed mechanisms, developed on the basis of QWC.

4. The most rational design of the pulsed wire feed mechanism should be regarded to be such a design, which incorporates two modulators with eccentrics, having quite close values of eccentricities and located opposite each other, thus allowing the maximal balancing out of the mechanism and minimising its vibrations.

REFERENCES

1. Lebedev, V.A., Nikitenko, V.P. (1983) Promising trends in design of the wire feed mechanisms. *Avtomaticheskaya Svarka*, **7**, 61 – 69.
2. Lebedev, V.A., Moshkin, V.F., Pichak, V.G. (1996) New electrode wire feed mechanisms. *Ibid.*, **5**, 39 – 44.
3. Voropaj, N.M. (1996) Parameters of the modes and process capabilities of arc welding with pulsed feed of electrode and filler wire. *Ibid.*, **10**, 3 – 9.
4. Lebedev, V.A., Svetnikov, B.G. (1986) Influence of initial curvature of electrode wire on its resistance in the guide. *Ibid.*, **2**, 35 – 38.
5. Lebedev, V.A., Moshkin, V.F., Pichak, V.G. (1998) Semiautomatic machines of the same modular design for welding, surfacing and cutting. *Svarochnoye Proizvodstvo*, **1**, 24 – 28.
6. Shejko, P.P., Pavshuk, V.M. (1992) Power source for consumable electrode pulsed-arc welding with smooth adjustment of parameters. In: *New welding power sources*. Kyiv.
7. Lebedev, V.A., Nikitenko, V.P. (1984) Grips for pulsed feed of electrode wire. *Avtomaticheskaya Svarka*, **10**, 52 – 58.

CLASSIFICATION OF WAVEGUIDES SHAPED AS BODIES OF REVOLUTION FOR ULTRASONIC WELDING OF POLYMERS AND COMPOSITES ON THEIR BASE

N.P. NESTERENKO[1] and **I.K. SENCHENKOV**[2]
[1]The E.O. Paton Electric Welding Institute, NASU, Kyiv, Ukraine
[2]S.P. Timoshenko Institute of Mechanics, NASU, Kyiv, Ukraine

ABSTRACT

The paper presents a classification and systemic method of selection of the configuration of waveguides shaped as the bodies of revolution, that are used as tools for ultrasonic welding of polymers and composites on their base. Known and new basic configurations of sonotrodes which can be used for producing large-diameter circumferential weld, are considered.

Key words: *ultrasonic welding, polymers and composites on their base, waveguides-tools (sonotrode), shape of oscillations, classification*

Paper [1] presents the classification and the main principles of design of plate waveguides used as tools (sonotrodes) for ultrasonic welding (USW) of polymers. Another important class of sodotrodes used both for spot and for contour welding are sonotrodes shaped as the bodies of revolution [2 – 11]. The task of designing the latter consists in determination of the geometrical shape of the sonotrode by the specified shape of the weld. Solution is greatly simplified by the presence of a systematised data base of reference configurations, differing in the required resonance frequencies and form of oscillations.

Analysis of publications shows that the diverse axially symmetric sonotrodes can be grouped into several classes by types of oscillations, characteristic of certain sections of branches in the resonance spectrum of a continuous circular cylinder [12]. Similar to the case of plate sonotrodes, classification of axially symmetric elements of USW acoustic systems, allows selection of their configuration, outlining the methods for controlling the shape and frequency of oscillations, as well as development of new types of sonotrodes.

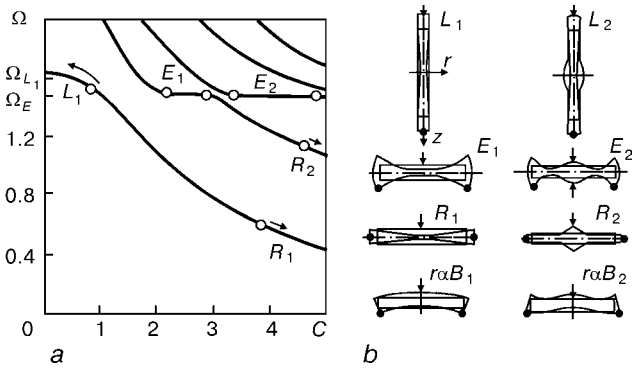

Figure 1. Types of axially symmetric motions in sonotrodes, having the shape of the body of revolution: *a* — characteristic sections of the branches of the frequency spectrum of a continuous cylinder; *b* — kinematics of the first two longitudinal, edge, radial and flexural axially symmetric modes

This paper is devoted to studying the formation of a system of basic sonotrode configurations, having the shape of the bodies of revolution, as well as their classification.

Let us characterise these elements by the resonance motion type. Historically, the sonotrodes in the form of rods of a variable cross-section, namely stepped, conical, exponential, etc., were the first to be used in ultrasonic acoustic systems. They are still used extensively, for instance, for spot USW. The task is made more complicated, when it is necessary to weld around a circular area or a circular contour of diameter $d_m \geq \lambda/3$. In this case «rod-like» sonotrodes turn out to be ineffective because of section warping, in terms of excitation and enhancement of oscillations, as well as uniformity of displacements at the working edge.

As in the case of plate elements, slot structures are widely used to generate reciprocating motions. Radial displacements of the outer and inner cylindrical surfaces of the discs, are applied, in particular, in seam USW with a rotating sonotrode and for activation of the wire drawing by superposition of ultrasound [4, 5]. Sonotrodes based on axially symmetric flexural mode of oscillations, can have the working surfaces both on the edges, and on the cylindrical surface. The first schematic is used in contour welding and the second — in seam welding [6]. Moving away from the traditional methods of formation of a uniform distribution of normal displacements u_z in a circular area of a large diameter is outlined in [7], devoted to analysis of the ability to use the edge mode of oscillations.

Modal characteristics of oscillations in the considered resonators have common features with the modes, corresponding to certain sections of the branches of the frequency spectrum of axially symmetric oscillations of a finite cylinder, in which height H and radius R' satisfy the conditions $|z| \leq H$; $0 < r < R'$. Part of such a spectrum for $\nu = 0.34$, corresponding to oscillations, symmetric relative to plane $z = 0$, is shown

Table 1. Types of sonotrodes, having the shape of the bodies of revolution

Oscillation type	*Waveguide type*	*Sonotrode configuration*
L	L_k	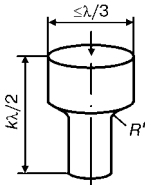
	$rmL_k^{(\alpha)}$	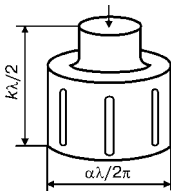
R	R_k	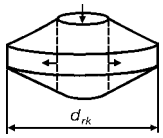
E	E_k	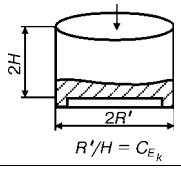
B	$r\alpha B_k$	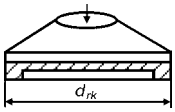

Table 2. Types of converter sonotrodes

Converter type	*Converter configuration*
L_kCR_n	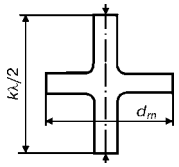
$L_kCr\alpha B_n$	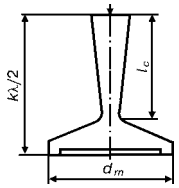
L_kCE_n	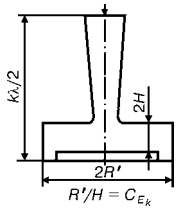
L_kCpB_n	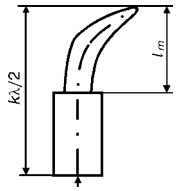

in Figure 1, *a*. In this case $\Omega = 2\omega H/\pi C_2$, $C = R'/H$. Letters L, E and R denote the type of mode, namely longitudinal, edge or radial; lower index is the number of the branch or plateau. The $r\alpha B_k$ designation is assumed for elements based on axially symmetric flexural modes. The small letters used in front, indicate more precisely that the body of revolution r is subjected to bending by axially symmetric α mode. Figure 1, *b* illustrates the kinematics of the first two modes of each of the considered types. Some sonotrode dimensions are given in fractions of the length of longitudinal wave λ, $\lambda = f^{-1}(\varepsilon/\rho)^{1/2}$, where ε is the Young's modulus; ρ is the material density; f is the oscillations frequency. The arrow indicates the excitation region; and the dot — the region of contact with the load. Such information is extremely useful for determination of the oscillation crests that are the zones of the most effective excitation of the specific modes.

Let us use Table 1 for further analysis. The protrusions in the lower part of E_k and $r\alpha B_k$ sonotrodes outline their working surfaces and indicate that they are used for contour welding of a circumferential weld. Formally, this list can include axially symmetric resonators of $(r)T$ type based on a quasithickness mode of oscillations [1]. However, practical implementation of such elements is made more complicated by a number of factors. Study [12] shows that the reciprocating motion of the disc edge is distorted by interaction of «pure» T-mode with R- and A-modes. It is enhanced with the increase of Poisson's ratio and for $0.28 \le \nu \le 0.35$ values, typical for the sonotrode materials, results in an abrupt deterioration of the positive qualities of T-mode. Compared to planar T-mode, the situation is aggravated by the closeness of the frequencies of thickness and thickness-shear resonance Ω_T and Ω_S at $\nu = 1/3$. This makes the spectrum more dense and tuning out of parasitic modes more complicated.

High-frequency parts of the spectra of symmetric modes of the rectangle and the cylinder, are specified by assigning the edge resonance frequency $\nu = 1/3$ as the lower limit [12]. In keeping with that, elements of the type of E, T and S can be regarded as high-frequency elements, and elements of L, R and B type — as low-frequency ones.

Single-mode resonators do not always comply with the functional requirements. This is usually related to the issue of effective excitation of some oscillation modes. In such cases converter-sonotrodes are used, in which easily-excited (for instance L_1) mode is converted into a weakly-excited type of motion, namely radial, edge, etc. [7, 12, 13]. Classification and marking of some types of converters are given in Table 2.

In the accepted marking, the first element indicated is the one, that is excited by the converter and

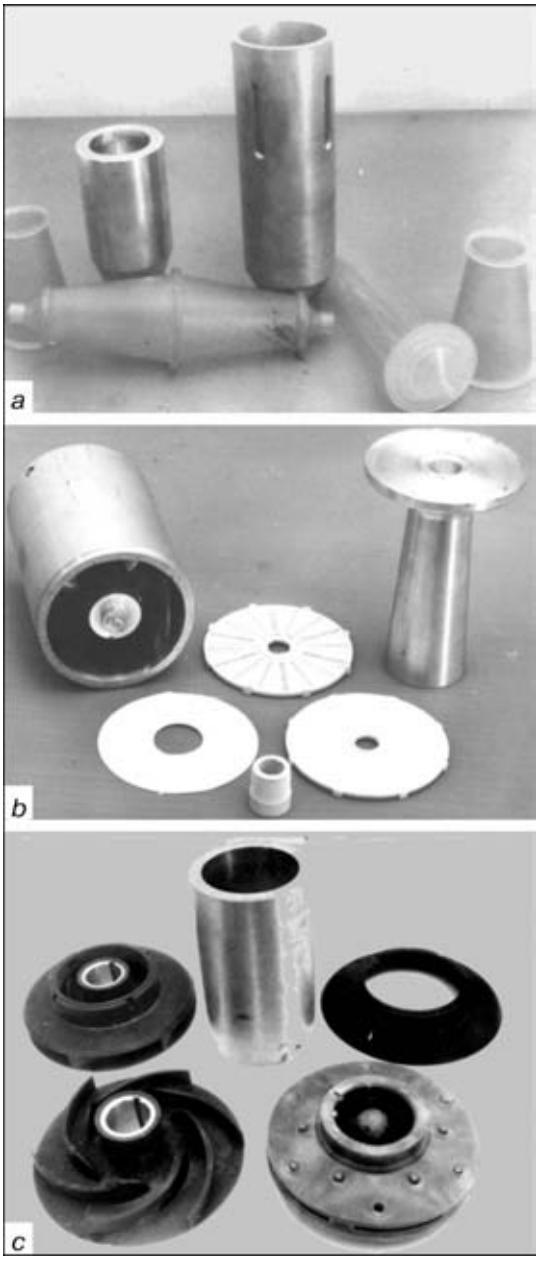

Figure 2. Waveguides for USW of hemisorption columns (*a*), polymer filters (*b*) and water pump wheels (*c*)

the energy of which is converted (letter *C*) into oscillations of another type of resonator, connected to it. The strongest interaction and conversion of the modes are in place when the partial system frequencies are close and equal to the excitation frequency.

The given classification allows selection of the sonotrode type following the specified shape of welded joint. Precise dimensions of the element for the specified working frequency of oscillations are determined in the second stage. It is necessary to tune out the parasitic frequencies in it, thus ensuring the required values of oscillation amplitude and uniformity of its distribution over the working surface of the sonotrode. The third stage includes evaluation of fatigue strength and temperature of the element heating by vibration. Implementation of the latter two stages envisages the use of mathematical simulation methods.

Problem definition in the cylindrical system of co-ordinates $r0z$ includes [14] kinematic equations, equations of axially symmetric oscillations, fundamental equations, heat conduction equations and expressions for the dissipative function:

$$\frac{\partial \tilde{\sigma}_{rr}}{\partial r} + \frac{1}{r}(\tilde{\sigma}_r - \tilde{\sigma}_0) + \frac{\partial \tilde{\sigma}_{rz}}{\partial z} + \rho\omega^2 \tilde{U}_r = 0,$$
$$\frac{\partial \tilde{\sigma}_{rz}}{\partial r} + \frac{1}{r}\tilde{\sigma}_{rz} + \frac{\partial \tilde{\sigma}_{zz}}{\partial z} + \rho\omega^2 \tilde{U}_r = 0, \quad (1)$$

$$\tilde{\sigma}_{ij} = 2\tilde{G}\left(\tilde{\varepsilon}_{ij} + \frac{\tilde{\nu}}{1-2\tilde{\nu}}\tilde{\varepsilon}_{kk}\delta_{ij}\right), \quad i, j = r, \theta, z, \quad (2)$$

$$c\dot{\theta} = \frac{1}{r}\frac{\partial}{\partial r}\left(kr\frac{\partial \theta}{\partial r}\right) + \frac{\partial}{\partial z}\left(k\frac{\partial \theta}{\partial z}\right) + D', \quad (3)$$

$$D' = \frac{\omega}{2}(\sigma''_{ij}\varepsilon'_{ij} - \sigma'_{ij}\varepsilon''_{ij}), \quad (4)$$

boundary and initial (for temperature) conditions [1]. In this case $\tilde{G}$ and $\tilde{\nu}$ are the complex shear modulus and Poisson's ratio; $\tilde{G} = G' + iG''$; $\tilde{\nu} = \nu' - i\nu''$; $\tilde{\varepsilon}_{ij}$ and $\tilde{\sigma}_{ij}$ are the complex amplitudes of the components of the vector of displacements, strain and stress tensors; c and k are the coefficients of bulk heat content and heat conductivity; θ is the temperature; ω is the circular frequency; $\omega = 2\pi f$.

At high oscillation frequencies, it is necessary to take into account the dependence of the shear modulus on the stress amplitude intensity

$$\tilde{G} = \tilde{G}(\omega, \theta, \sigma_i),$$

$$\sigma_i = \frac{1}{\sqrt{6}}(|\tilde{\sigma}_{rr} - \tilde{\sigma}_{\theta\theta}|^2 + |\tilde{\sigma}_{zz} - \tilde{\sigma}_{rr}|^2 + |\tilde{\sigma}_{\theta\theta} - \tilde{\sigma}_{rr}|^2 + 6|\tilde{\sigma}_{rz}|^2)^{1/2},$$

$$|\tilde{\sigma}_{rz}|^2 = \sigma'^2_{rz} + \sigma''^2_{rz}, \ \ldots$$

In order to ensure the fatigue strength of the sonotrode, the value of stress intensity maximal in volume V, should meet the condition $\max_V \sigma_i \le \chi\sigma_1$, where σ_1 is the cyclic fatigue limit of the material at a symmetric loading cycle; χ is the coefficient of the strength margin.

Considering the complexity of the sonotrode geometry and non-linearity of the problem (1) – (4) in the general case, it is rational to apply numerical methods for solving it. The finite element method [15] is the most convenient of them for this class of problems.

The main stages of designing axially symmetric sonotrodes are the same as for plate elements [1]. The developed approach was used to design and make a number of sonotrodes for USW of plastic items. They are shown in Figure 2.

CONCLUSIONS

1. Diversity of sonotrodes, having the shape of the body of revolution and used for USW of polymers and composites on their base, allows classifying them by the type of resonance form of oscillations. The

types of motions, implemented in them, namely longitudinal, radial, bending, etc., can be correlated with the characteristic sections of the branches of the frequency spectrum of a continuous circular cylinder.

2. Marking of axially symmetric sonotrodes is proposed and the main stages of their design are outlined.

3. The developed classification enables applying a well-grounded approach to selection of the basic configuration of the sonotrode, proceeding from the weld shape. The sonotrode shape is further determined more precisely by numerical simulation.

4. Two-dimensional objects are reliably designed now, whereas oscillations in sonotrodes of $rmL_k^{(\alpha)}$ type are three-dimensional. Development of software for three-dimensional analysis determines the direction for work performance in this field in the near future. Its implementation will allow a marked widening of the capabilities of the most efficient contour USW.

REFERENCES

1. Nesterenko, N.P., Senchenkov, I.K. (2001) Classification and design of plate wavegides-tools for ultrasonic welding of polymers and composites on their base. *Avtomaticheskaya Svarka*, **4**, 51 – 53.
2. Silin, L.L., Balandin, G.F., Kogan, M.G. (1962) *Ultrasonic welding*. Moscow: Mashinostroyeniye.
3. Machetner, B.Kh. (1965) Concentrators — tools for ultrasonic treatment and methods of their fastening. In: *NIIMASh Review*. Moscow.
4. Vasiliev, P.E., Savitskaya, T.A. (1979) Calculation of circular concentrators of radial oscillations. *Akustich. Zhurnal*, **2**, 208 – 212.
5. Vasiliev, P.E. (1980) Composite piezoelectric converter of radial oscillations. *Ibid.*, **4**, 517 – 521.
6. Volkov, S.S. (1969) Ultrasonic contour welding of cylindrical items of polymer materials. *Svarochnoye Proizvodstvo*, **5**, 39 – 45.
7. Senchenkov, I.K., Vasilenko, O.N., Kozlov, V.I. (1995) Axially symmetric sonotrodes based on the edge oscillation mode. *Dopovidi NAN Ukrainy*, **3**, 44 – 45.
8. Senchenkov, I.K., Nesterenko, N.P. (1995) Design of a tool with axially symmetric longitudinally-flexural mode of oscillations for contour ultrasonic welding of plastics. *Avtomaticheskaya Svarka*, **6**, 39 – 42.
9. Senchenkov, I.K., Nesterenko, N.P., Tarasenko, O.V. *et al.* (1989) Finite element analysis of contour waveguides for ultrasonic welding of plastics. In: *New developments on welding and adhesion bonding of plastics*. Kyiv: PWI.
10. Sechenkov, I.K., Kozlov, V.I., Chervinko, O.P. *et al.* (1990) On design of resonance characteristics of axially symmetric waveguides by the finite element method. *Prikladnaya Mekhanika*, **11**, 35 – 39.
11. Volkov, S.S., Chernyak, B.Ya. (1986) *Welding of plastics by ultrasound*. Moscow: Khimiya.
12. Grinchenko, V.T., Meleshko, V.V. (1981) *Harmonic oscillations and waves in elastic bodies*. Kyiv: Naukova Dumka.
13. Iton, K., Mori, E. (1974) Studies on resonator with directional converter (R–L-type converter disc of various thickness). *J. Acoust. Soc. Jap.*, **11**, 587 – 591.
14. Karnaukhov, V.G., Senchenkov, I.K., Gumenyuk, B.P. (1985) *Thermomechanical behaviour of viscoelastic bodies at harmonic loading*. Kyiv: Naukova Dumka.
15. Motovilovets, I.A., Kozlov, V.I. (1987) Mechanics of coupled bodies in structural elements. Kyiv: Naukova Dumka.

10 YEARS OF THE INTERNATIONAL ASSOCIATION «WELDING»

O.N. IVANOVA, Director of IAW
The Paton Electric Welding Institute, NASU, Kyiv, Ukraine

The International Association «Welding» (IAW) was founded in May, 1991 at the facility of the E.O.Paton Electric Welding Institute of NAS of Ukraine and became a successor of the Coordination Center on the problem «Welding» at the former CMEA. The activity of the association is based on the new principles of market mutual relations. The aim of its activity is to create favourable conditions for its members in study of their scientific-technical potential, to render practical assistance in promoting the competitive developments at the markets.

The association incorporates different research institutions, industrial enterprises, entities of business and financial activity of a number of countries. As a legal body it is functioning by the Agreement of the interested parties, on the basis of Status, and registered in Ukraine in accordance with existing laws.

The scientific-technical cooperation in the field of welding, one of the most widely spread processes of metal treatment, is a powerful key factor in the development and intensification of production. The direct scientific, industrial and trade relations between organizations and companies, included to IAW, create favourable conditions for the effective scientific-technical and economical development of each member of the association. This is due, in particular, to providing the express information about all the achievements in the field of welding science and technology, information about demands and offers at the welding market.

The main trends in the IAW activity are as follows: scientific-technical, production-business, financial-economical, information-advertizing, foreign economical, etc. This very wide range of trends of activity makes it possible, depending on the situation, to select the most effective trend and to concentrate efforts on it for obtaining the desired result. The analysis of the economical situation and feasibility of selecting the most rational trend allows realization of the main aim of cooperation and quick solution of the arising problems.

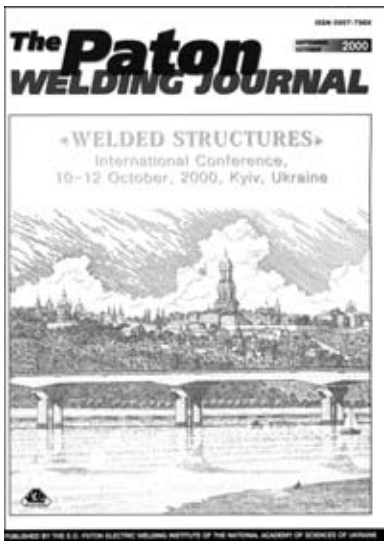

Proceedings of International conferences

During recent three-four years the IAW is active in three main trends, such as information-advertizing, scientific-technical and financial-economical.

The information-advertizing activity is associated, first of all, with the organizing and conductance of international conferences and seminars. Over the recent years about 30 international conferences and seminars in different countries, namely in Bulgaria, Germany, Poland, Georgia, Macedonia, Russia, Ukraine, were held by the IAW. The subjects of the conferences were rather diverse. These are the problems of quality and certification of products, hygienic conditions of application of welding processes, new technologies of welding, problems of welding application in shipbuilding, construction of tanks, railways and rolling stocks, metallurgy and related technologies. Scientists from Belarus, Russia, Hungary, Poland, Slovakia, Czech Republic, Bulgaria, Uzbekistan, Germany, France, Romania, Japan, USA, Korea, China, Ukraine participated in the conferences. Among the conducted conferences such large conferences can be outlined as «Welding and Related Technologies to the XXI Century» (November 1998, Kyiv) and «Welded Structures» (October 2000, Kyiv).

The information activity is not limited by organizing the conferences and seminars. The IAW issues the express-informations, each devoting to a definite problem, for example, computer systems in welding production, problems of quality and economical manufacturing of welded structures and so on. Each issue consists of four chapters including the abstracts of subject papers presented at the conferences; description of new developments offered by organizations-IAW members, and also their demands in new developments; information about the scheduled international conferences; list of organizations-IAW members. Express informations are distributed among the IAW members free of charge.

In 2001 the IAW together with the National Academy of Sciences of Ukraine and the E.O. Paton Electric Welding Institute became co-founders of the journals «Avtomaticheskaya Svarka», «Problemy Spetsialnoy Elektrometallurgii», «Tekhnicheskaya Diagnostika i Nerazrushayushchiy Kontrol», «The Paton Welding Journal».

In the scope of the scientific-technical trend, the IAW, using its status possibilities as an object of a foreign activity and results of information-advertizing work, is active in searching for investors to realize the R&D projects by signing the contracts for the fulfilment of research and experimental-designing works. Over this period a number of works was fulfilled in cooperation with such organizations and companies as Instytut Spawalnictwa (Gliwice, Poland), «Linge-KCA-Drezden», «Binzel Industries GmbH» (Germany), «Airbus Industrie» (France), «Consortium Service Management Group, Inc.» «Performance Alloys Materials, Inc.» (USA), «Farrik van Plaatwerken van Dam» (the Netherlands), Korea Institute of Machines and Materials, the E.O. Paton Electric Welding Institute (Ukraine), Gas Institute of NAS of Ukraine, Institute of Surgery and Transplantology of AMS of Ukraine, NPO «More», Kharkov Aviation Institute.

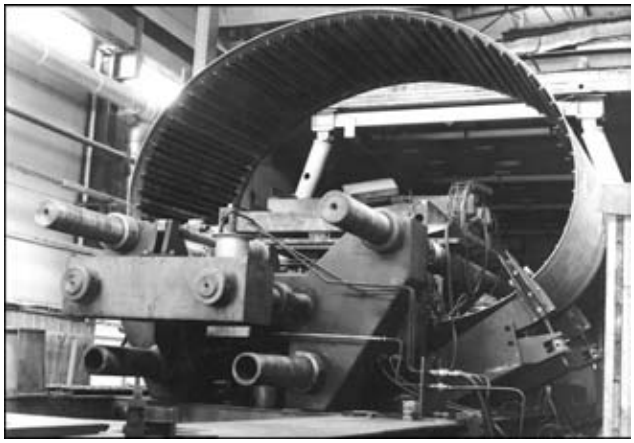

Welded stringer shell in the process of manufacture (shell diameter 4000 mm, length 2200 mm, sheath thickness 5 mm; 72 stiffeners are welded to the sheath using the electron beam welding)

Owing to international mutual relations, a very wide scope of developments was fulfilled, among which are the EBW of large-sized thin-walled aluminium alloy structures, explosion stress relieving in welded samples of high-pressure vessels, inner cladding of steel cylindrical billets using explosion welding, welding of soft vital tissues and other projects. Only some of the developments made by the PWI in collaboration with IAW, are illustrated.

Each year the IAW accumulates the experience in attraction of financial resources and searches for partners to realize the projects using both the new challenging developments and implementation of ready developments. At a definite interest of organizations there are all necessary conditions for cooperation within the scope of the joint projects.

To make the financial-economical activity more active the IAW established a local charity funds «Cooperation of Welders» intended for rendering assistance in realization of scientific-educational programs and financing the definite purposeful programs. This made it possible to attract attention of legal and physi-

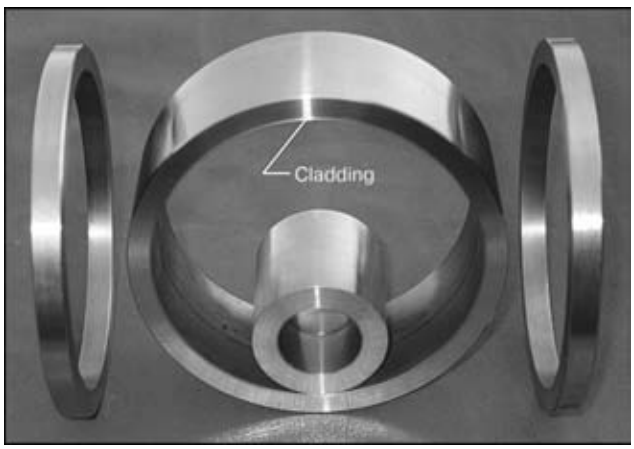

Steel hollow cylinders with 30 and 120 mm inner diameter after inner explosion cladding with special material

Welding complex for joining soft vital tissues

cal persons of Ukraine to cooperation for mobilization of financial, material-technical and other resources, to widen the sources of incomings. Due to funds of sponsors two International conferences were held.

It is seen that the trends of IAW activity are interconnected in such a way that information and advertizing contribute to the creation of projects, and the funds, obtained from their realization, can promote to a certain extend the development of information-advertising activity.

Summarizing the ten-year activity of IAW, it can be concluded that the activity of the association was successful and useful in spite of natural difficulties accompanying this transition period. It made it possible to preserve the many-year earlier established creative relations of scientists and specialists working in the field of welding science and technology.

The active work of co-founders within the scopes of IAW, i.e. Institute of Welding (Gliwice, Poland), Industrial Group OSC «Rotex-K» (Moscow), Georgian Welding Association (Tbilisi), KZU Holding, Ltd. (Sofia), Institute of Welding and Protective Coatings (Minsk), Otto-von-Guericke Universitat (Magdeburg, Germany), «Consortium Service Management Group, Inc.» (Corpus Christi, USA) should be outlined. The activity of IAW gives opportunity to find new partners, to establish the multilateral and bilateral business contacts, to realize the fast exchange of information about the newest achievements in science and technology, and also in the solution of arising problems, to participate jointly in the developments of scientific and technical projects, financed by special funds, to search for orders and their fulfilment by the joint efforts, to accumulate and further develop the unique experience of multilateral cooperation of partners on the mutually beneficial conditions.

SYNTHESIS OF INDUCTION SYSTEMS FOR WELDING AND BRAZING OF PIPE JOINTS BY USING PRESET DISTRIBUTION OF POWER IN THE WELD ZONE

A.S. PISMENNY
The E.O. Paton Electric Welding Institute, NASU, Kyiv, Ukraine

ABSTRACT

Method of synthesis of electromagnetic field and design of inductor, realized in use of impedance boundary conditions and preset distribution of specific power at the workpiece surface being heated are described.

Key words: *welding, brazing, synthesis, electromagnetic fields, inductors, coils (windings), pipes, tubes, flanges*

To produce the quality weld for joining the workpieces during welding and brazing, it is important to attain the preset (from technological requirements) distributions of temperature and specific power in the weld zone.

When the induction heating is used for the mentioned purpose it is important to define the design and dimensions of the inductor, a gap between the inductor and workpieces being heated, and also the inductor electrical parameters providing the preset heating conditions.

The above-mentioned problem is solved traditionally by the methods of successive approximations, usually in statement of a boundary problem of the electromagnetic field, exited by an inductor current (current, shape and dimensions of the inductor are preset coming from the designer experience, i.e. a zero approximation), in the workpieces heated and also in the surrounding space. Dimensions and other parameters of the inductor are determined during calculation of a specific power in the weld zone, thus repeating the process of calculation until reaching the required result.

It is evident that this approach is labour-intensive and not optimum (from the point of view of developers of the technological processes and equipment for their realization).

For these purposes it is rational to use such methods of synthesis at which the necessary parameters of the electromagnetic field and design of the inductor are determined directly from the preset distribution of vectors of the field along the surface of the workpieces being heated.

There is a limited number of analytical or numerical solutions of similar problems [1 – 3]. For example, in case of plane electromagnetic fields it is necessary to solve the Cauchy's problem for the Laplace's equation on the half-plane. This corresponds mostly to the cases in which the time is an independent variable unlike the problems when a space coordinate serves an independent argument, as in the problem being considered.

An additional limitation in the solution of the synthesis problems, is, firstly, the feasibility of presetting either a limiting value of the potential or its normal derivative at the boundary. The independent presetting of one and another brings a mathematical contradiction, resulting in the fact that the problem becomes insoluble at a strict statement. Secondly, the solutions of the Cauchy's problem for the Laplace's equation are not stable with respect to small changes in boundary conditions that leads to a necessary significant limitation of the field area in which an approximate solution can be obtained [1, 2].

However, there is a feasibility to regulate the problems of synthesis, to provide the stability and ability of their solution by using the impedance boundary conditions (IBC) in the problem statement. These conditions bind unambiguously the values of potential and its normal derivative (intensities of electrical, E, and magnetic, H, fields). The use of boundary conditions of the new type is also rational, i.e. power conditions connecting the value of the potential at the boundary of bodies with a specific power (surface, P_e, or volume, P_{ev}) [4 – 7].

Let us consider the procedure of solution of the mentioned problems in terms of a vector potential of the magnetic field $\vec{A}(r, \theta, z)$ in a cylindrical system of coordinates.

The problem of determination of design, dimensions and electromagnetic parameters of the inductor, which is arranged outside the surface of the body being heated, providing the preset distributions of the electromagnetic field and specific power in the weld zone, and so the preset condition of its heating, is stated.

The vector potential in the area, which is outside with respect to the body heated, should satisfy the Laplace's equation

$$\Delta\vec{A} = 0 \qquad (1)$$

and condition of radiation at infinity [8]

$$\lim_{r,\, z \to \infty} \vec{A} = 0. \qquad (2)$$

At the surface of the body heated the IBC is fulfilled, that is justly in a general case for the calculation of two- and three-dimensional fields including that for bodies with curvilinear boundaries:

$$[\vec{n} \times \vec{E}_e] = Z_e[\vec{n} \times [\vec{n} \times \vec{H}_e]], \qquad (3)$$

where $\vec{n}$ is the unit vector of normal to the surface of the body heated; Z_e is the wave resistance of the body surface (normal surface impedance) in the same point; $\vec{E}_e = -j\omega\vec{A}_e$ for complex amplitudes of vectors of the electromagnetic field and the case of problems with an axial symmetry of bodies heated and current-carrying circuits, considered here; $\vec{H}_e = (1/\mu_0)\mathrm{rot}_n\vec{A}_e$.

In the present problem $\vec{A}_e$ is the known function of coordinates and specific power [4 – 7]:

$$\vec{A}_e = jZ_e(2P_e\mathrm{Re}\,[Z_e])^{1/2}/\omega \qquad (4)$$

at a preset distribution of P_e and

$$\vec{A}_e = (\rho P_{ev})^{1/2}/\omega \qquad (5)$$

at a preset distribution P_{ev}.

The method of analytical continuation on the basis of the uniform approximation of unknown function by the Taylor's series is most simple and convenient for the solution of the boundary problem (1) – (4) or (1) – (3), (5) [1]. In addition, the condition at infinity cannot be always satisfied (2). However, it has no often a practical importance as it is necessary to provide the preset accuracy in determination of an electromagnetic field in the close vicinity of the workpieces heated (within the air gap between workpieces and inductor).

After the field determination it is necessary to fulfil the stage of a physical realization of boundary conditions beyond the preset vicinity of the workpieces, but within the area in which the field was determined by arrangement of the field sources along the selected boundary: linear density of current (numerically equal to a tangent component of the field intensity) and ferromagnetic materials (magnetic conduits) — along the equipotential regions of the boundary. Here, the solution of the synthesis problem is completed [1].

Taking into account the conditions of technical ability of realization of the perfect design of the inductor it is not almost possible to realize the real distribution of the current density. The problem consists in the fact that the current circuits and systems of circuits (winding turns) are the real sources of the inductor electromagnetic field. They have finite dimensions and the distribution of current density along the inductor turns surface, faced the workpieces, which is low-dependent on current in the workpieces heated.

Therefore, in the solution of the problem it is rational at once to take into account the known information about the field sources and to introduce it in an appropriate form for consideration, because by virtue of cylindrical asymmetry their structure is known. And it possible to make the procedure of synthesis much simpler.

To take into account the known structure of the field sources in the new statement it is necessary to introduce the condition of an allowable error of realization of a vector potential $\vec{A}_e$, being preset at the surface of the workpieces heated:

$$|\vec{A}_e - \vec{A}_{ei}| < \varepsilon, \qquad (6)$$

where $\vec{A}_{ei}$ is the vector potential of the magnetic field, generated at the surface of workpieces heated with an inductor current; $\varepsilon \geq 0$ is a random small value determining an allowable error in realization of the field at the surface of the workpieces.

Here, it is rational to change the statement of the synthesis problem and to formulate it as the problem of functional minimizing

$$F = \iint_S [\vec{A}_e(r_{ek}, z_{ek}) - \vec{A}_{ei}(I_i, r_i, z_i)]^2 dr dz, \qquad (7)$$

where I_i is the inductor current; index i is referred to the coordinates of the electromagnetic field sources (inductor), and index k — to the coordinates of the zone of surface of the workpieces heated, in which the distribution (4) or (5) is preset.

Due to this, the functional (7) is to be solved for surface of the workpieces. It is simplified significantly and takes the form

$$F = \int_L [\vec{A}_e(r_{ek}, z_{ek}) - \vec{A}_{ei}(I_i, r_i, z_i)]^2 dx. \qquad (8)$$

In case when the functions (4) or (5) are preset in a limited number of points of the surface of the workpieces heated (points of collocation), then it is possible to use the functional (8) in the form

$$F = \sum_{k=1}^{N} [\vec{A}_e(r_{ek}, z_{ek}) - \vec{A}_{ei}(I_i, r_i, z_i)]^2 = 0, \qquad (9)$$

where k is the number of point of collocation; N is the number of points of collocation.

The obtained solution of the problem of synthesis, as was defined, satisfies the equations of the electromagnetic field and boundary conditions. Therefore, it is the desired solution by virtue of the theorem of uniqueness of solution for the system of Maxwell's equations [8].

Using the above-mentioned procedure the synthesis of definite induction systems for heating pipes for

welding and brazing [4] and flange joints [6] of pipes was made.

The experimental checking showed that the error in calculations using the method developed lies within the units of percents. This makes it possible to recommend this method for use in the development and designing of equipment for the technological processes.

REFERENCES

1. Kolesnikov, E.V. (1966) Synthesis of two-dimensional magnetic field in ferromagnetic plane. *Izv. Vuzov, Elektromekhanica*, **5**, 487 – 505.
2. Kolesnikov, E.V. (1966) Synthesis of magnetic field using magnetic materials of a finite permeability. *Ibid.*, **7**, 691 – 709.
3. Volynsky, B.A., Bukhman, V.E. (1960) *Models for solution of boundary problems*. Moscow: Fizmatgiz.
4. Pismenny, A.S. (1990) Synthesis of induction systems for welding and brazing. *Avtomaticheskaya Svarka*, **5**, 11 – 15.
5. Pismenny, A.S. (1991) Calculation of induction systems of electrothermal bending of welded pipelines. *Ibid.*, **10**, 39 – 42.
6. Pismenny, A.S., Prokofiev, A.S., Shinlov, M.E. (1999) Synthesis of induction systems for brazing of pipe flange joints using the preset distribution of power in the weld zone. *Ibid.*, **8**, 17 – 21.
7. Pismenny, A.S. (1995) Impedance boundary conditions at the surface of electroconductive bodies in the problems of electrothermics. *Dopovidi NAN Ukrainy*, **1**, 64 – 66.
8. Koshlyakov, N.S., Gliner, E.B., Smirnov, M.M. (1970) *Equaitions in partial derivatives of mathematical physics*. Moscow: Vysshaya Shkola.

STRAIGHTENING OF ELECTRODE WIRE USING AUTOMATIC DEVICES

S.A. VASILISHIN
KPO «Prigma-Press», Khmelnitsky, Ukraine

ABSTRACT

Types and peculiarities of technological processes of straightening of metallic materials from bundles are described. Designs of straightening cases and differences in their operations are considered. The modified design of the straightening case is suggested, which makes it possible to set different schemes of its adjustment depending upon the diameter and type of a material being straightened.

Key words: *straightening of wire, roller straightening, all-sided straightening, straightening case, designs, adjustment schemes*

Despite a wide variety of available technological processes and designs, the equipment used for making parts from wire (electrodes in particular) shares some operations. The most important of them is straightening of wire from a bundle.

Depending upon requirements to the quality of straightening and profile of the cross section of a source material, there are two basic cardinally different processes used for straightening of the material in the bundle:

• roller straightening in two mutually perpendicular planes by multiple plastic transverse bending (using roller-type straightening machines);

• all-sided straightening by multiple plastic transverse bending in blocks (drawing dies) of a rotating straightening case.

Straightening of metal using rollers is usually employed for bars and shaped rolled stock. To cause this process to occur in two planes, part of the rollers is installed in a horizontal plane and part — in a vertical plane. Straightening in these machines is done between two rows of rollers, the rollers of one row being placed in a staggered arrangement with respect to the rollers of the other row. While passing between the rollers, the material treated is subjected to multiple transverse bends (reverse bends), alternating in opposite directions, with stresses which exceed the yield strength of the material. It is this fact that provides straightening.

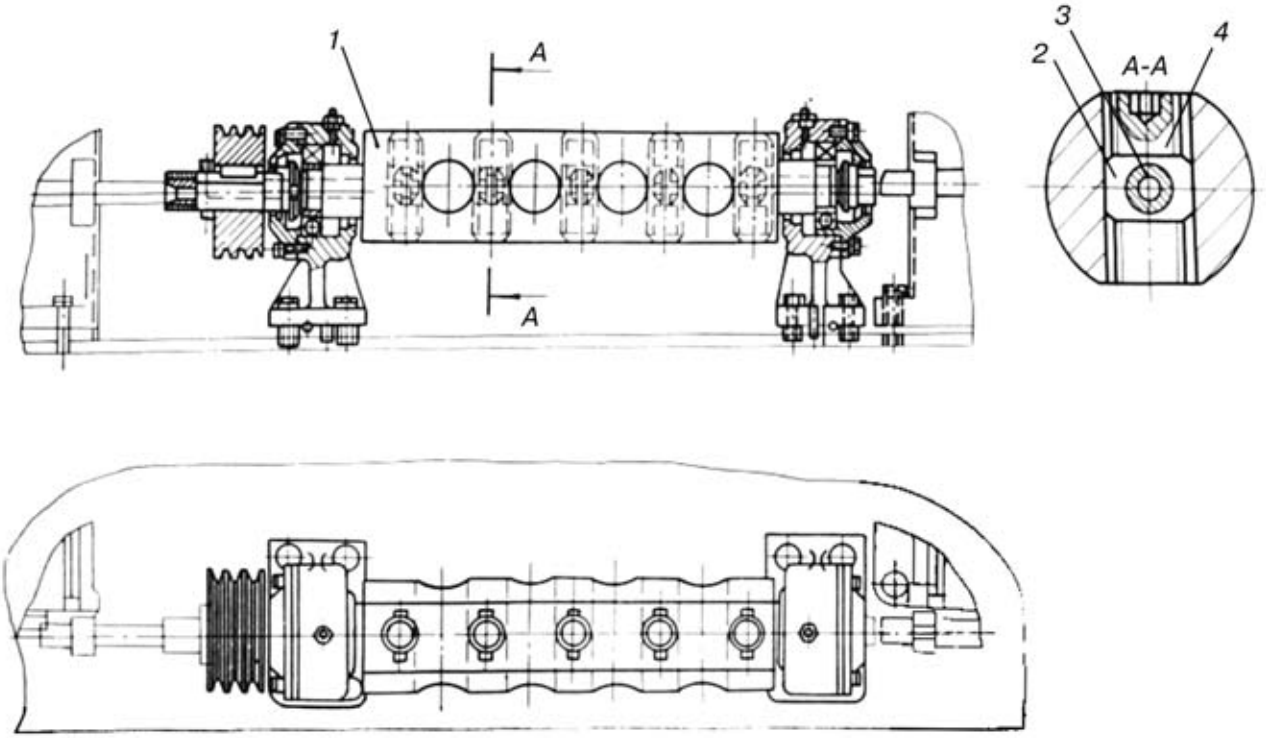

Figure 1. Straightening case with straightening sleeves. See designations of *1 – 4* in the text

The roller-type straightening devices are used to advantage in spring, washer-coiling, wire-nail and net-knitting machines. For straightening shaped rolled stock, they are used also in straightening-cutting automatic devices.

All-sided straightening of wire can be used only for straightening of metal of a round cross section. It is performed using a rapidly rotating straightening case with special blocks. The material drawn in rotation of the case through the blocks shifted with regard to the case axis is straightened by multiple plastic transverse bends alternating in opposite directions. The main advantage of the process of straightening using the rotating straightening case, as compared with the process of straightening using rollers, is a much higher quality of the material treated. A drawback of this process consists in the fact that it is impossible to perform straightening of a shaped material.

Straightening cases of straightening-cutting automatic devices are employed for straightening of only round bars. There are different types of the straightening cases which are used in practice. One of the most widespread type of the cases is that which involves straightening sleeves (Figure 1). They are employed with straightening-cutting automatic devices of the I6119 and I6122 models and manufactured by the Khmelnitsky Plant KPO «Prigma-Press».

As to its design, the straightening case is cylindrical shaft *1* installed on two bearing supports. The shaft has a through channel formed by the holes made in two mutually perpendicular planes and shifted with respect to each other by a pitch of location of the straightening sleeves. Blocks *2* with straightening sleeves *3*, which are fixed in a radial direction on the two sides by screws *4*, are placed in the hole. The reverse bend of the wire in the straightening case is set by shifting the axis of the sleeves using these screws. An advantage of such a straightening case is simplicity of manufacture of the straightening sleeves, and drawbacks include fast wear of the straightening sleeves on the inside diameter, despite the fact that they are made from high-quality tool steels, and necessity to install the sleeves on the axis in loading the wire into the straightening case. To eliminate the latter, some companies that use such automatic devices employ straightening sleeves made from hard alloys. Then their strength increases dozens of times. If it is necessary to minimize deformation of the external surface of the wire being straightened (for non-ferrous metals and alloys), it is recommended that the straightening sleeves be made from soft materials.

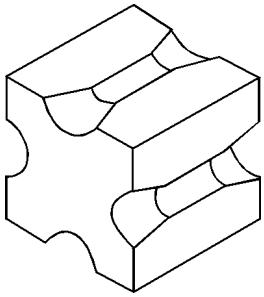

Figure 2. Tetrahedral straightening block

A modification of the straightening case with straightening sleeves is the case with split straightening blocks of a tetrahedral shape (Figure 2).

Joining of two straightening blocks forms a hole through which a wire is drawn in the straightening case. An advantage of such blocks consists in the fact that in wear of one of the channels the blocks are turned to 90° to put into operation a new channel.

The straightening case manufactured by the «Prigma-Press», which is mounted on a straightening-cutting automatic device of the IA6218 model used for electrode billets, has such a design.

Some foreign companies install combined straightening cases with rotating rollers and straightening blocks on their straightening-cutting automatic devices. Schematic of the straightening case made by the Israeli Company «Videx», comprising four pairs of rotating globoidal rollers and three blocks in the form of straightening sleeves, is shown in Figure 3.

This design of the straightening case allows the wire to be fed using no special mechanism, due to an axial component formed in rotation of the crossed rollers together with the straightening case. Drawbacks of this design are the inconsistent feed speed and complicated design of the case. The Greek Company «Pratto» uses in its straightening-cutting automatic devices the straightening cases with rotating straightening sleeves mounted on bearings in the casings. The casings are moved along the inclined slots made in the case, which allows the sleeves to be moved about the axis of feeding the wire. In rotation of the straightening case, the bearings are rotated around the sleeves, while the sleeves in turn are rotated due to the axial movement of the wire through the straightening case. As a result, the sliding friction in the sleeves is minimized.

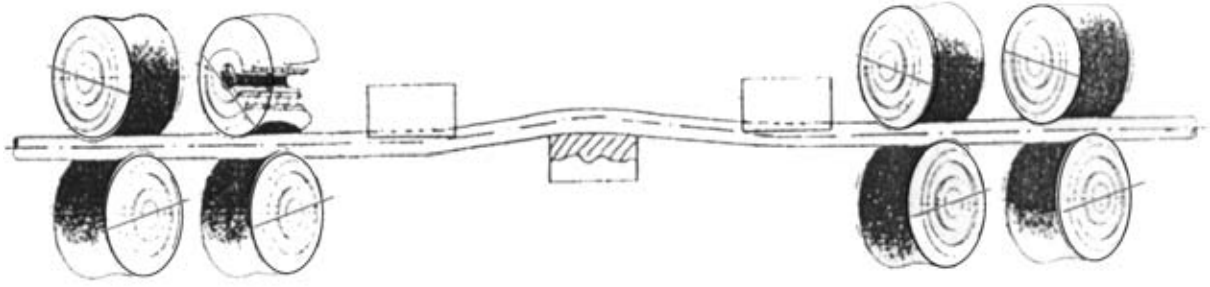

Figure 3. Schematic of the straightening case with rotating rollers and straightening blocks

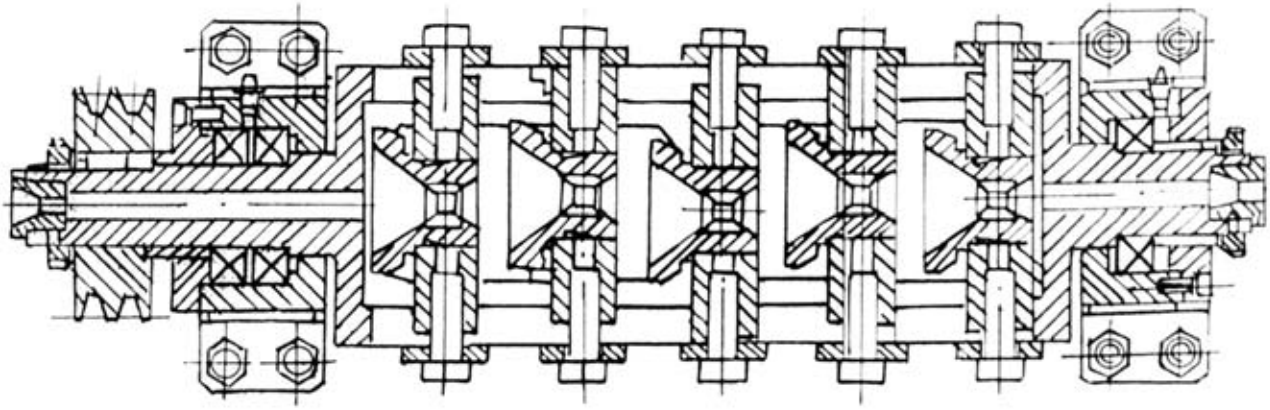

Figure 4. Straightening case with shifted blocks in two planes

A new design of the straightening case (Figure 4) was developed on the basis of the above cases for the I6120 automatic device. It is a cast hollow shaft with the encased guides and pressed-in straightening sleeves fixed inside it. The slots, through which the casings can be moved along and across the straightening case, are made on both sides of the straightening case along its axis. Such a design allows different diagrams of adjustment of the straightening case to be used for different diameters and materials. In addition, this makes it possible to vary the distance between the straightening sleeves and shift about the feed axis by choosing the optimal treatment conditions. The guides have an increased inlet cone, which makes it possible to load the wire without displacement of the straightening sleeves to the feed axis.

TECHNOLOGY AND EQUIPMENT FOR REFINING OF RAW RARE-EARTH METALS (REM)

KEY WORDS

technology for refining of REMs, induction remelting, sectional mould, ingot

BRIEF DESCRIPTION

Metal-thermic reduction is the most common commercial method for production of the majority of rare-earth metals. Raw REMs produced by this technology contain from 0.7 to 2.0 % calcium. Therefore, they are subjected to additional refining in arc skull furnaces. This process is characterized by an increased power and labour consumption.

The E.O. Paton Electric Welding Institute developed the technology and manufactured a pilot-commercial installation for refining of raw REMs. The technology is based on induction remelting with the formation of an ingot in the sectional water-cooled mould (IRSM). Intensive stirring of the metal melt in the high-frequency electromagnetic field causes a several times increase in the rate of evaporation from the metal melt, as compared with traditional arc melting. The refining process is realized in the inert gas atmosphere. Pressure inside the melting chamber can be varied over wide ranges. The pilot-commercial installation makes it possible to melt ingots of refined raw REMs with a diameter from 100 to 200 mm and mass of up to 80 kg. The annual output of the installation is up to 30 t.

PURPOSE AND FIELDS OF APPLICATION

The technology is intended for refining of raw REMs with a melting point of not less than 1200 °C. The technology and equipment were applied at the Kirkgisia Mining-Metallurgical Plant for producing pure yttrium of the Itm1 grade, containing up to 0.01 % calcium.

STATE-OF-THE-ART AND LEVEL OF DEVELOPMENT

Experimental-commercial validation at the Kirkgisia Mining-Metallurgical Plant.

PROPOSALS FOR COOPERATION

Open possibilities for cooperation.

Tel.: (380 44) 227 74 46

Fax: (380 44) 268 04 86

E-mail: office@paton.kiev.ua

TECHNOLOGY AND EQUIPMENT FOR REFINING MASTER ALLOYS

KEY WORDS

induction melting, sectional mould, vanadium-containing master alloy, ingot

BRIEF DESCRIPTION

Aluminothermic reduction from oxides is a traditional commercial technology used for production of many types of complex-composition master alloys. Spontaneous occurrence of oxidation-reduction reactions leading to reduction of metals is caused by a higher chemical affinity of aluminium for oxygen.

Ingots of master alloys produced by this method have a number of drawbacks, such as segregation of main elements, contamination of metal with non-metallic inclusions and increased oxygen content. For these reasons, up to 30 % of master alloys are rejected.

Based on the method of induction melting in a sectional mould (IMSM), the E.O. Paton Electric Welding Institute developed the technology for refining vanadium-containing master alloys (up to 55 % vanadium), which allows master alloy wastes to be returned to production.

The installation was developed for refining the vanadium-containing master alloy wastes. This installation makes it possible to produce high-quality ingots with a diameter of up to 200 mm and mass of up to 100 kg. The annual output of this installation is up to 50 t.

The technology developed provides remelting lumpy wastes in a sectional mould in the inert gas atmosphere. Flux on the CaF2 base can be utilized to ensure deeper refining.

PURPOSE AND FIELDS OF APPLICATION

The technology and equipment developed are intended for refining master alloys with a melting point of 1500 – 1700 °C. The technology and equipment passed the experimental-commercial tests in refining vanadium-containing master alloys at the Leninabad Plant for Rare Metals (Tajikistan).

STATE-OF-THE-ART AND LEVEL OF DEVELOPMENT

Experimental-commercial validation.

PROPOSALS FOR COOPERATION

Open possibilities for cooperation

Tel.: (380 44) 227 74 46

Fax: (380 44) 268 04 86

E-mail: office@paton.kiev.ua

HIGH-FREQUENCY WELDING OF THIN-WALLED SPIRAL PIPES

KEY WORDS

high-frequency welding of pipes, equipment for high-frequency welding, spirally-welded pipes

BRIEF DESCRIPTION

The technology is based on the use of the method of welding of helical-butt joints with edges flashing by high-frequency currents with simultaneous rolling of the welding zone. The materials being welded are St.08(rimmed), St.3 (cold- or hot- rolled, coiled, without scale). The mill for HFW of pipes is serviced by one operator.

The specification of the equipment is as follows:

Welding speed, m/min ..... 40 – 80
Speed of pipe yield, m/min ..... 8 – 12
Efficiency, km of pipes per shift ..... 1.0 – 1.5
HFC generator power (440 kHz frequency), kW ..... 160 – 250
Motor drive power, kW 8
Pipe length, m ..... 2 – 6 and more
Working area, m^2 110

The diameters of the pipes being welded depending on the thickness and width of the used strip, are given in the Table.

Pipe diameter, mm	*Strip thickness (pipes), mm*	*Strip width, mm*
75 – 100	0.5 – 1.5	100
100 – 200	0.8 – 2.0	100
200 – 250	0.8 – 2.5	200
300 – 700	1.0 – 3.0	200, 300, 500

PURPOSE AND FIELDS OF APPLICATION

Thin-walled spirally-welded pipes are used for air ducts, water conduits (with cladding of the pipe walls), pipelines for bulky products (flour, saw dust, etc.), cases of apparatuses and equipment, metal structures.

STATE-OF-THE-ART AND LEVEL OF DEVELOPMENT

Production technology and design documentation for equipment for welding pipes of 75 to 700 mm diameter on the shop floor have been developed. The welded pipes are produced to the current standards.

PROPOSALS FOR COOPERATION

Any form of cooperation for supply of equipment and production of pipes is possible.

Tel.: (380 44) 227 74 46

Fax: (380 44) 268 04 86

E-mail: office@paton.kiev.ua

CONSTRUCTION OF CURVILINEAR SECTIONS OF PIPELINES BY THE INCREMENT AND ELECTROTHERMAL BENDING METHOD

KEY WORDS

curvilinear sections of pipelines, electrothermal bending, pipeline construction

BRIEF DESCRIPTION

The process of construction of the curvilinear section of a pipeline by the increment method, consists in that the required number of straight pipes are welded to the end of the rectilinear section of the pipeline, whose total length is equal to the length of the curvilinear section. Then electrothermal bending (ETB) of the pipeline section is performed to achieve the design angle. The ETB process consists of local induction heating of the pipe wall up to the maximal temperature on the internal side of the future bend. In order to stabilize the bending parameters, mechanical stresses are induced in the place of the future bend on the level of stresses arising in the pipe during its fabrication. The pipe bending results in metal upsetting in the axial direction and formation of an outer corrugation on the bend inner side with the specified limits. The considered process of pipe bending does not create any conditions which could lead to stretching or reduction of the thickness of the walls of the bend outer part, characteristic of the traditional technology of fabrication of the curvilinear pipes in the cold and hot bending machines.

Investigations, field and route trials showed that the modes of ETB of pipes of 1220 and 1420 mm diameter with the wall thickness of 18 to 20 mm, provide bend angles of up to 0.5 to 0.7 deg. per one heating cycle. The required design angle of pipeline bending is achieved by successive repetition of ETB cycles. According to the interdepartamental statement (VNIIST and E.O.Paton Electric Welding Institute) made from the results of investigation of ETB influence on the properties of 1420 mm diameter pipes from steels of X60 – X70 grades, the performance of the curvilinear sections produced by ETB technology, is not inferior to that of the pipes in the initial condition. This allowed the developed technology to be recommended for use in construction of the curvilinear sections of the line pipelines from steels of different grades, produced the controllable rolling.

PURPOSE AND FIELDS OF APPLICATION

Technology of electrothermal bending (ETB) of pipelines in the field conditions is used mainly for production of the curvilinear sections with the angle of pipeline turning of up to 1 degree per 1 meter of the pipeline length for large-diameter pipes.

STATE-OF-THE-ART AND LEVEL OF DEVELOPMENT

Design documentation has been developed for fabrication of equipment for ETB of pipes of 720, 820, 1220 and 1420 mm diameter in the field conditions. Pilot samples of equipment for ETB of pipes of 1420 mm diameter have been manufactured. The equipment and technology have passed pilot-production trials in mounting of a pilot section of a line pipeline. Provisional instructions on the technology of construction of curvilinear pipelines by the increment method have been elaborated and approved.

PROPOSALS FOR COOPERATION

Any form of cooperation.

Tel.: (380 44) 227 74 46

Fax: (380 44) 268 04 86

E-mail: office@paton.kiev.ua

TECHNOLOGY OF STRENGTHENING OF DIFFERENT PURPOSE TOOL BY THE METHOD OF THERMO-REACTIVE DIFFUSION SATURATION IN SALT MELTS

KEY WORDS

thermoactive diffusion saturation, coatings, vanadium carbides, strengthening technology, salt melt, tool

BRIEF DESCRIPTION

The technology of strengthening of different purpose tool by thermoactive diffusion saturation in salt melts was developed. The treatment is carried out in shaft electro-heat-treating furnaces in salt melt with additions, containing carbide-forming elements. Operating temperature is 800 – 1200 °C. The process is performed at atmosphere pressure in borax-based melt at temperature of 800 – 1200 °C, holding time is 0.5 – 3.0 h. The product to be strengthened must contain not less than 0.3% C and not more than 2% Ni in surface layer. The technology makes it possible to compare an oxygen-free heating for quenching with the process of carbide-formation in surface layer of the part.

Initial materials are reusable. The technology is environmentally clean without dangerous gas emissions and draining wastes. The thickness of coatings, for example, of vanadium carbide, produced by developed technology, is 5 – 20 μm, microhardness is 26000 – 28000 MPa (for comparison, the microhardness of steel, quenched up to *HRC* 60, is 7000 MPa), surface roughness is not increased. Service temperature of the coatings can be up to 400 °C.

PURPOSE AND FIELDS OF APPLICATION

The process was developed for strengthening of machine parts, operating under friction and wear conditions, including impact loads, as well as cutting, bending, drawing, press-stamping and blade tools. The coating has increased factor of friction and, in some cases, it can efficiently operate without lubrication.

STATE-OF-THE-ART AND LEVEL OF DEVELOPMENT

Industrial application.

PROPOSALS FOR COOPERATION

Signing of contracts, establishment of a joint venture.

Tel.: (380 44) 227 74 46

Fax: (380 44) 268 04 86

E-mail: office@paton.kiev.ua

DEVELOPMENT OF METHODS AND TECHNOLOGIES OF REPAIR AND RESTORATION OF CRITICAL BUILDING METAL STRUCTURES AFTER LONG-TERM SERVICE

KEY WORDS

methods of repair, evaluation of the technical conditions, loads and impacts, verifying calculation, reinforcement of the preserved elements, technology of repair and reinforcement by electric arc welding

BRIEF DESCRIPTION

Methods and technology of repair and restoration of critical building metal structures after long-term service have been developed. The technology of reinforcement and repair is elaborated taking into account the statement on the technical condition of the structures in service, made by the results of their examination, and verifying calculations. In this case the causes leading to appearance of defects and damage are considered, and methods are sought to prevent their formation during further service. The developed technology of repair, restoration and reinforcement allows for and specifies the use of the base and auxiliary materials, welding process, preheating, structure unloading prior to repair, application of thermal jackets, sequence of deposition of the welding beads, use of the required inspection and diagnostic systems and other elements of technology.

PURPOSE AND FIELDS OF APPLICATION

The development is aimed at extension of the life of critical building metal structures, namely bridges, cranes and crane girders, truss towers, pipes, etc.

STATE-OF-THE-ART AND LEVEL OF DEVELOPMENT

The examination procedure, and the developed technology of reinforcement and repair of metal structures have been tried out with success in repair of a large motor road bridge in Kyiv.

PROPOSALS FOR COOPERATION

Technology transfer under contract.

Tel.: (380 44) 227 74 46

Fax: (380 44) 268 04 86

E-mail: office@paton.kiev.ua

AIR-TIGHT PERMANENT PIPE JOINT «POLYETHYLENE-STEEL» WITH A HYDROINSULATING THERMOSHRINKABLE COATING

KEY WORDS

permanent joint «polyethylene-steel», polyethylene branch pipe, steel branch pipe

BRIEF DESCRIPTION

Pipe permanent joint consists of a steel and polyethylene branch pipes and has special grooves at the surface of a steel branch pipe and a steel squeezing ring over the polyethylene branch pipe in the area of their joining. The hydroinsulating thermoshrinkable coating is deposited on the area of joining. When assembling the joint, the polyethylene branch pipe is first welded to the polyethelene pipeline and then a steel branch pipe is welded to the metallic pipeline.

The results of investigations showed that the permanent joint, which was designed, is equal by strength to the polyehylene pipe, i.e. the predicted service life of joints from the polyethelene pipes will be not less than 50 years, according to TS 6-19-352–87 at safety factor 3.25 (operating pressure of natural gas is 0.4 MPa at temperature +20 °C), and at 0.6 MPa pressure the safety factor will equal to 2.17.

PURPOSE AND FIELDS OF APPLICATION

The pipe permanent joint is used in construction of gas-, water pipelines, etc. in field conditions and at the territory of settlements with their laying under the ground.

STATE-OF-THE-ART AND LEVEL OF DEVELOPMENT

Experimental-industrial testing.

PROPOSALS FOR COOPERATION

Making contracts.

Tel.: (380 44) 227 74 46

Fax: (380 44) 268 04 86

E-mail: office@paton.kiev.ua

TECHNOLOGY AND EQUIPMENT FOR MANUFACTURE OF WELDED JOINING PARTS OF POLYEHYLENE PIPELINES OF UP TO 315 MM DIAMETER

KEY WORDS

welding of polyethylene, polyethylene pipes, welded joining parts, equipment for welding polyethylene pipes

BRIEF DESCRIPTION

Technological recommendations and designing documentation are developed for pilot models of machines for manufacture of welded joining parts from sections of polyethylene pipes for polyethylene pipelines of two types and sizes: diameter 63 – 160 mm and 160 – 315 mm. Butt welding is performed with a heated tool.

The joining parts manufactured by the developed technology have higher (by 20 – 30 %) strength of welded joints, thus permitting to increase, respectively, the service reliability both of parts proper and the pipeline system as a whole.

Implementation of technology and equipment will reduce also the labour consumption and increase the welding efficiency by 30-40% and save currency due to refuse of purchasing the imported welding equipment.

PURPOSE AND FIELDS OF APPLICATION

Technology and equipment developed are designed for manufacture of welded joining parts, used in construction of polyethylene pipelines of different diameters.

STATE-OF-THE-ART AND LEVEL OF DEVELOPMENT

Experimental-industrial testing.

PROPOSALS FOR COOPERATION

Different forms of cooperation.

Tel.: (380 44) 227 74 46

Fax: (380 44) 268 04 86

E-mail: office@paton.kiev.ua

TECHNOLOGY AND EQUIPMENT FOR METAL-ELECTRODE IMPULSE-ARC WELDING AND SURFACING WITH MODULATED FEED OF SHIELDING GASES

KEY WORDS

impulse-arc welding, equipment for impulse-arc welding, shielding gases, modulation of gas feed, metal electrode

BRIEF DESCRIPTION

Metal-electrode impulse-arc welding with modulated feed of shielding gases into the arc zone allows solving the problems of controlling the processes proceeding at the electrode tip, in the arc and in the weld pool. Equipment has been developed for automatic and semi-automatic welding.

The equipment for welding consists of a specialized power source, block of modulation of the shielding gas composition and a device for synchronizing the kind of welding current passing through the arc with the shielding gas composition. Such a system allows welding joints on different types of steels of small, medium and large thicknesses in the range of currents of 50 to 500 A.

Equipment specification:

Kind of welding current	constant, impulse
Range of welding current adjustment, A	50 – 500
Frequency of current pulses, Hz	50 – 300
Amplitude of current pulses, A	500 – 1000
Duration of shielding gases feed, s	$25 - 1000 \cdot 10^{-3}$

The new technology allows improvement of the energy and process parameters of the electric arc, widening the capabilities of mechanized welding processes, saving of welding consumables and power.

The main advantages of the new technology over the traditional processes (welding in CO_2, Ar-based mixtures, impulse-arc welding in Ar + CO_2 mixture) are as follows:

- improvement of the mechanical properties, in particular, of impact toughness at below zero temperatures, by 30 %;
- reduction by 2.5 to 3.0 times of shielding gas consumption;
- improvement of weld appearance;
- ability to control the penetration depth and shape;
- reduction of spatter by 25 %;
- ability to perform sound welding of sheet metal in the gravity position.

PURPOSE AND FIELDS OF APPLICATION

Automatic and semi-automatic metal-arc welding and surfacing of low-carbon structural steels, aluminium-base alloys in ship-building, chemical, petroleum and food machinery engineering

STATE-OF-THE-ART AND LEVEL OF DEVELOPMENT

Results of technology studies and design documentation are available, pilot- production trials have been conducted and pilot samples have been manufactured.

PROPOSALS FOR COOPERATION

Making a contract.

Tel.: (380 44) 227 74 46

Fax: (380 44) 268 04 86

E-mail: office@paton.kiev.ua

TRANSISTORIZED SOURCE FOR CONSUMABLE-ELECTRODE IMPULSE- ARC WELDING

KEY WORDS

impulse-arc welding, transistorized source, consumable electrode

BRIEF DESCRIPTION

The transistorized source for consumable-electrode impulse-arc welding allows more flexibility in solving the arising technological problems, At approximately equal cost with its prototype, namely I-169 source, the weight, overall dimensions and labour consumption for its fabrication have been reduced. It has no analogs in Ukraine or CIS; allows any shape of welding current to be formed.

Equipment specification:

Three-phase mains voltage, V	380
Maximal average welding current, A	515
Average arc voltage, V	16 – 40
Impulse current amplitude, smoothly adjustable, A	400 – 800
Pulse duration, smoothly adjustable, s	$(1.5 - 5.0) \cdot 10^{-3}$
Pulse frequency, smoothly adjustable, Hz	30 – 300

PURPOSE AND FIELDS OF APPLICATION

Automatic and semi-automatic consumable-electrode arc welding and surfacing of low- and high-alloyed steels, aluminium-, copper-, titanium-base alloys in ship-building, automotive industry, chemical and food processing engineering.

STATE-OF-THE-ART AND LEVEL OF DEVELOPMENT

Pilot sample has been manufactured.

PROPOSALS FOR COOPERATION

Open possibilities for cooperation.

Tel.: (380 44) 227 74 46

Fax: (380 44) 268 04 86

E-mail: office@paton.kiev.ua